Supporting Information

Dodecamannosylated Fullerenes as *Escherichia coli* FimH Ligands and Bacterial Antiadhesives

Maxime Durka,[a] Kevin Buffet,[a] Julien Iehl,[b] Michel Holler,[b]

Jean-François Nierengarten,*[b] Joemar Taganna,[c] Julie Bouckaert,*[c]

Stéphane P. Vincent*[a]

[a] University of Namur (FUNDP), Département de Chimie, Laboratoire de Chimie Bio-Organique, rue de Bruxelles 61, B-5000 Namur, Belgium; E-mail: stephane.vincent@fundp.ac.be

[b] Laboratoire de Chimie des Matériaux Moléculaires, Université de Strasbourg et CNRS (UMR 7509), Ecole Européenne de Chimie, Polymères et Matériaux (ECPM), 25 rue Becquerel, 67087 Strasbourg Cedex 2 (France). E-mail: nierengarten@chimie.u-strasbg.fr

[c] Structural Biology Brussels at the Vrije Universiteit Brussel Pleinlaan 2, 1050 Brussels (Belgium); E-mail: bouckaej@vub.ac.be

TABLE OF CONTENTS

SYNTHESIS **3**

Experimental section **3**

Characterization of compound 3 **13**

HAEMAGLUTINATION INHIBITION ASSAYS (HIA) **17**

ISOTHERMAL TITRATION CALORIMETRY (ITC) **19**

SURFACE PLASMON RESONANCE (SPR) **28**

NMR DATA **42**

MODEL STRUCTURE OF MANNOSYLATED FULLERENE IN INTERACTION WITH 6 FIMH MOLECULES **77**

Acknowledgements - We are grateful to Swaine Chen for strain UTI89, and to Mehdi Almant for the amide-functionalised heptyl mannoside**.**

SYNTHESIS

Experimental Section

General. Reagents and solvents were purchased as reagent grade and used without further purification. Compounds **1**,[1] **2**,[1] **18**,[2] **23**[1,3] and **24**[1,4] were prepared according to previously reported procedures. All reactions were performed in standard glassware under an inert Ar or N_2 atmosphere. Microwave irradiation reaction was performed in a Biotage Initiator™. Evaporation and concentration were done at water aspirator pressure and drying in vacuo at 10^{-2} Torr. Column chromatography: silica gel 60 (230-400 mesh, 0.040-0.063 mm) was purchased from E. Merck. Thin Layer Chromatography (TLC) was performed on glass or aluminium sheets coated with silica gel 60 F_{254} purchased from E. Merck, visualization by UV light or by revelation with ethanolic phosphomolybdic acid. IR spectra (cm^{-1}) were measured on an ATI Mattson Genesis Series FTIR instrument. NMR spectra were recorded on a Bruker AC 300, AC 400 or JEOL ECX 400 with solvent peaks as reference. Compounds were characterized by ^1H, ^{13}C, and NMR as well as by ^1H-^1H correlation and ^1H-^{13}C experiments when necessary. All The following abbreviations were used to describe the multiplicities: s=singlet, d=doublet, t=triplet, m=multiplet, quint.=quintuplet br s=broad singlet.

[1] J.-F. Nierengarten, J. Iehl, V. Oerthel, M. Holler, B. M. Illescas, A. Muñoz, N. Martín, J. Rojo, M. Sánchez-Navarro, S. Cecioni, S. Vidal, K. Buffet, M. Durka, S. P. Vincent, *Chem. Commun*. 2010, **46**, 3860.
[2] J. Iehl and J.-F. Nierengarten, *Chem. Eur. J*. 2009, **15**, 7306.
[3] R. J. Kaufman and R. S. Sidhu et al. *J. Org. Chem.* 1982, **47**, 4941; M. Touaibia, A. Wellens, T. C. Shiao, Q. Wang, S. Sirois, J. Bouckaert and R. Roy, *ChemMedChem*, 2007, **2**, 1190; P. van der Peet, C. T. Gannon, I. Walker, Z. Dinev, M. Angelin, S. Tam, J. E. Ralton, M. J. McConville and S. J. Williams, *ChemBioChem* 2006, **7**, 1384; . Ferrandiz-Huertas, J. Isac-García, F. Pérez-Balderas and F. Santoyo-González, *Synthesis* 2005, **6**, 939.
[4] Y. Yamada, K. Matsuura and K. Kobayashi, *Bioorg. Med. Chem.* 2005, **13**, 1913.

Compound 4

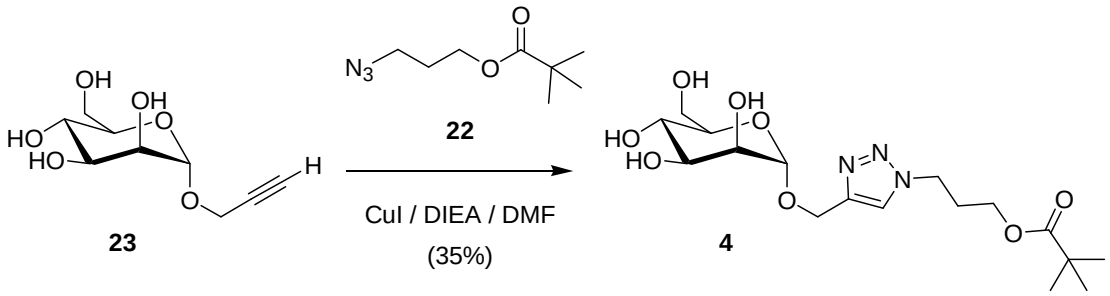

A solution of **23** (22 mg, 0.1 mmol, 1 eq.), **22** (18 mg, 0.12 mmol, 1.2 eq.), DIEA[5] (41.8 µL, 0.24 mmol, 2 eq.) and CuI (9.5 mg, 0.05 mmol, 0.5 eq.) in dry DMF (200.0 µL) was warmed to 80°C under microwave irradiation during 1 hour. The solvents were then evaporated under reduced pressure. Column chromatography (SiO_2, EtOAc to EtOAc/EtOH 8:2) gave **4** (14 mg, 35%) as a yellow oil. $[\alpha]_D^{20}$ (MeOH, c = 0.5) = +26.2. ^{1}H NMR (21.1°C, 400 MHz, D_2O) δ = 7.95 (s,1 H), 4.82 (d, *J* = 1.4 Hz, 1 H), 4.62 (AB, *J* =12.4 Hz, 2 H), 4.43 (t, *J* = 6.4 Hz, 2 H), 3.97 (t, *J* = 5.5 Hz, 2 H), 3.78 (dd, *J* = 1.6 and 3.2 Hz, 1 H), 3.71 (m, 1 H), 3.64-3.58 (m, 1 H), 3.62 (m, 1 H), 3.52 (t, *J* = 9.9 Hz, 1 H), 3.54-3.48 (m, 1 H), 2.17 (quint., *J* = 5.9 Hz, 2 H), 0.95 (s, 9 H). ^{13}C NMR (21.6°C, 101 MHz, D_2O) δ = 181.8, 125.4, 99.5, 72.9, 70.5, 69.9, 66.7, 62.6, 60.8, 59.7, 48.1, 38.5, 28.2, 26.18. MS (TOF-MS-ES+): m/z: 242.15 (100%, $[M-C_6H_{11}O_6+NH_4]^+$), 404.2041 (88%, $[M+H]^+$). HRMS: calcd for $C_{17}H_{30}N_3O_8$, $[M+H]^+$: 404.2027, found: 404.2041.

Compound 5

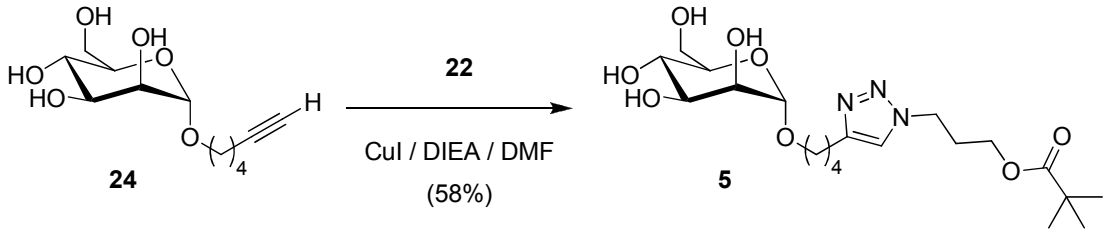

The same procedure described for compound **4** was applied with **24** (15 mg, 0.058 mmol, 1 eq.), **22** (12 mg, 0.069 mol, 1.2 eq.), DIEA (20.0 µL, 0.115 mmol, 2 eq.) and CuI (5.0 mg, 0.0262

[5] DIEA : Diisopropyl Ethylamine

mmol, 0.5 eq.) in dry DMF (120 µL). The solution was warmed to 80°C under microwave irradiation during 1 hour. The solvents were then evaporated under reduced pressure. Column chromatography (SiO_2, EtOAc to EtOAc/EtOH 9:1) gave **5** (15 mg, 58%) as a yellow oil. $[\alpha]_D^{20}$ (MeOH, c = 0.2) = +4.7. ^{1}H NMR (21.8°C, 400 MHz, D_2O) δ = 7.73 (s,1 H), 4.74 (s, 1 H), 4.29 (t, *J* = 6.2 Hz, 2 H), 3.99 (t, *J* = 5.5 Hz, 2 H), 3.82 (m, 1 H), 3.75 (d, *J* = 11.9 Hz, 1 H), 3.69-3.62 (m, 3 H), 3.57-3.43 (m, 3 H), 2.65 (t, *J* = 7.1 Hz, 2 H), 2.20 (m, 2 H), 1.67-1.51 (m, 4 H), 1.00 (s, 9 H). ^{13}C NMR (22.0°C, 101 MHz, D_2O) δ = 181.7, 99.7, 72.7, 70.6, 70.1, 67.4, 66.7, 62.6, 60.9, 48.0, 38.5, 28.2, 27.9, 26.2, 25.2, 24.3. MS (TOF-MS-ES+): m/z: 468.23 (100%, $[M+Na]^+$), 913.47 (21%, $[2M+Na]^+$). HRMS: calcd for $C_{20}H_{35}N_3O_8Na$, $[M+Na]^+$: 468.2316, found: 468.2292. Rf = 0.16 (EtOAc/EtOH).

Compound 6

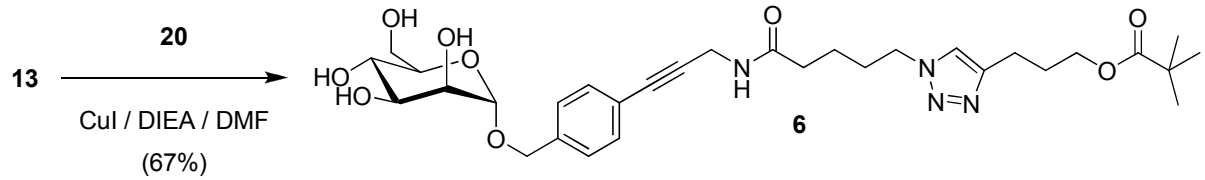

A solution of **13** (67 mg, 0.15 mmol, 1 eq.), **20** (see structure below, 63 mg, 0.37 mmol, 2.5 eq.), DIEA (52 µL, 0.30 mmol, 2 eq.) and CuI (3 mg, 0.015 mmol, 0.5eq.) in dry DMF (2 mL) was stirred 24 hours at room temperature. The solvents were then evaporated under reduced pressure. Column chromatography (SiO_2, EtOAc to EtOAc/EtOH 85/15) gave **6** (41mg, 67%) as a yellow oil. $[\alpha]_D^{20}$ (MeOH, c = 1.2) = 20.2. ^{1}H NMR (19.7°C, 400 MHz, CD_3OD) δ = 7.74 (s, 1 H), 7.36 (d, *J* = 8.5 Hz, 2 H), 7.31 (d, *J* = 8.5 Hz, 2 H), 4.81 (d, *J* = 1.6 Hz, 1 H), 4.61 (AB, *J* = 12.4 Hz, 2 H), 4.37 (t, *J* = 7.1 Hz, 2 H), 4.15 (s, 2 H), 4.07 (t, *J* = 6.4 Hz, 2 H), 3.82 (m, 1 H), 3.81 (dd, *J* = 1.8 and 3.4 Hz, 1 H), 3.70 (dd, *J* = 3.9 and 9.4Hz, 1 H), 3.67 (m, 1 H), 3.60 (*br* t, *J* = 9.9 Hz, 1 H), 3.54 (ddd, *J* = 2.3, 5.7 and 9.9 Hz, 1 H), 2.74 (t, *J* = 7.8 Hz, 2 H), 2.26 (t, *J* = 7.3 Hz, 2 H), 2.00-1.88 (m, 4 H), 1.61 (quint., *J* = 7.6 Hz, 2 H), 1.17 (s, 9 H). ^{13}C NMR (22°C, 100 MHz, CD_3OD) δ = 178.7, 173.8, 138.2, 131.3, 127.7, 122.2, 99.5, 84.9, 81.8, 73.7, 71.3, 70.8, 68.0, 67.3, 63.4, 61.6, 49.6, 34.6, 29.4, 28.9, 28.2, 26.2, 22.3, 21.6. MS (TOF-MS-ES+): m/z: 617.32 (100%, $[M+H]^+$), 639.30 (100%, $[M+Na]^+$). HRMS: calcd for $C_{31}H_{45}N_4O_9$, $[M+H]^+$: 617.3181, found: 617.3189. Rf = 0.23 (EtOAc/EtOH 8:2).

Compound 8

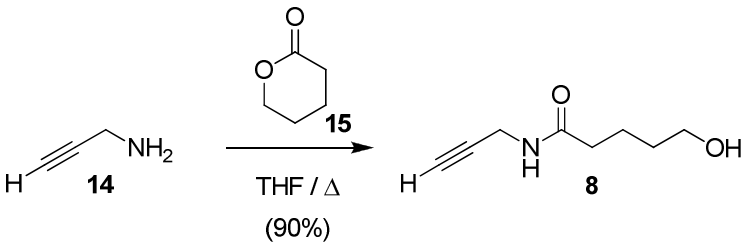

A solution of **14** (5.93 mL, 92.40 mmol, 2 eq.) and **15** (4.63 mL, 46.20 mmol, 1 eq.) in dry THF (30.0 mL) was heated under reflux for 3 days. The solvent was evaporated under reduced pressure. Column chromatography (SiO_2, EtOAc/MeOH 85:15) afforded **8** (6.48 g, 90%) as a yellow solid. ^{1}H NMR (21.8°C, 400 MHz, $CDCl_3$) δ = 5.74 (bs, 1 H), 4.05 (dd, *J* = 2.5 Hz, *J* = 5.3 Hz, 2 H), 3.65 (q, *J* = 6.0 Hz, 2 H), 2.26 (t, *J* = 7.1 Hz, 2 H), 2.23 (t, *J* = 2.5 Hz, 1 H), 1.76 (m, 3 H), 1.60 (m, 2 H). ^{13}C NMR (22.0°C, 101 MHz, $CDCl_3$) δ = 172.9, 79.7, 71.7, 62.2, 35.8, 31.9, 29.3, 21.7. MS (TOF-MS-ES+): m/z: 178.0835 (100%, $[M+Na]^+$), 278.1318 (32%, $[M+C_5H_8O_2+Na]^+$). HRMS-ESI: calcd for $C_8H_{13}NO_2Na^+$ $[M+Na]^+$: 178.0838, found: 178.0835. Rf = 0.4 (EtOAc/MeOH 9:1).

Compound 9

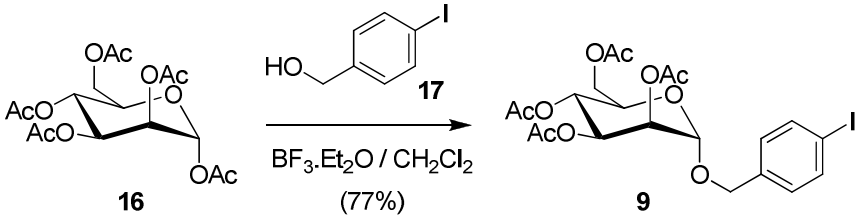

Alcohol **17** (5.12 g, 21.80 mmol, 1.7 eq.) and $BF_3.Et_2O$ (8.11 mL, 64.00 mmol, 5 eq.) were added dropwise to a solution of **16** (5.00 g, 12.80 mmol, 1 eq.) in dry CH_2Cl_2 (100.0 mL) at 0°C under an argon atmosphere. The mixture was allowed to warm to room temperature and stirred at this temperature for 24 hours. The solution was then washed with a saturated aqueous $NaHCO_3$ solution (2x 100 mL), then water (100 mL). The aqueous phase was extracted with CH_2Cl_2 (3 x 100 mL). The combined organic layers were dried over $MgSO_4$, filtered and concentrated.

Column chromatography (SiO_2, Cy/EtOAc 9:1 to Cy/EtOAc 5:5) afforded **9** (5.57 g, 77%) as a white solid. $[\alpha]_D^{20}$ ($CHCl_3$, c = 1) = + 44.3. ^{1}H NMR (23.4°C, 400 MHz, $CDCl_3$) δ = 7.69 (d, *J* = 8.2 Hz, 2 H), 7.08 (d, *J* = 8.2 Hz, 2 H), 5.35 (dd, *J* = 3.4 and 9.9 Hz, 1 H), 5.30 (d, *J* = 9.9 Hz, 1 H), 5.27 (dd, *J* = 3.4 and 1.6 Hz, 1 H), 4.85 (d, *J* = 1.4 Hz, 1 H), 4.57 (AB, *J* = 12.1 Hz, 2 H), 4.28 (m, 1 H), 4.06 (m, 1 H), 3.97 (ddd, *J* = 2.5, 5.3 and 9.6 Hz, 1 H), 2.14, 2.11, 2.03, 1.98 (4 s, 12 H). ^{13}C NMR (23.1°C, 101 MHz, $CDCl_3$) δ = 170.7, 170.1, 170.0, 169.8, 137.8, 135.9, 130.0 (2C), 96.8, 94.0, 69.6, 69.1, 69.1, 68.9, 66.2, 62.5, 21.0, 20.86, 20.79 (2C). MS (TOF-MS-ES+): m/z: 587.0384 (100%, $[M+Na]^+$), 582.0824 (38%, $[M+NH_4]^+$). HRMS-ESI: calcd for $C_{21}H_{25}IO_{10}Na^+$, $[M+Na]^+$: 587.0385, found: 587.0384. Rf = 0.68 (Cy/EtOAc 1:1).

Compound 10

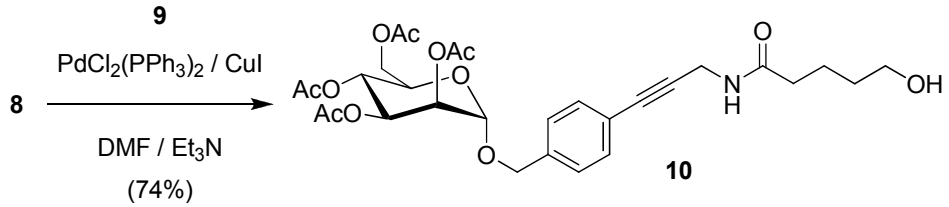

A mixture of mannoside **9** (1.00 g, 1.77 mmol, 1 eq.), **8** (830.0 mg, 5.31 mmol, 3 eq.), Et_3N (0.49 mL, 3.54 mmol, 2 eq.), $PdCl_2(PPh_3)_2$ (124.0 mg, 0.18 mmol, 0.1 eq.) and CuI (6.7 mg, 0.35 mmol, 0.2 eq.) in dry and degazed DMF (10 mL) was heated under microwave irradiation (6 minutes at 120°C). The mixture was cooled to 0°C, diluted with EtOAc and washed with brine (3 x 50 mL). The combined aqueous layers were extracted with EtOAc. The combined organic layers were dried over $MgSO_4$, filtered and concentrated. Column chromatography (SiO_2, EtOAc to EtOAc/MeOH 8:2) gave **10** (0.77 g, 74%) as a yellow oil. $[\alpha]_D^{20}$ ($CHCl_3$, c = 1.0) = + 53.9. ^{1}H NMR (22.9°C, 400 MHz, $CDCl_3$) δ = 7.40 (d, *J* = 8.2 Hz, 2 H), 7.27 (d, *J* = 8.5 Hz, 2 H), 5.97 (bs, 1 H), 5.35 (dd, *J* = 3.2 and 10.1 Hz, 1H), 5.28 (bt, *J* = 9.9 Hz, 1 H), 5.27 (dd, *J* = 1.6 and 3.4 Hz, 1 H), 4.86 (d, *J* = 1.4 Hz, 1 H), 4.61 (AB, *J* = 12.4 Hz, 2 H), 4.28 (d, *J* = 5.0 Hz, 2 H), 4.28-4.23 (m, 1 H), 4.03 (m, *J* = 2.3 Hz, *J* = 12.4 Hz, 1 H), 3.96 (ddd, *J* = 2.3, 5.0 and 9.9 Hz, 1 H), 3.65 (t, *J* = 6.2 Hz, 2 H), 2.28 (t, *J* = 7.3 Hz, 2 H), 2.13, 2.10, 2.02, 1.98 (4 s, 12 H), 1.77 (m, 2 H), 1.61 (m, 2 H). ^{13}C NMR (21.5°C, 101 MHz, $CDCl_3$) δ = 172.8, 170.8, 170.2, 170.1, 169.8,

136.7, 122.5, 132.0, 128.1, 97.0, 85.4, 83.1, 69.6, 69.4, 69.2, 68.8, 66.1, 62.4, 62.2, 35.9, 32.0, 30.1, 21.7, 21.0, 20.9, 20.8. MS (TOF-MS-ES+): m/z: 592.24 (100%, $[M+H]^+$), 614.22 (70%, $[M+Na]^+$), 1183.48 (50%, $[2M+H]^+$). HRMS-ESI: calcd for $C_{29}H_{37}NO_{12}H^+$, $[M+H]^+$: 592.2389,found: 592.2387. Rf = 0.60 (EtOAc/MeOH 9:1)

Compound 11

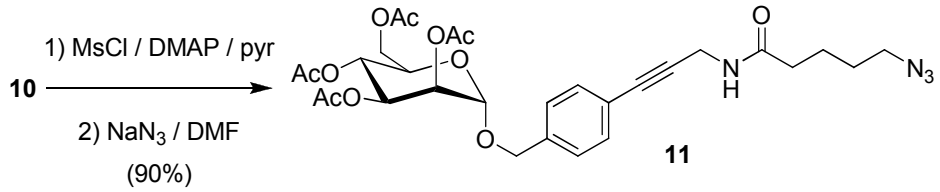

MsCl (0.40 mL, 5.15 mmol, 4 eq.) was added to a solution of alcohol **10** (0.762 g, 1.29 mmol, 1 eq.) and DMAP (0.031 g, 0.26 mmol, 0.2 eq.) in dry pyridine (13 mL) under argon atmosphere at 0°C. The mixture was stirred during 1 hour then diluted with EtOAc and washed with brine (3 x 50 mL). The combined aqueous layers were extracted with EtOAc. The combined organic layers were dried over $MgSO_4$, filtered and concentrated. The residue was used in the next step without further purification. The mesylated intermediate was dissolved in DMF (13 mL) and NaN_3 (0.41 g, 6.44 mmol, 5 eq.) was added. The solution was stirred at 60°C during 4 hours. The mixture was then diluted with EtOAc and washed with a saturated solution of NH_4Cl. The aqueous layer was extracted with EtOAc and the combined organic layers dried over $MgSO_4$, filtered and concentrated. Column chromatography (SiO_2, Cy/EtOAc 8:2 to Cy/EtOAc 5:5) afforded **11** (0.72 g, 90%) as a colorless oil. $[\alpha]_D^{20}$ ($CHCl_3$, c = 1.0) = + 45.9. IR (neat): υ = 2099 (N_3). ^{1}H NMR (19.9°C, 400 MHz, $CDCl_3$) δ = 7.41 (d, *J* = 8.2 Hz, 2 H), 7.28 (d, *J* = 8.2 Hz, 2 H), 5.71 (s, 1 H), 5.36 (dd, *J* = 3.4 and 10.1 Hz, 1 H), 5.30 (dd, *J* = 9.9 Hz, 1 H), 5.27 (dd, *J* = 1.6 and 3.4 Hz, 1 H), 4.86 (d, *J* = 1.6 Hz, 1 H), 4.62 (AB, *J* = 12.1 Hz, 2 H), 4.28 (d, *J* = 5.0 Hz, 2 H), 4.26 (m, 1 H), 4.03 (m, 1 H), 3.96 (ddd, *J* = 2.3, 5.0 and 9.9 Hz, 1 H), 3.30 (t, *J* = 6.6 Hz, 2 H), 2.26 (t, *J* = 7.1 Hz, 2 H), 2.14, 2.10, 2.03, 1.99 (4 s, 12 H), 1.80-1.71 (m, 2 H), 1.69-1.61 (m, 2 H). ^{13}C NMR (22.1°C, 100 MHz, $CDCl_3$) δ = 171.9 170.7 170.1 170.0 169.8, 136.7, 132.0, 128.0, 122.5, 97.0, 85.3 83.2, 69.6, 69.4, 69.2, 68.8, 66.1, 62.5, 51.2, 35.8, 30.1, 28.5, 22.8, 21.0, 20.9, 20.8. MS (TOF-MS-ES-): m/z: 661.24 (100%, $[M+COOH]^-$) 1277.47 (25%, $[2M+COOH]^-$). HRMS-ESI:

calcd for $C_{29}H_{36}N_4O_{11}COOH$, $[M+COOH]^-$: 661.2363, found: 661.2352. Rf = 0.32 (Cy/EtOAc 1:1).

Compound 12

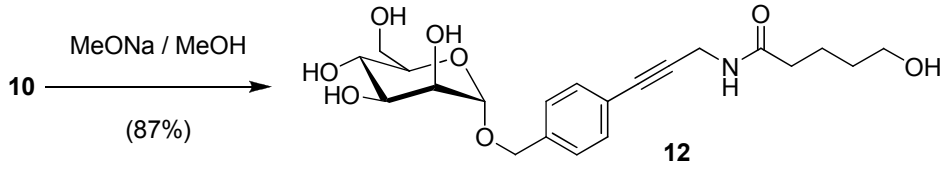

MeONa (3.8 mg, 70.6 µmol, 1.1 eq.) was added to a solution of **10** (38.0 mg, 64.2 µmol, 1 eq.) in dry MeOH (1.0 mL) at 0°C. After 15 minutes, the resulting solution was filtered over a short column of Dowex 50WX8-200 (H^+ form). The resin was washed with H_2O/MeOH 1/1 (50 mL) and MeOH (20 mL) and the solvents were evaporated to afford **12** (23.7 mg, 87%) as a white foam. ^{1}H NMR (21.3°C, 400 MHz, D_2O) δ = 7.35 (d, *J* = 8.0 Hz, 2 H), 7.26 (d, *J* = 8.0 Hz, 2 H), 4.82 (d, *J* = 1.4 Hz, 1 H), 4.52 (AB, *J* = 11.9 Hz, 2 H), 4.02 (s, 2 H), 3.83 (dd, *J* = 1.6 and 3.2 Hz, 1 H), 3.70 (d, *J* = 11.5 Hz, 1 H), 3.67-3.58 (m, 2 H), 3.55-3.49 (m, 2 H), 3.46 (t, *J* = 6.4 Hz, 2 H), 2.17 (t, *J* = 7.3 Hz, 2 H), 1.54-1.48 (m, 2 H), 1.45-1.40 (m, 2 H). ^{13}C NMR (22.1°C, 101 MHz, D_2O) δ = 176.8, 137.4, 131.9, 128.5, 121.9, 99.5, 85.4, 82.3, 73.0, 70.6, 70.0, 66.7, 69.0, 66.7, 61.2, 60.8, 35.3, 30.7, 29.5, 21.7. MS-ESI (TOF-MS-ES+): m/z: 424.1973 (100%, $[M+H]^+$), 262.1433 (33%, $[M-C_6H_{11}O_6+NH_4]^+$). HRMS-ESI: calcd for $C_{21}H_{29}NO_8H^+$, [M+H]: 424.1966, found: 424.1973. Rf = 0.10 (EtOAc/MeOH 9/1).

Compound 13

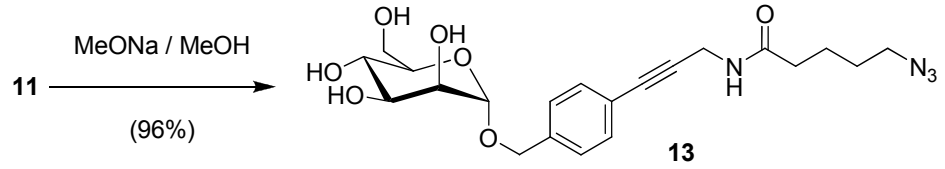

MeONa (10 mg, 0.18 mmol, 1.1 eq.) was added to a solution of **11** (100 mg, 0.16 mmol, 1 eq.) in dry MeOH (1.5 mL) at 0°C. After 15 minutes, the resulting solution was filtered over a short column of Dowex 50WX8-200 (H^+ form). The resin was washed with MeOH then water and the solvents were evaporated to afford **13** (70 mg, 96%) as a white foam. $[\alpha]_D^{20}$ (MeOH, c = 1.0) = +

53.2. IR (neat): υ = 2099 (N_3). ^{1}H NMR (22°C, 400 MHz, CD_3OD) δ = 7.37 (d, *J* = 8.0 Hz, 2 H), 7.31 (d, *J* = 8.0 Hz, 2 H), 4.81 (d, *J* = 1.4 Hz, 1 H), 4.60 (AB, *J* = 12.1 Hz, 2 H), 4.16 (s, 2 H), 3.83 (m, 1 H), 3.81 (dd, *J* = 1.8 and 3.4 Hz, 1H), 3.69 (m, 1 H), 3.68 (dd, *J* = 8.9 Hz, 1 H), 3.60 (dd, *J* = 8.9 and 9.9 Hz, 1 H), 3.56 (ddd, *J* = 1.8, 5.7 and 9.6 Hz, 1 H), 3.29 (m, 2 H), 2.25 (t, *J* = 2.25 Hz, 2 H), 1.72 (m, 2 H), 1.59 (m, 2 H). ^{13}C NMR (21.9°C, 100 MHz, CD_3OD) δ = 174.0, 138.2, 131.4, 127.7, 122.2, 99.5, 85.0, 81.8, 73.6, 71.3, 70.8, 68.0, 67.3, 61.6, 50.8, 34.9, 28.9, 28.0, 22.7. MS (TOF-MS-ES-): m/z: 493.1926 (100%, $[M+COOH]^-$), 941.3866 (61%, $[2M+COOH]^-$). HRMS: calcd for $C_{21}H_{28}N_4O_7COOH$, $[M+COOH]^-$: 493.1940, found: 493.1926. Rf = 0.10 (EtOAc).

Compound 20

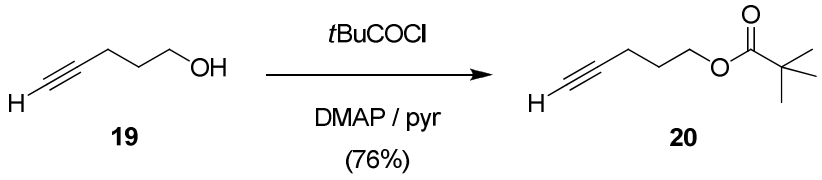

Pivaloyl chloride (1.72 ml, 14.30 mmol, 1.2 eq.) was added to a solution of **19** (1.1 mL, 11.90 mmol, 1 eq.) and DMAP (0.14 g, 1.19 mmol, 0.1eq.) in dry pyridine (10 mL) at 0°C. The solution was then stirred overnight at room temperature. The solvents were evaporated under reduced pressure. Column chromatography (SiO_2, Cy to Cy/AcOEt 8/2) gave **20** (1.54 g, 76%) as a colorless oil. ^{1}H NMR (22°C, 400 MHz, $CDCl_3$) δ = 4.15 (t, *J* = 6.4 Hz, 2 H), 2.28 (dt, *J* = 2.8 and 7.1 Hz, 2 H), 1.96 (t, *J* = 2.8 Hz, 1 H), 1.86 (tt, *J* = 6.9 and 6.4 Hz, 2 H), 1.19 (s, 9 H). MS (TOF-MS-APCI+): m/z: 169.1221 ($[M+H]^+$). HRMS: calcd for $C_{10}H_{17}O_2$, $[M+H]^+$: 169.1223, found: 169.1221. Rf = 0.67 (Cy/AcOEt 9:1).

Compound 22

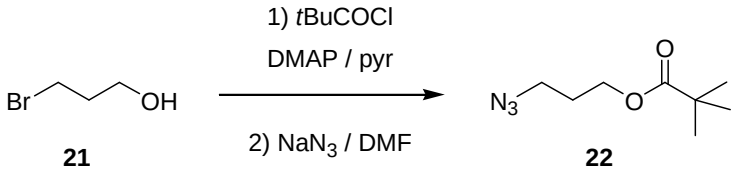

Pivaloyl chloride (2 mL, 16.7 mmol, 1.2 eq.) was added to a solution of alcohol **21** (2.0 g, 13.9 mmol, 1 eq.) and DMAP (0.24 g, 1.39 mmol, 0.1 eq.) in dry pyridine (10 mL) at 0°C. The mixture was then stirred for 15 hours at room temperature and a saturated aqueous NH_4Cl solution (50 mL) was added. The aqueous layer was extracted with CH_2Cl_2 (3x 50 mL). The combined organic layers were dried over $MgSO_4$, filtered and concentrated. The residue was used in the next step without further purification. The residue was diluted in dry DMF (10 mL) and NaN_3 (4.51 g, 69.5 mmol, 5eq.) was added. The resulting solution was stirred during two days at 60°C. The misture was cooled to room temperature and a saturated aqueous NH_4Cl solution (50 mL) was added. The aqueous layer was extracted with CH_2Cl_2 (3x 50 mL). The combined organic layers were dried over $MgSO_4$, filtered and concentrated. The residue was used in the next step without further purification. IR (neat): υ = 2100 (N_3). ^{1}H NMR (22°C, 400 MHz, $CDCl_3$) δ = 4.10 (t, *J* = 6.2 Hz, 2 H), 3.34 (t, *J* = 6.8 Hz, 2 H), 1.87 (m, 2 H), 1.15 (s, 9 H). ^{13}C NMR (22°C, 100 MHz, $CDCl_3$) δ = 178.4, 61.2, 48.3, 38.8, 28.2, 27.2.

Compound 3

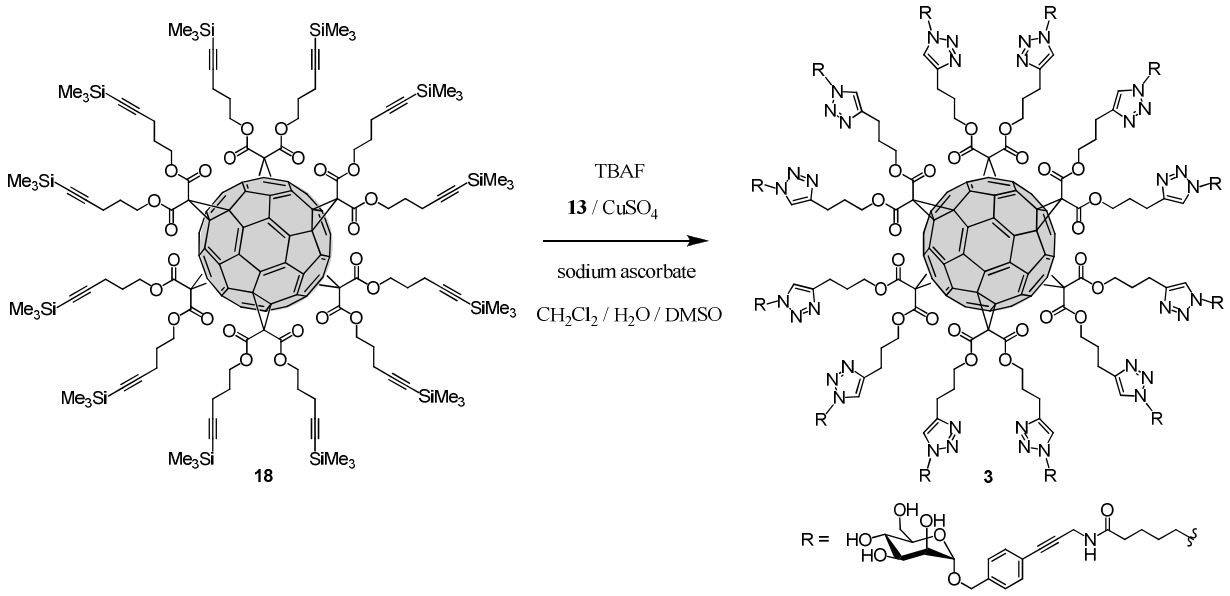

A 1 M solution of TBAF in THF (0.37 mL, 0.37 mmol) was added to a mixture of **18** (80 mg, 0.027 mmol), **13** (156 mg, 0.35 mmol), $CuSO_4.5H_2O$ (0.4 mg, 0.003 mmol) and sodium ascorbate (1.6 mg, 0.008 mmol) in CH_2Cl_2/MeOH/DMSO (1:1:1, 3 mL). The resulting mixture was stirred

at room temperature. After 24 h, methanol (10 mL) was added to the mixture and the resulting orange precipitate filtered, extensively washed with methanol then CH_2Cl_2 and dried under high vacuum to give **3** (172 mg, 86%) as a red solid. IR (neat): υ = 3385 (O-H), 2129 (C≡C), 1740 (C=O), 1648 (C=O). ^{1}H NMR (DMSO-d_6, 300 MHz): δ = 8.33 (*br* s, 12 H), 7.82 (*br* s, 12 H), 7.26-7.46 (m, 48 H), 4.40-4.80 (m, 84 H), 4.20-4.38 (m, 36 H), 4.04-4.16 (m, 24 H), 3.60-3.75 (m, 24 H), 3.47-3.57 (m, 24 H), 3.33-3.45 (m, 36 H), 2.55-2.75 (m, 24 H), 2.10-2.20 (m, 24 H), 1.88-2.00 (m, 24 H), 1.70-1.85 (m, 24 H), 1.40-1.55 (m, 24 H). ^{13}C NMR (DMSO-d_6, 100 MHz): δ = 171.5, 162.7, 145.6, 145.0, 140.7, 138.3, 131.2, 127.7, 121.7, 121.3, 99.1, 87.0, 81.4, 74.2, 71.0, 70.2, 68.8, 67.1, 67.0, 66.5, 61.2, 48.9, 45.6, 40.3, 34.3, 29.2, 28.5, 27.6, 22.0, 21.3.

Characterization of compound 3

As shown in Figures S1 and S2, the ^{13}C NMR spectrum of fullerene hexakis-adduct **3** is in full agreement with its *T*-symmetrical structure and shows the expected signals for the 6 equivalent malonate addends. Only 3 signals out of the 5 expected ones are however observed for the fullerene C atoms (δ = 68.8 for the sp3 C atom; 140.7 and 145.0 ppm for the sp2 C atoms). Indeed, these 3 signals are reminiscent of those of the three non-equivalent fullerene C atoms of the hexakis-adduct carrying achiral addends (overall T_h symmetry). No influence of the overall symmetry of **3** which is *T* could be deduced and the two pairs of diastereotopic sp2 C atoms are pseudo-equivalent. Similar observations have been reported for related C_{60} derivatives.[1] Mass spectra of **3** were recorded under different conditions (MALDI-TOF and ESMS). However, as reported for related fullerene-sugar conjugates,[1] high level of fragmentation prevented the observation of the expected molecular ion peak.

Fig. S1. ^{13}C NMR (top) and DEPT (bottom) spectra of compound **3** recorded in DMSO-d_6.

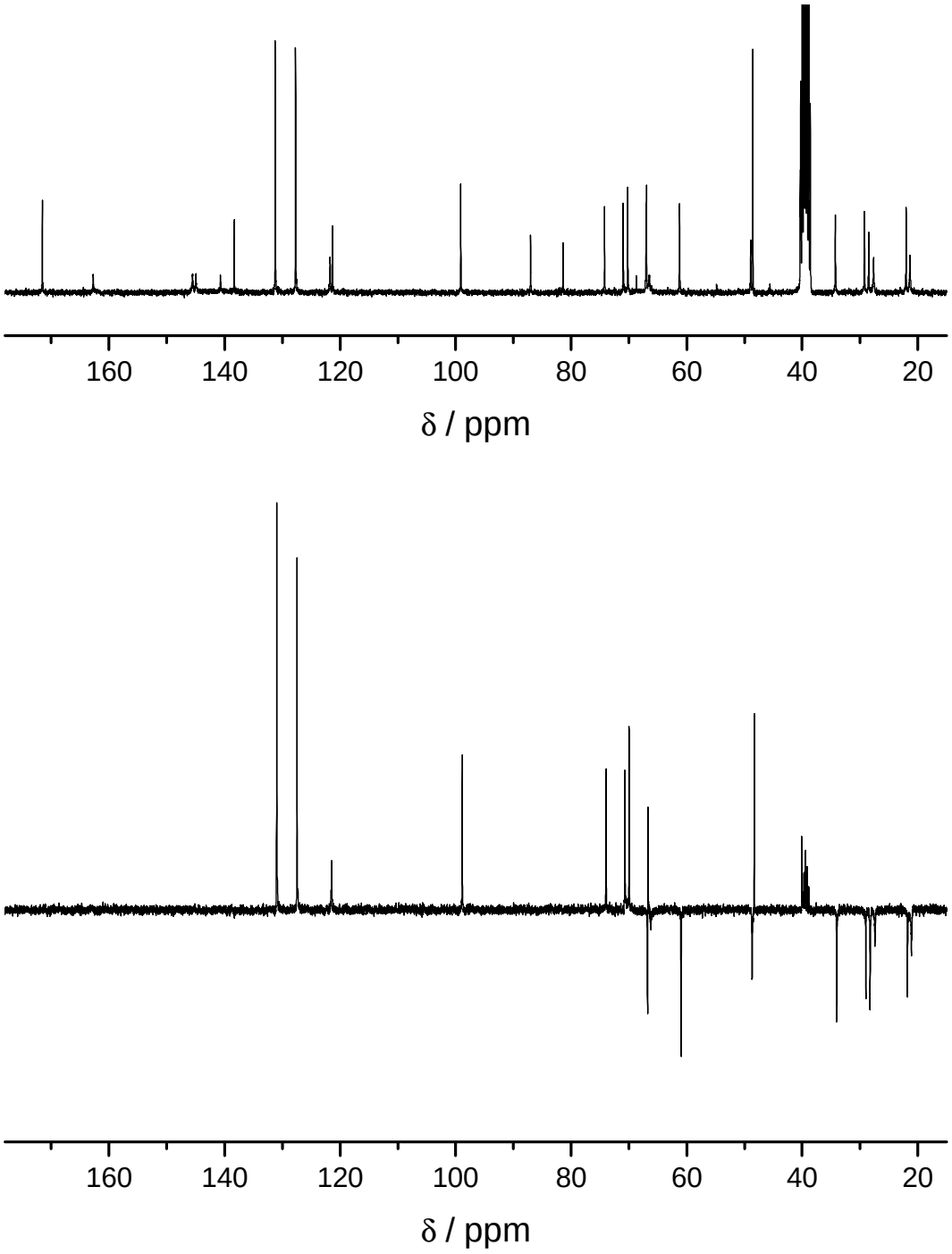

Fig. S2. ^{13}C NMR spectrum of compound **3** recorded in DMSO-d_6 (* = residual MeOH); unambiguous assignment was achieved with the help of the corresponding DEPT spectrum (see Fig. S1).

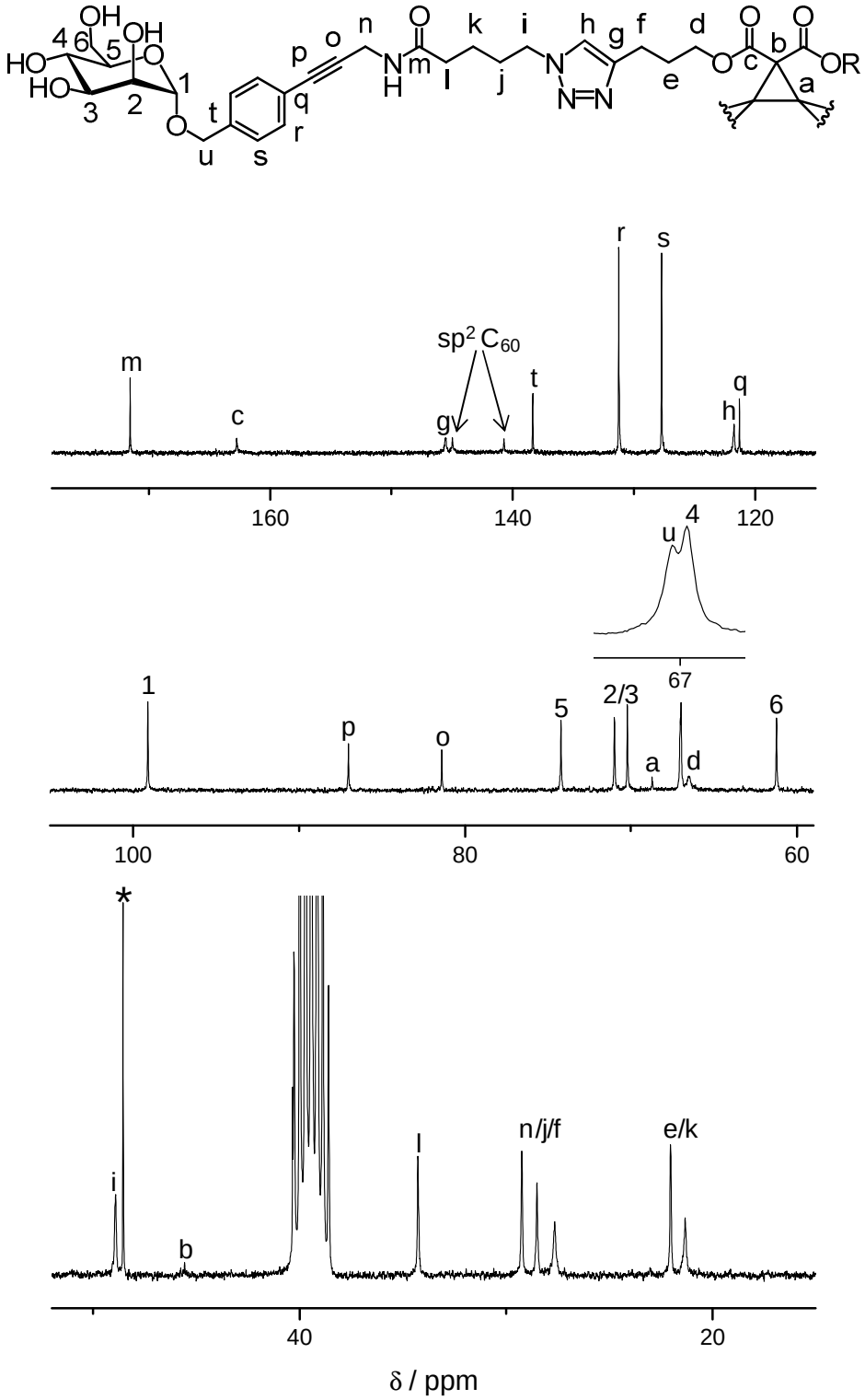

Fig. S3. ^{1}H NMR spectrum of compound **3** recorded in DMSO-d_6.

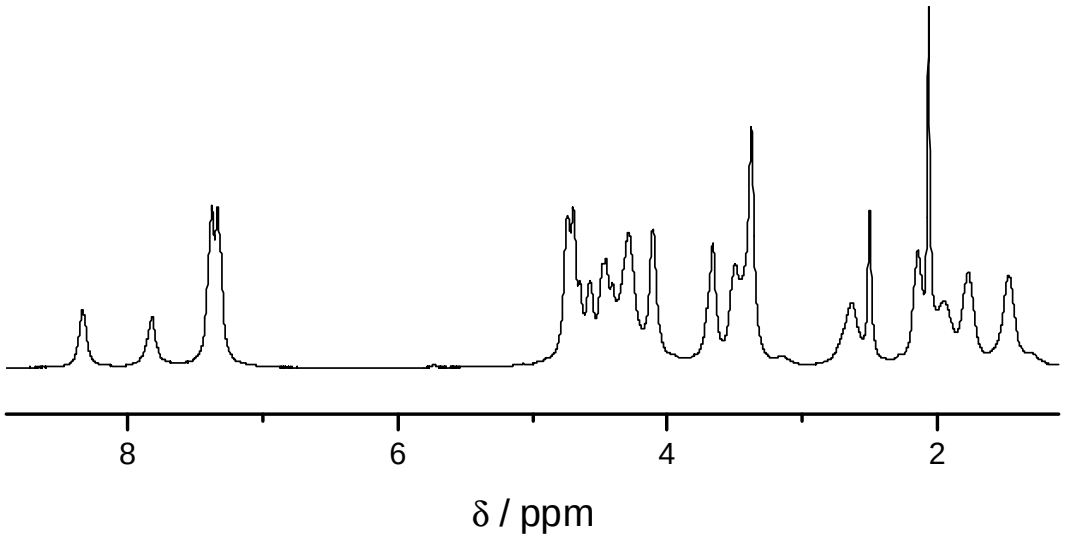

HAEMAGGLUTINATION INHIBITION ASSAYS

General method

Inhibition of haemagglutination by FimH, multivalently displayed as the fimbrial tip adhesin of type-1 fimbriated Eschrichia coli uropathogenic strains, allow a first biological evaluation of the multivalent character of the mannoside-functionalised fullerenes. Haemagglutination is observed as the red blood cells being held in suspension through the formation of a space-filling cross-linked network with the fimbriated bacteria.

The UTI89 clinical isolate engineered for continuous type-1 fimbriation was grown statically at 37ºC for 48 hours in LB medium and analyzed for haemagglutination of guinea pig red blood cells (Harlan Laboratories). Both bacteria and red blood cells (RBCs) were washed 3 times in ice-cold PBS (17mM K/NaH_2PO_4, 150mM NaCl). PBS was used for all dilutions. 96-well round-bottom microtiter plates were used for the dilutions.

The titer for agglutination was determined in a 2-fold dilution series in PBS of the bacteria in a volume of 25 μL. Well 1 is a negative control without bacteria but 25 μL PBS. 25 μL PBS and 50 μL 5% RBCs were added to a final 100 μL volume. Upon 1 hour at 4°C, the titer was determined as the lowest concentration of bacteria that led to haemagglutination.

A bacterial concentration of twice the determined haemagglutination titer was kept constant in the haemagglutination inhibition assays. First, a 2-fold dilution series of the inhibitory compounds was performed in 25 μL PBS with 10% DMSO. Instead, in well 1 only 25 μL PBS was added as a negative control. 25 μL of the bacterial solution and 50 μl of 5% red blood cells were added to reach a final volume of 100 μL. The plate was left at 4°C for 1 hour before read-out minimum inhibition concentration (MIC) is presented in table S1.

We observed that Fullerene **1** is not only inhibiting haemagglutination. It also shows clustering of the bacteria at the concentrations in wells 3 and 4, similarly this is observed for fullerene **3** in well 3.

Table S1: Inhibition of Haemagglutination.

Compound	Initial concentration of compound in well 2 (μM)	MIC (μM) (minimum concentration required for inhibition of haemagglutination)
4	1,611	100
1	434	3.4
5	1,700	6.6
2	394	1.5
12	1,889	29.4
3	333	10.4

ISOTHERMAL TITRATION CALORIMETRY

General method

A VP-ITC (Microcal Llc., Northampton, MA, USA) was operated at 22°C using 36 injections of 8 μL or 48 injections of 6 μL into the 1.458 mL cell. All titration were direct, where the compound was titrated into the FimH in solution in the cell, except for fullerene **3** where reverse titration was performed. Prior the ITC, FimH was dialyzed extensively against 20 mM HEPES pH 7,4 and 150 mM NaCl (buffer). The last dialysis exchange buffer was kept for dilution of the FimH and compound stock solutions, prepared into 5% DMSO. For the monomers **4, 5, 6** and **12**, intervals between injections were 300 secs, for the fullerenes **1, 2** and **3** intervals were at 600 secs.

The Origin program supplied by Microcal Inc. was used to fit the isotherm with the binding constant (Ka, M^{-1}), molar ratio (n) and enthalpies (cal/mole of injectant) using the model for one type of binding sites and the entropic contributions ($cal.mole^{-1}.°C^{-1}$) was derived from these fittings.

The monomers **4**, **5**, **6** and **12** were titrated at 120 to 140 μM concentrations into 15 to 20 μM FimH in the cell. Fullerenes **1** and **2** were used at 15 μM and 40 μM concentrations into 12,5 μM to 15 μM FimH in the cell in direct titrations. Direct titrations of **3** with the previous fullerene ITC conditions failed. Reverse titration of fullerene **3** at 1 μM in the cell with 10 μM FimH and including 5% DMSO led to a visible first binding phase indicating nanomolar affinity, whereas in 20% DMSO in the same buffer, 48 titrations of 6 μL of 36.2 μM FimH into 2 μM fullerene **3** clearly showed FimH-fullerene aggregation with a mid-point at half-occupation (n = 0.5) of fullerene **3**.

Fig. S4. **Titration of FimH with fullerene 1** in HEPES (20 mM, pH 7.4) and 150 mM NaCl with 5% DMSO (in cell: FimH @ 15 µM; in syringe: **1** @ 40 µM) Top: raw calorimetric data. Bottom: plot of the area under the peaks against the molar ratio of **1** to FimH (black squares) and the best fit (solid line).

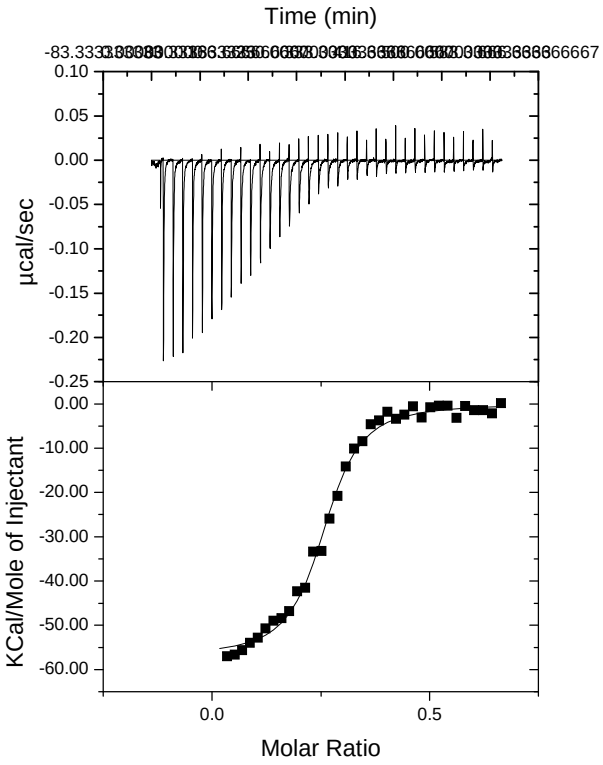

Fig. S5. **Titration of FimH with fullerene 2** in HEPES (20 mM, pH 7.4) and 150 mM NaCl with 5% DMSO (in cell: FimH @ 12.5 µM; in syringe: **2** @ 25 µM) Top: raw calorimetric data. Bottom: plot of the area under the peaks against the molar ratio of **2** to FimH (black squares) and the best fit (solid line).

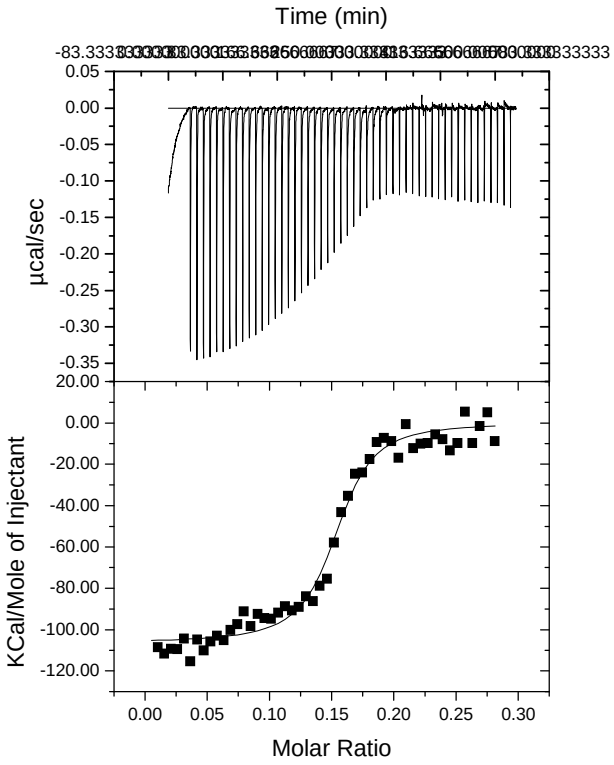

Fig. S6. **Titration of fullerene 3 with FimH** in HEPES (20 mM, pH 7.4) and 150 mM NaCl with 5% DMSO (in cell: **3** @ 1 µM; in syringe: FimH @ 10 µM) Top: raw calorimetric data. Bottom: plot of the area under the peaks against the molar ratio of FimH to **3** (black squares).

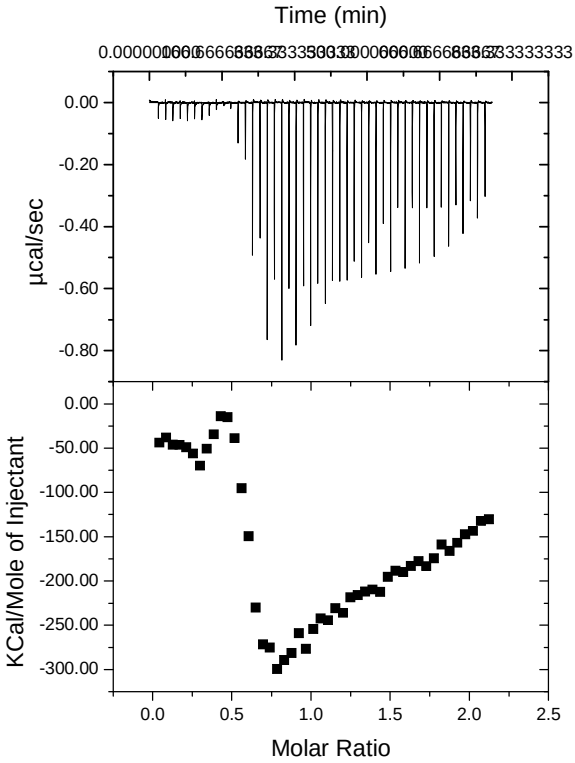

Fig. S7. **Titration of fullerene 3 with FimH** in HEPES (20 mM, pH 7.4) and 150 mM NaCl with 20% DMSO (in cell: **3** @ 2 µM; in syringe: FimH @ 32.6 µM) Top: raw calorimetric data. Bottom: plot of the area under the peaks against the molar ratio of FimH to **3** (black squares) and the best fit (solid line).

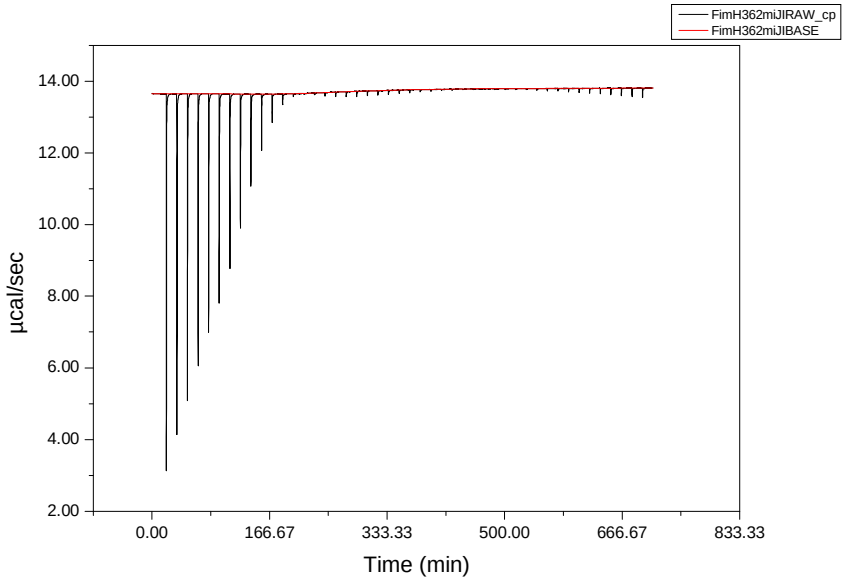

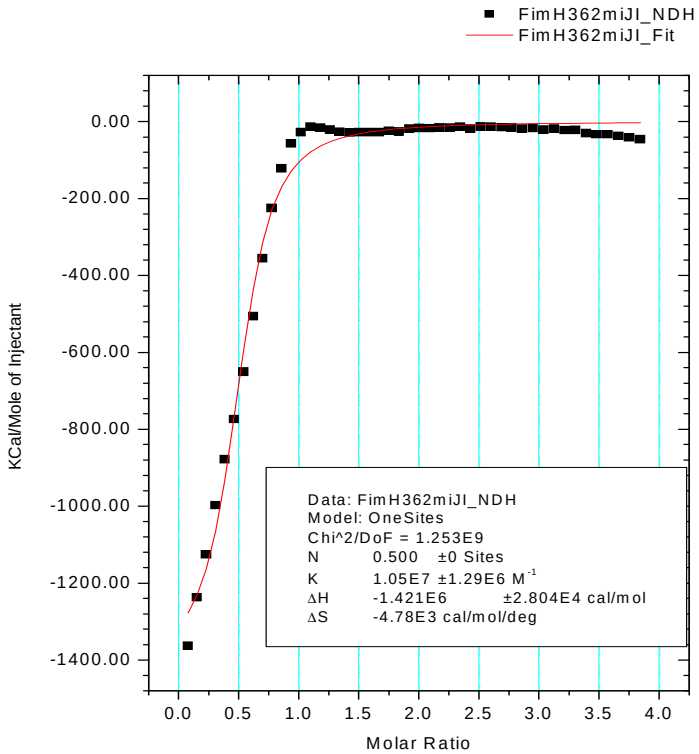

Fig. S8. **Titration of FimH with monomer 4** in HEPES (20 mM, pH 7.4) and 150 mM NaCl with 5% DMSO (in cell: FimH @ 20 µM; in syringe: **4** @ 120 µM) Top: raw calorimetric data. Bottom: plot of the area under the peaks against the molar ratio of **4** to FimH (black squares) and the best fit (solid line).

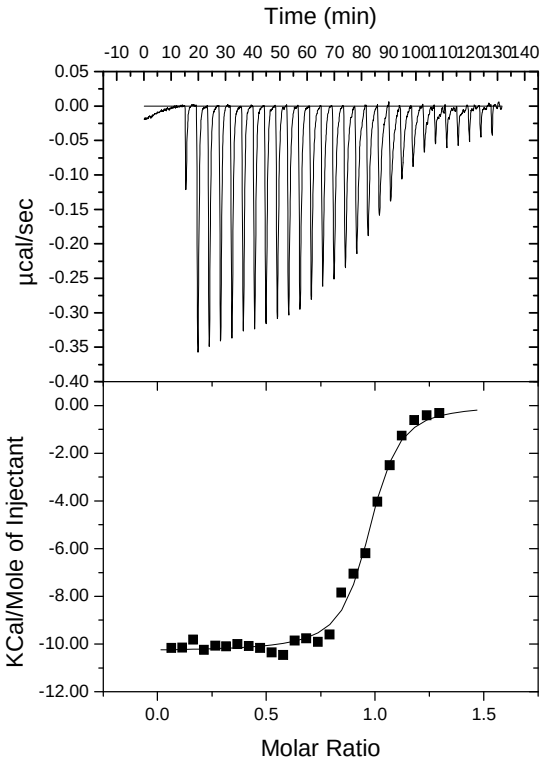

Fig. S9. **Titration of FimH with monomer 5** in HEPES (20 mM, pH 7.4) and 150 mM NaCl with 5% DMSO (in cell: FimH @ 20 µM; in syringe: **5** @ 120 µM) Top: raw calorimetric data. Bottom: plot of the area under the peaks against the molar ratio of **4** to FimH (black squares) and the best fit (solid line).

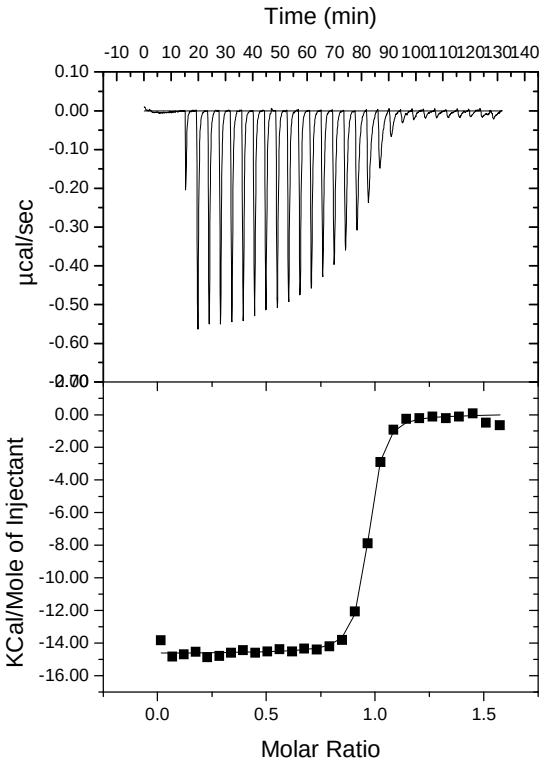

Fig. S10. **Titration of FimH with monomer 6** in HEPES (20 mM, pH 7.4) and 150 mM NaCl with 5% DMSO (in cell: FimH @ 15 µM; in syringe: **6** @ 140 µM) Top: raw calorimetric data. Bottom: plot of the area under the peaks against the molar ratio of **6** to FimH (black squares) and the best fit (solid line).

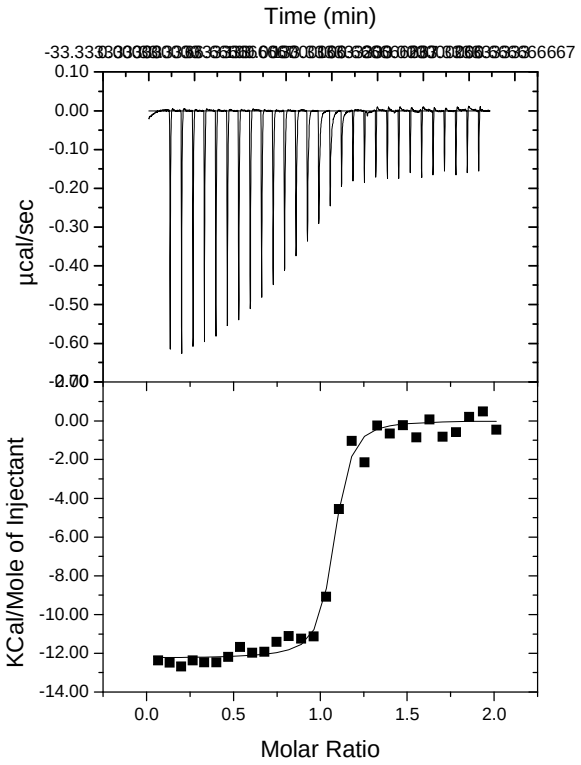

Fig. S11. **Titration of FimH with monomer 12** in HEPES (20 mM, pH 7.4) and 150 mM NaCl with 5% DMSO (in cell: FimH @ 20 µM; in syringe: **12** @ 120 µM) Top: raw calometric data. Bottom: plot of the area under the peaks against the molar ratio of **12** to FimH (black squares) and the best fit (solid line).

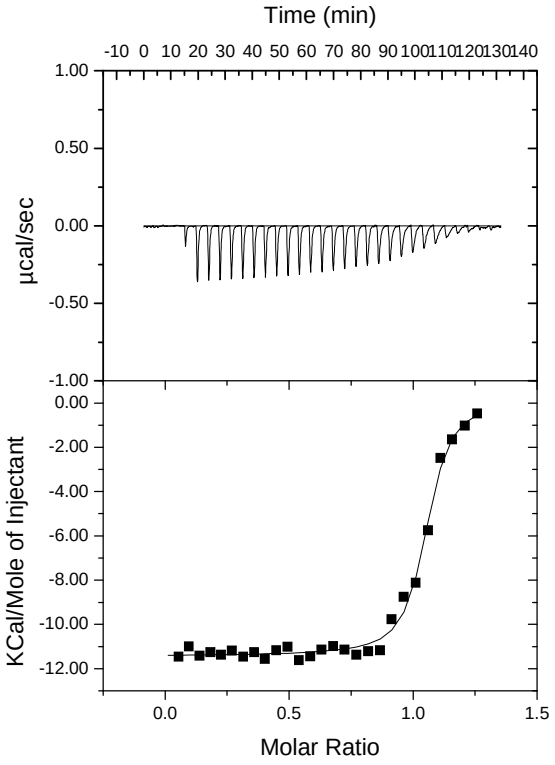

SURFACE PLAMON RESONANCE

General method

The lectin domain of FimH was expressed as described previously and purified at pH 4.0 in 50 mM HCOOH on a SPFF (sulfopropyl fast flow) ion exchange column (GE Healthcare). A CM5 sensor chip (Biacore, GE Healthcare) has been coated with a layer of amino-functionalized monovalent heptyl mannoside to 60 RU (response units) and the kinetics of FimH binding to the sensor chip has been determined. All data collections were performed in HBS buffer complemented with 3 mM EDTA and 0.01% Tween20. Regeneration was done with a single 10 s injection of 50-100 mM NaOH in water.

A solution affinity inhibition experiment was set up as follows: a constant FimH concentration (concentration B, a parameter that is fitted in the solution affinity equation) was inhibited with a series of 24 increasing concentrations (0 – 750 nM) of the compound (concentrations A, a variable in the solution affinity equation). The kinetic constants, k_a and k_d, and R_{max}, derived from the prior experiment, were kept constant to determine the non-inhibited FimH concentrations that displayed binding to the heptyl mannoside on the chip.

The solution affinity provided by the Biacore software using the equation:

$$(B-A-Kd)/2+(0.25*(A+B+Kd)\text{^}2-A*B)\text{^}0.5$$

with B presenting the uninhibited concentration of FimH, and A the variable compound concentration.
The lowest chi^2 for fitting this equation was calculated as a function of the functional valency n of the compound, by multiplying the molar concentration of the fullerene by $n > 1$.

Fig. S12. (A) SPR raw data for fullerene **1 (**Chi^2 = 0.761); (B) Inhibition curve without the fitting for the multivalency (n = 1) for fullerene **1**; (C) Chi^2 = f(n) for fullerene **1**; (D) Inhibition curve with the fitting for the multivalency (n = 3.4) of fullerene **1** (see Table S2).

(A)

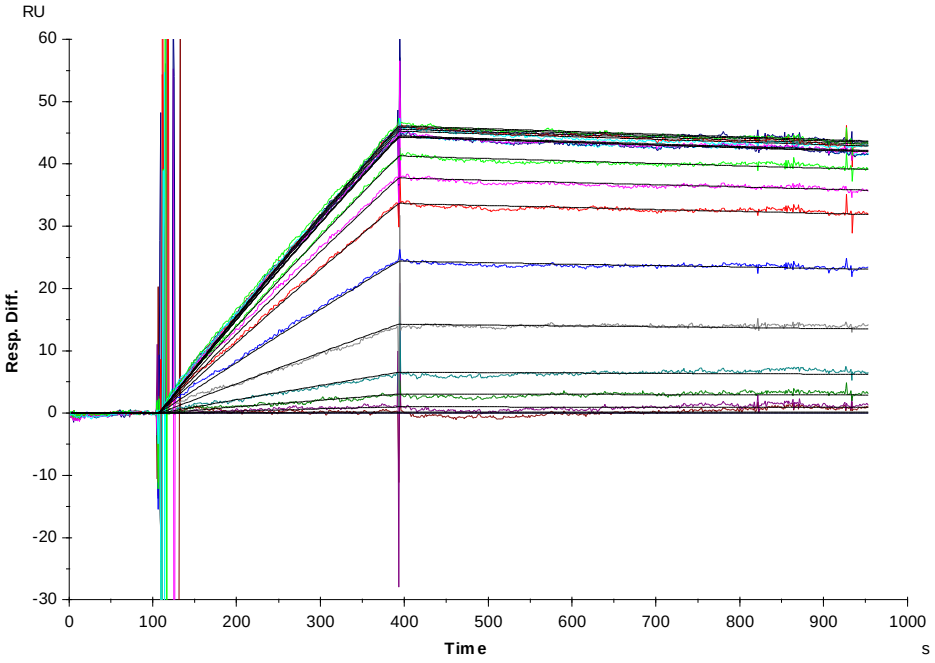

(B)

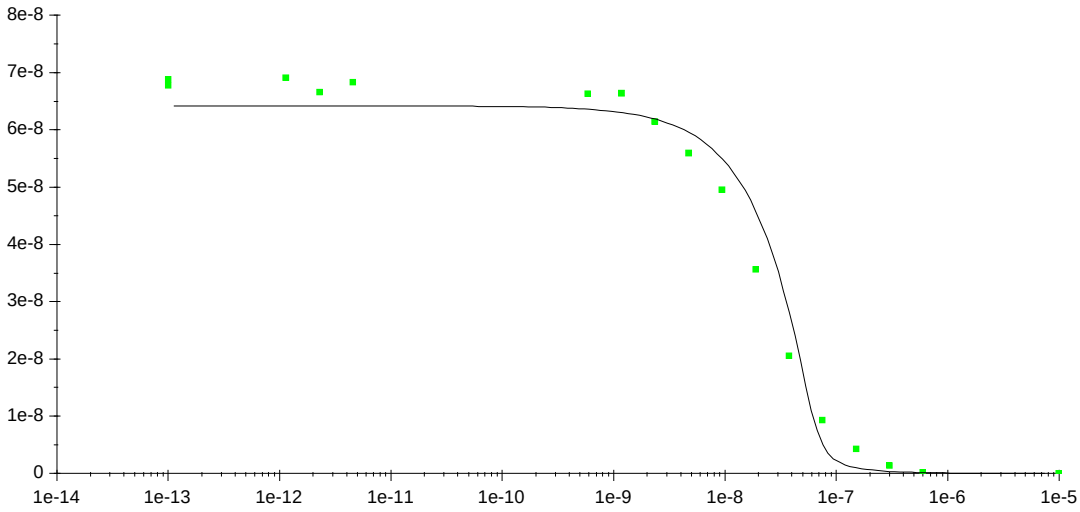

(C)

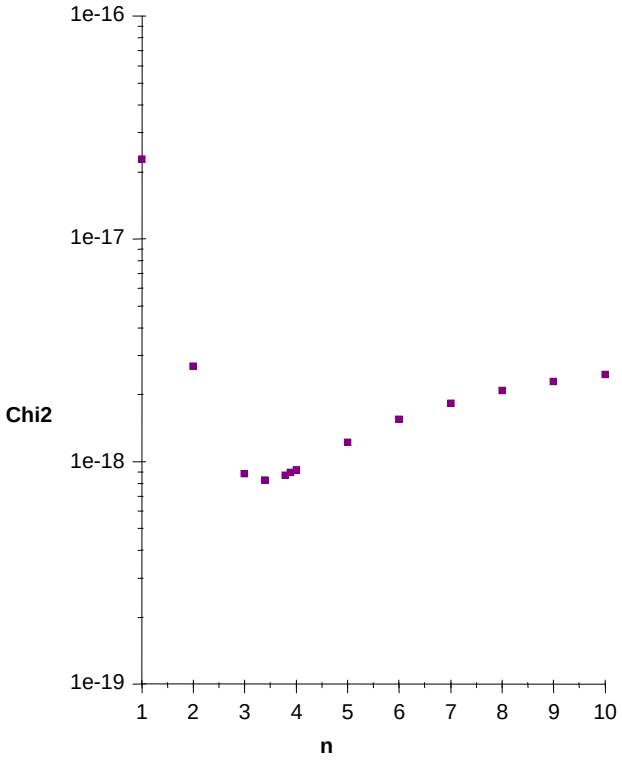
1e-16
1e-17
1e-18
1e-19
Chi2
1
2
3
4
5
6
7
8
9
10
n

(D)

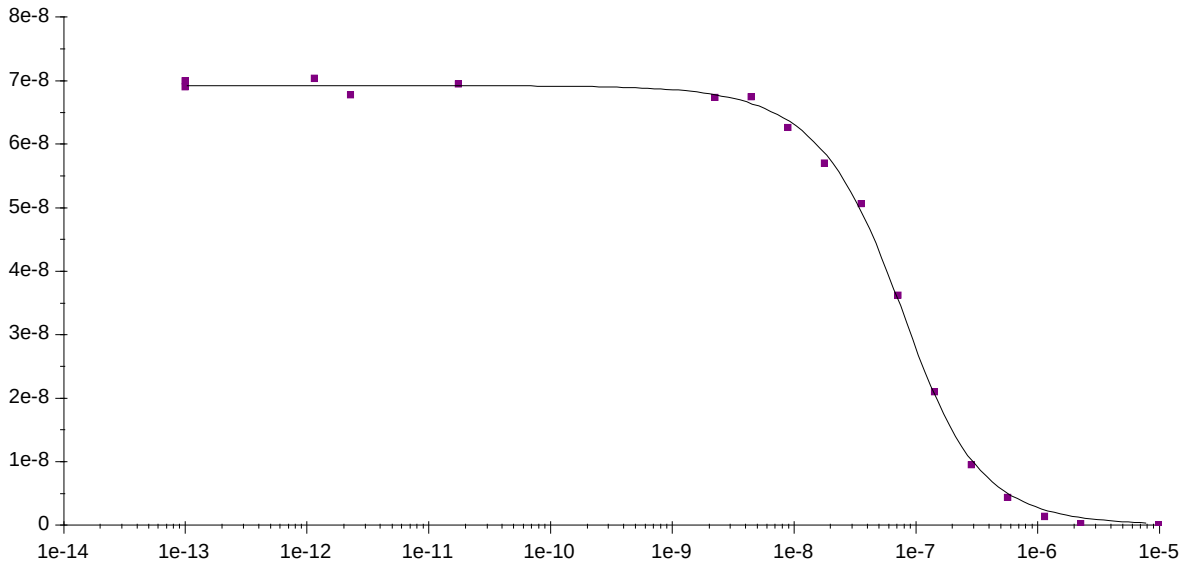
8e-8
7e-8
6e-8
5e-8
4e-8
3e-8
2e-8
1e-8
0
1e-14
1e-13
1e-12
1e-11
1e-10
1e-9
1e-8
1e-7
1e-6
1e-5

Table S2: Parameters K_a, K_d, B (uninhibited concentration of FimH) and their standard error SE, to search the lowest chi^2 for the fitting in function of functional valency n of fullerene **1**.

n	KA(1/M)	KD(M)	Initial Conc B	Chi^2	KD	SE(KD)	B	SE(B)
1	7,30E+08	1,37E-09	6,42E-08	2,27E-17	1,37E-09	1,63E-09	6,42E-08	1,42E-09
2	8,84E+07	1,13E-08	6,71E-08	2,68E-18	1,13E-08	1,49E-09	6,71E-08	5,06E-10
3	3,76E+07	2,66E-08	6,78E-08	8,83E-19	2,66E-08	1,43E-09	6,78E-08	3,01E-10
3.4	**3,01E+07**	**3,32E-08**	**6,79E-08**	**8,22E-19**	**3,32E-08**	**1,61E-09**	**6,79E-08**	**2,94E-10**
3.8	2,50E+07	4,00E-08	6,81E-08	8,71E-19	4,00E-08	1,88E-09	6,81E-08	3,04E-10
3.9	2,40E+07	4,17E-08	6,81E-08	8,92E-19	4,17E-08	1,96E-09	6,81E-08	3,09E-10
4	2,30E+07	4,34E-08	6,81E-08	9,16E-19	4,34E-08	2,04E-09	6,81E-08	3,13E-10
5	1,64E+07	6,08E-08	6,83E-08	1,22E-18	6,08E-08	3,04E-09	6,83E-08	3,67E-10
6	1,27E+07	7,86E-08	6,84E-08	1,55E-18	7,86E-08	4,17E-09	6,84E-08	4,16E-10
7	1,04E+07	9,65E-08	6,85E-08	1,83E-18	9,65E-08	5,37E-09	6,85E-08	4,56E-10
8	8,73E+06	1,15E-07	6,85E-08	2,08E-18	1,15E-07	6,59E-09	6,85E-08	4,88E-10
9	7,54E+06	1,33E-07	6,85E-08	2,28E-18	1,33E-07	7,83E-09	6,85E-08	5,13E-10
10	6,63E+06	1,51E-07	6,86E-08	2,46E-18	1,51E-07	9,08E-09	6,86E-08	5,35E-10

Fig. S13. (A) SPR raw data for fullerene **2** (Chi^2 = 0.237); (B) Chi^2 = f(n) for fullerene **2**. (C) Inhibition curve with the fitting for the multivalency (n = 6.5) of fullerene **2**.

(A)

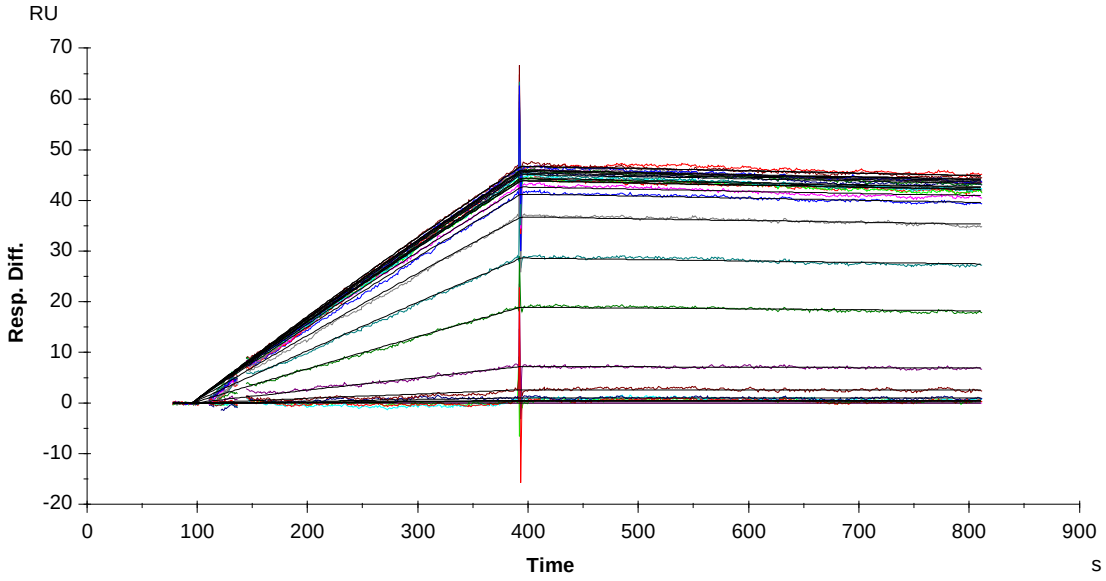

(B)

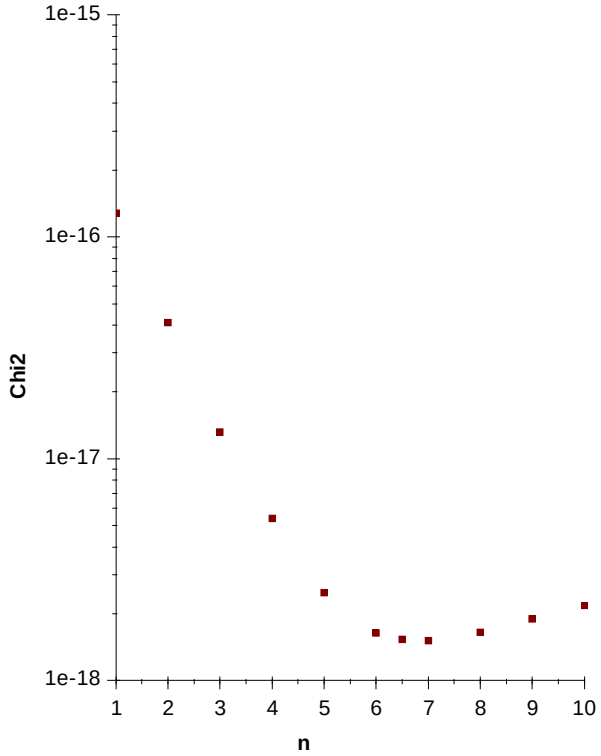

(C)

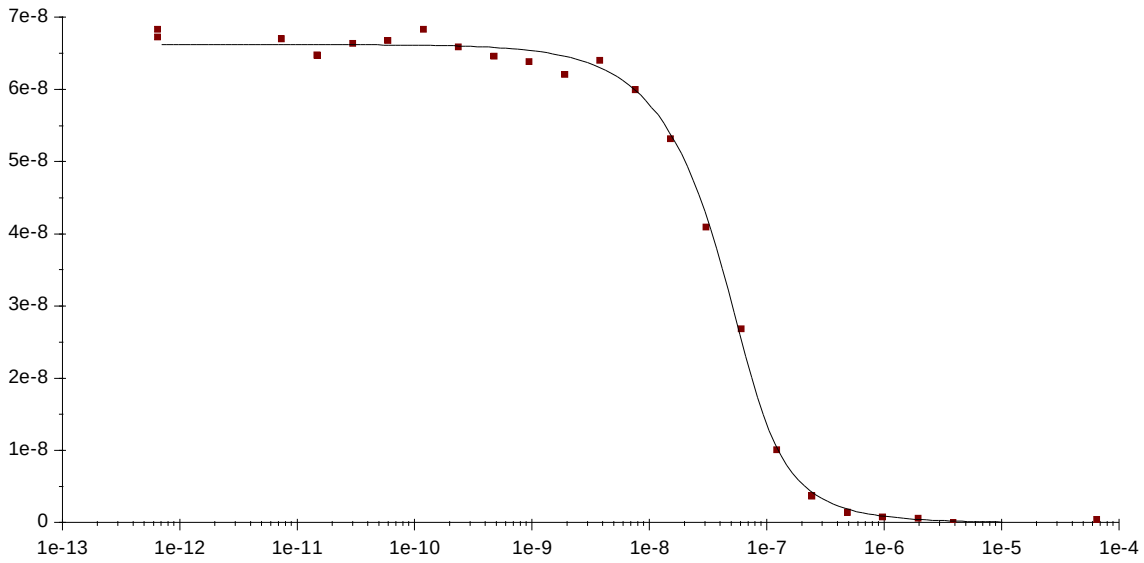

Table S3: Parameters K_a, K_d, B (uninhibited concentration of FimH) and their standard error SE, to search the lowest chi^2 for the fitting in function of functional valency n of fullerene **2**.

n	KA(1/M)	KD(M)	Initial Conc B	Chi2	KD	SE(KD)	B	SE(B)
1	7,52E+09	1,33E-10	5,88E-08	1,28E-16	1,33E-10	1,45E-09	5,88E-08	2,67E-09
2	9,90E+10	1,01E-11	6,21E-08	4,11E-17	1,01E-11	6,44E-10	6,21E-08	1,56E-09
3	4,46E+09	2,24E-10	6,41E-08	1,32E-17	2,24E-10	6,98E-10	6,41E-08	9,20E-10
4	4,08E+08	2,45E-09	6,51E-08	5,37E-18	2,45E-09	9,92E-10	6,51E-08	5,98E-10
5	1,77E+08	5,64E-09	6,57E-08	2,49E-18	5,64E-09	1,02E-09	6,57E-08	4,17E-10
6	1,01E+08	9,93E-09	6,60E-08	1,64E-18	9,93E-09	1,09E-09	6,60E-08	3,44E-10
6,5	8,14e7	1,23e-8	6,62e-8	1,53E-18	1,23E-08	1,18E-09	6,62E-08	3,34E-10
7	**6,78E+07**	**1,48E-08**	**6,63E-08**	**1,51E-18**	**1,48E-08**	**1,30E-09**	**6,63E-08**	**3,34E-10**
8	5,03E+07	1,99E-08	6,64E-08	1,65E-18	1,99E-08	1,62E-09	6,64E-08	3,53E-10
9	3,96E+07	2,52E-08	6,65E-08	1,90E-18	2,52E-08	2,02E-09	6,65E-08	3,81E-10
10	3,25E+07	3,08E-08	6,66E-08	2,18E-18	3,08E-08	2,47E-09	6,66E-08	4,12E-10

Fig. S14. (A) SPR raw data for fullerene **3** (Chi^2 = 0.197); (B) Inhibition curve without the fitting for the multivalency (n = 1) for fullerene **3**; (C) Chi^2 = f(n) for fullerene **1**; (D) Inhibition curve with the fitting for the multivalency (n = 6.5) of fullerene **3** (see Table S4).

(A)

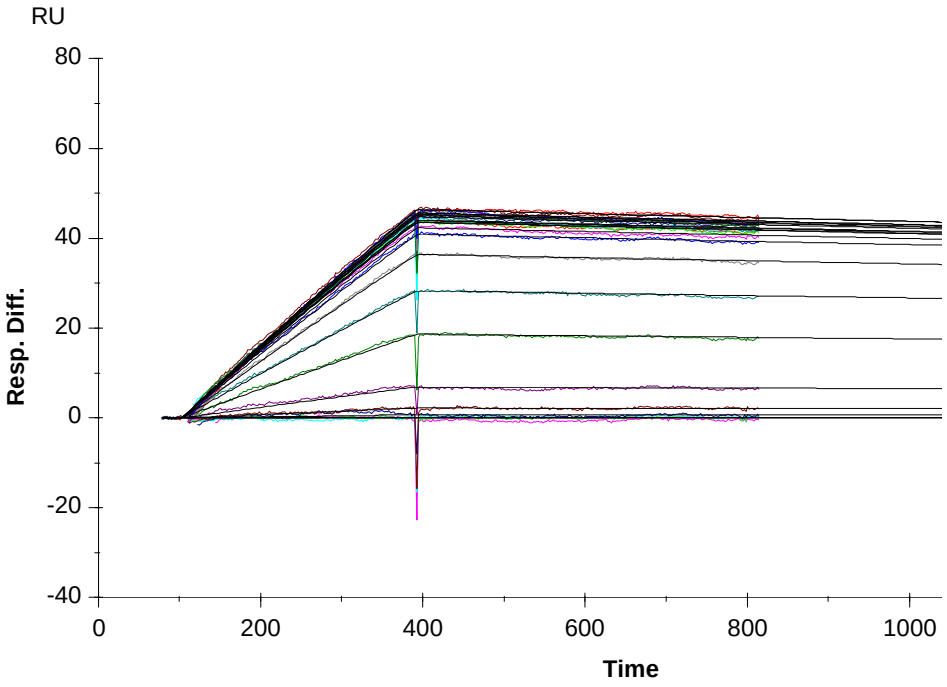

(B)

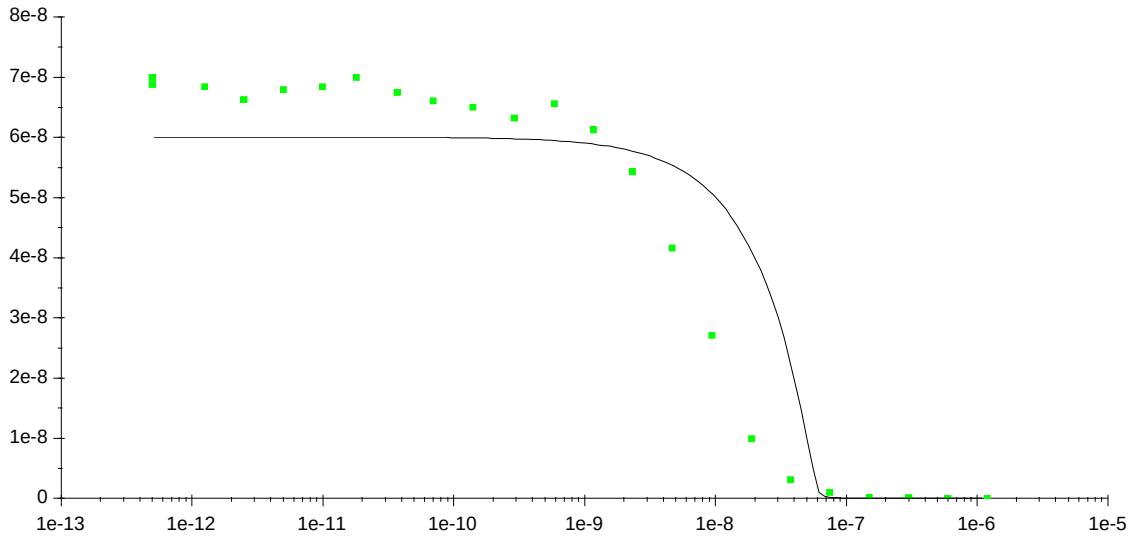

(C)

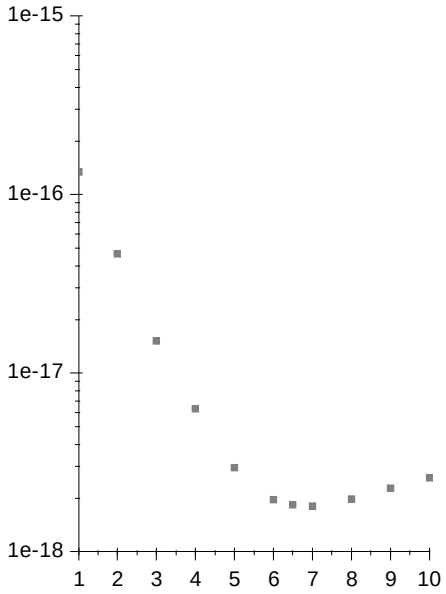

(D)

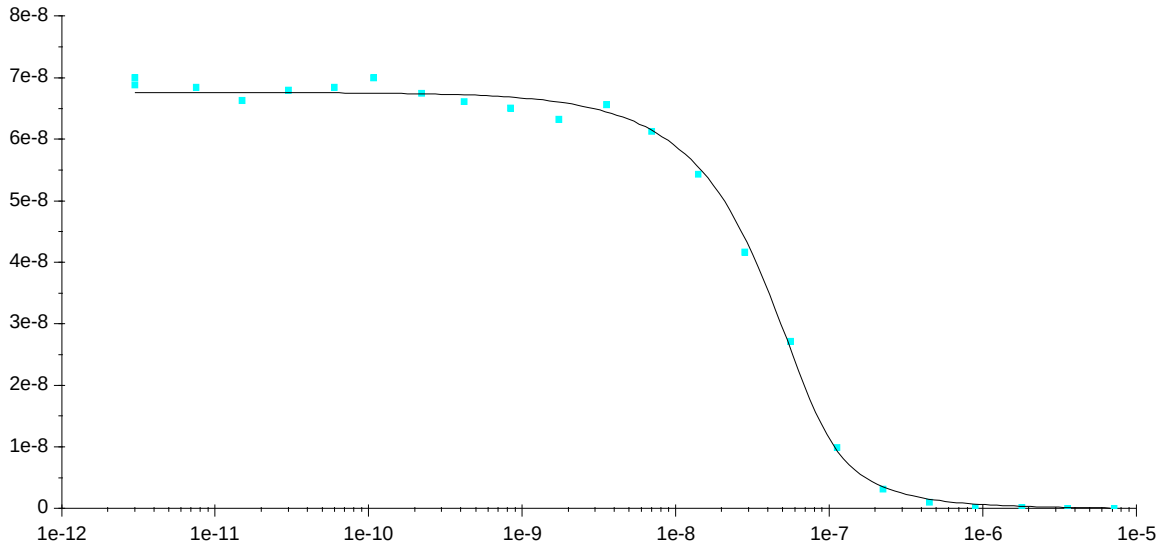

Table S4: Parameters K_a, K_d, B (uninhibited concentration of FimH) and their standard error SE, to search the lowest chi^2 for the fitting in function of functional valency n of fullerene **3**.

n	KA(1/M)	KD(M)	Initial Conc B	Chi_2	KD	SE(KD)	B	SE(B)
1	2,12E+10	4,71E-11	6,01E-08	1,34E-16	4,71E-11	2,70E-09	6,01E-08	2,75E-09
2	1,99E+11	5,02E-12	6,34E-08	4,68E-17	5,02E-12	5,86E-10	6,34E-08	1,66E-09
3	1,02E+12	9,76E-13	6,55E-08	1,52E-17	9,76E-13	6,36E-10	6,55E-08	9,84E-10
4	4,95E+08	2,02E-09	6,65E-08	6,34E-18	2,02E-09	9,69E-10	6,65E-08	6,47E-10
5	2,07E+08	4,84E-09	6,72E-08	2,95E-18	4,84E-09	1,02E-09	6,72E-08	4,53E-10
6	1,13E+08	8,87E-09	6,76E-08	1,96E-18	8,87E-09	1,11E-09	6,76E-08	3,76E-10
6,5	8,99E+07	1,11E-08	6,77E-08	1,83E-18	1,11E-08	1,21E-09	6,77E-08	3,65E-10
7	**7,42E+07**	**1,35E-08**	**6,78E-08**	**1,81E-18**	**1,35E-08**	**1,33E-09**	**6,78E-08**	**3,65E-10**
8	5,43E+07	1,84E-08	6,80E-08	1,98E-18	1,84E-08	1,67E-09	6,80E-08	3,85E-10
9	4,24E+07	2,36E-08	6,81E-08	2,27E-18	2,36E-08	2,08E-09	6,81E-08	4,16E-10
10	3,46E+07	2,89E-08	6,82E-08	2,60E-18	2,89E-08	2,55E-09	6,82E-08	4,48E-10

Fig. S15. (A) SPR raw data for the monomere **4** (Chi^2 = 0.2); (B) Inhibition curve of compound **4** (with the fitting n = 1).

(A)

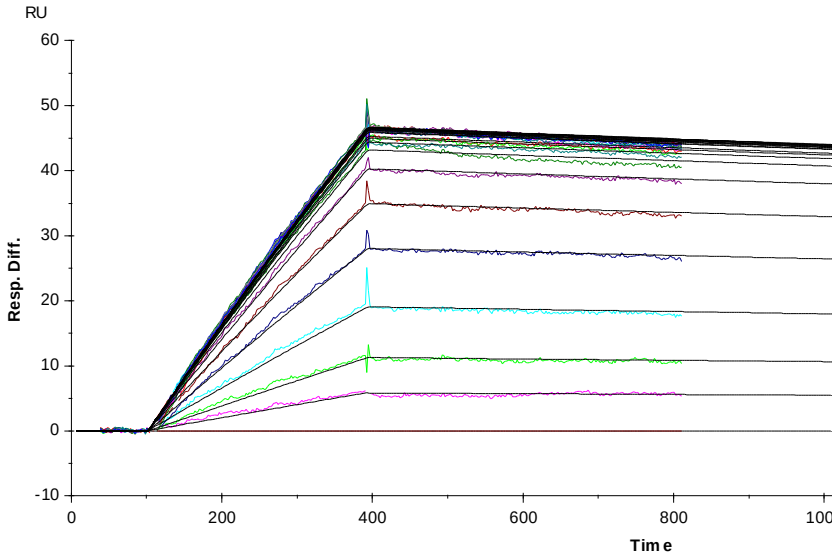

(B)

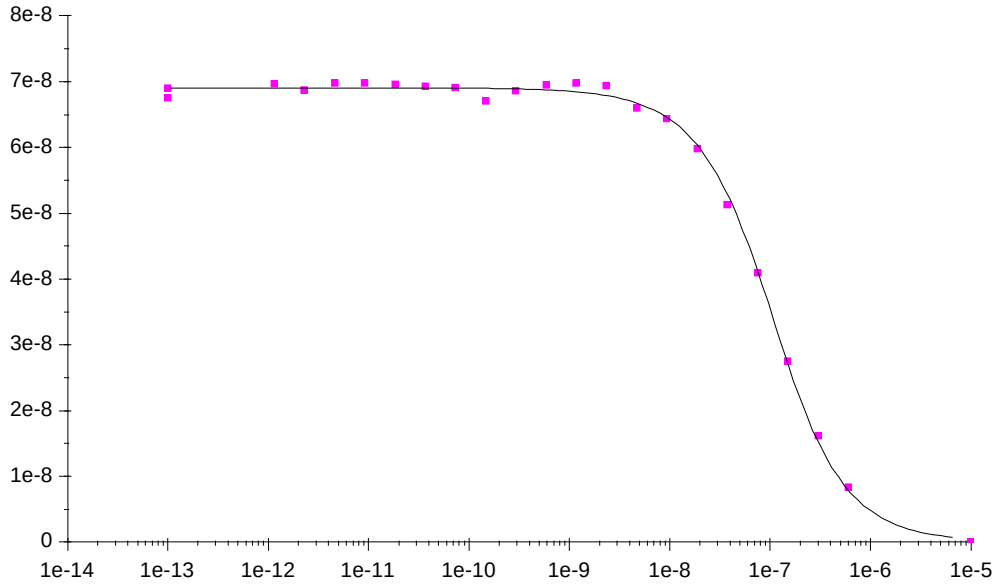

Fig. S16. (A) SPR raw data for monomere **5** (Chi^2 =0.169); (B) Inhibition curve of compound **5** (with the fitting n = 1).

(A)

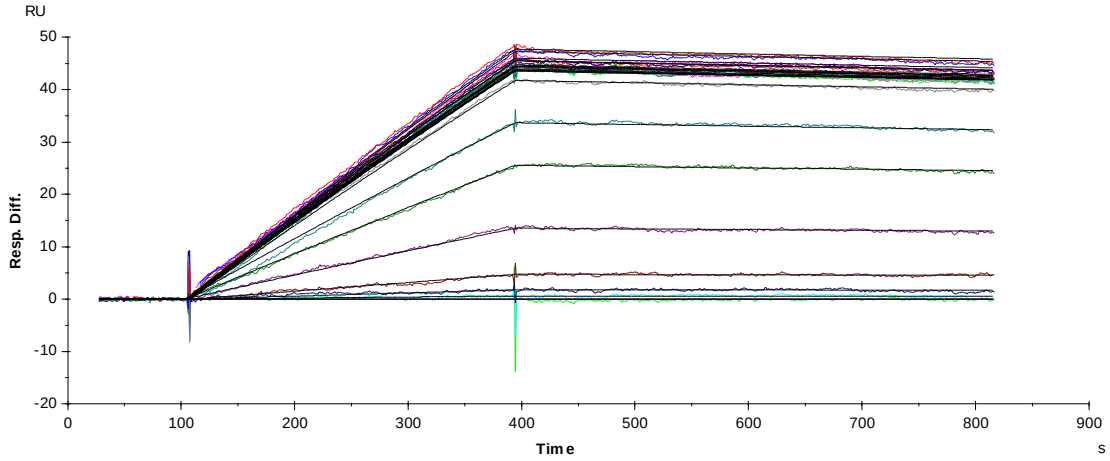

(B)

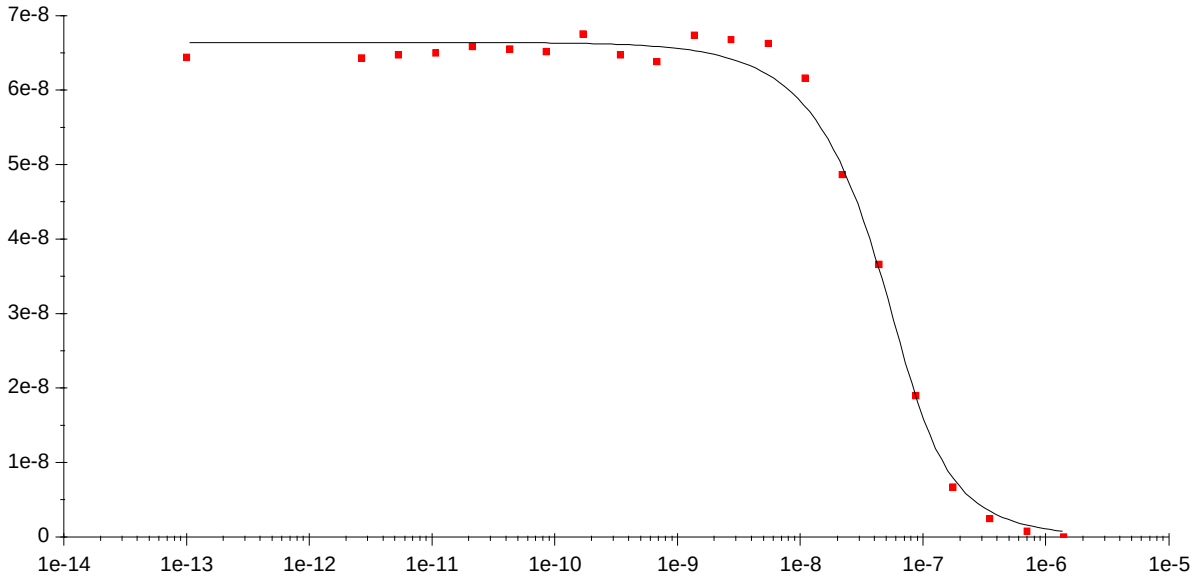

Fig. S17. (A) SPR raw data for monomere **6** (Chi^2 = 0.616); (B) Inhibition curve of compound **6** (with the fitting n = 1).

(A)

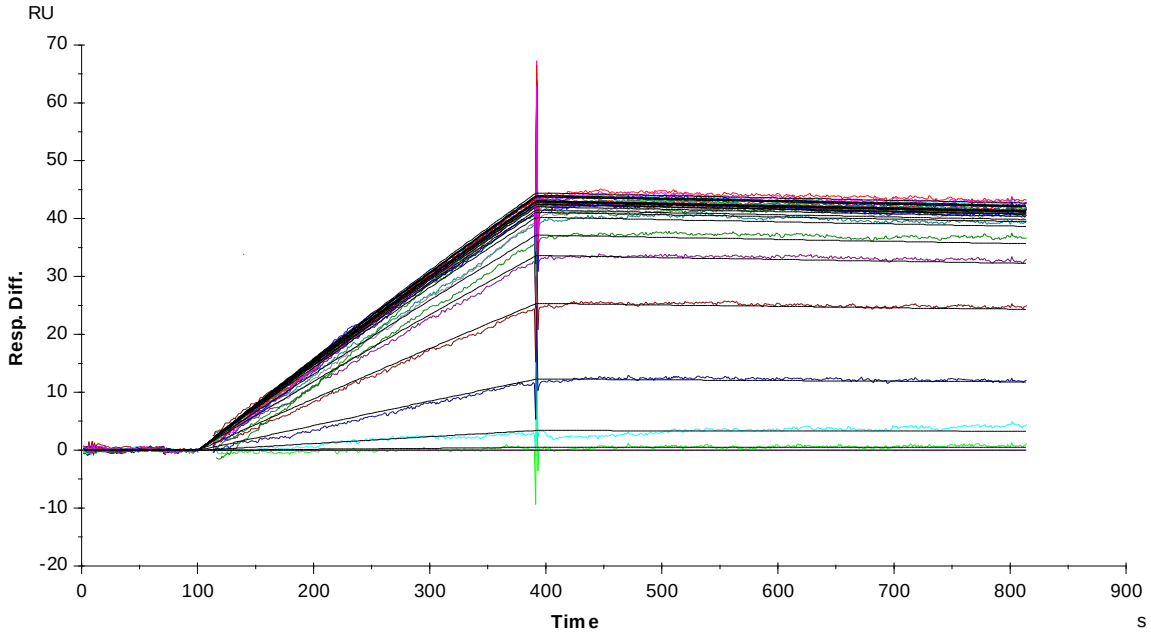

(B)

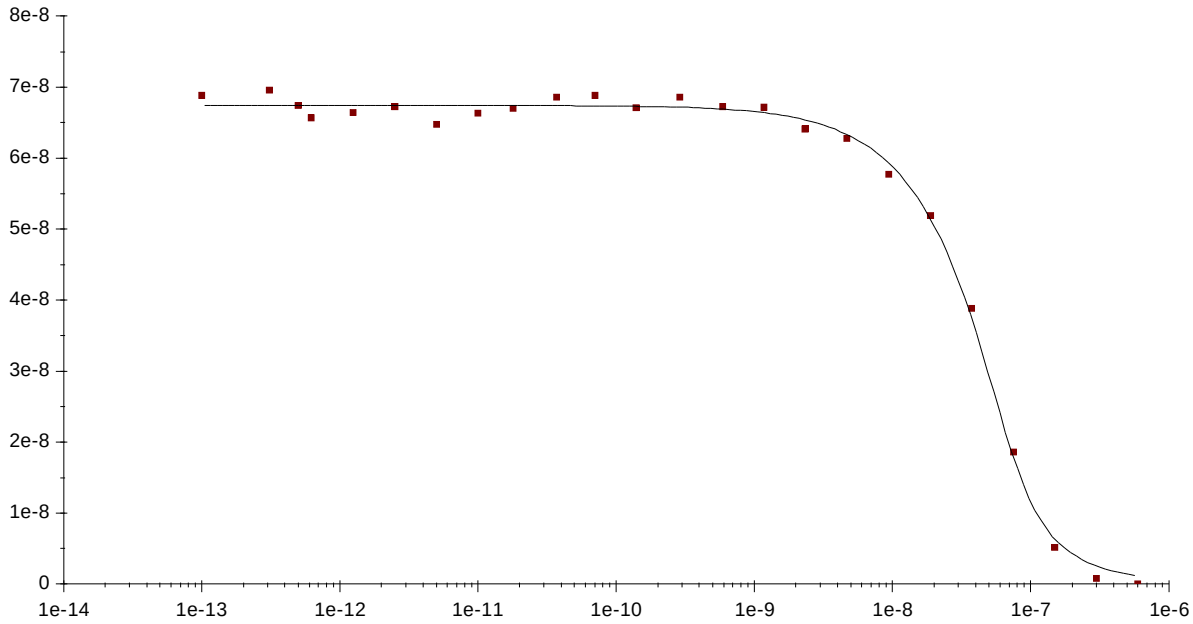

Fig. S18. (A) SPR raw data for monomere **12** (Chi^2 = 0.239); (B) Inhibition curve of compound **12** (with the fitting n = 1).

(A)

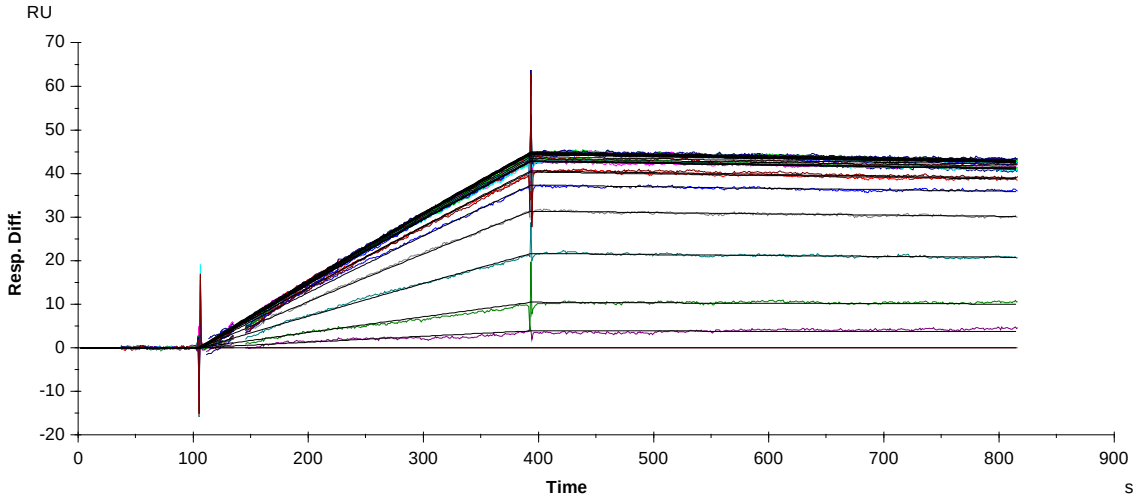

(B)

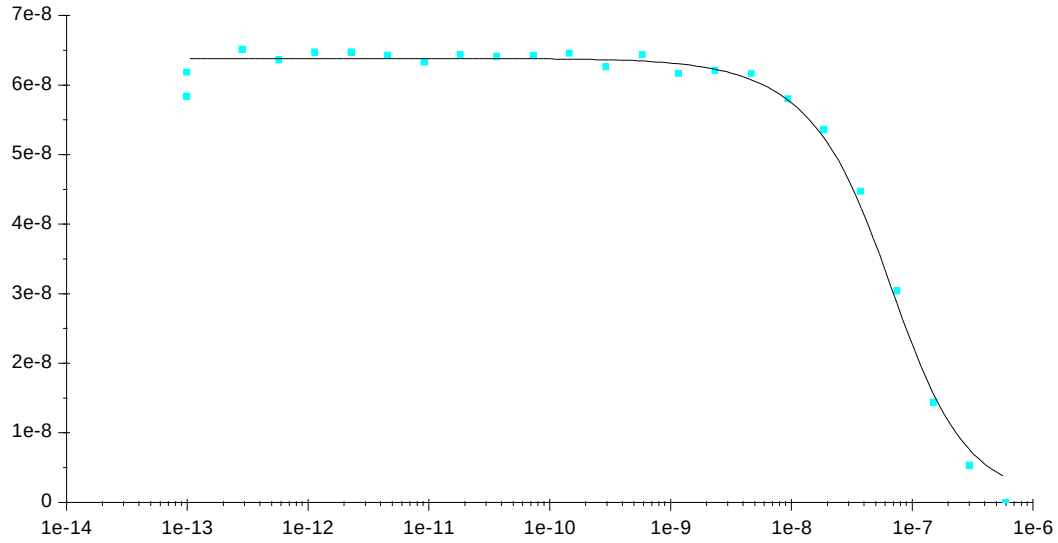

Table S5: Parameters K_a, K_d, B and their standard error SE, measured for monomer **4** (n = 1).

n	KA(1/M)	KD(M)	Initial Conc B	Chi^2	KD	SE(KD)	B	SE(B)
1	1,43e7	7e-8	6,91e-8	8,23E-19	7,00E-08	2,70E-09	6,91E-08	2,24E-10

Table S6: Parameters K_a, K_d, B and their standard error SE, measured for monomer **5** (n = 1).

n	KA(1/M)	KD(M)	Initial Conc B	Chi^2	KD	SE(KD)	B	SE(B)
1	9,35e7	1,07e-8	6,62e-8	3,30E-18	1,07E-08	1,60E-09	6,62E-08	4,78E-10

Table S7: Parameters K_a, K_d, B and their standard error SE, measured for monomer **6** (n = 1).

n	KA(1/M)	KD(M)	Initial Conc B	Chi^2	KD	SE(KD)	B	SE(B)
1	1,08e8	9.25e-9	6,74e-8	1,74E-18	9,25E-09	1,05E-09	6,74E-08	3,07E-10

Table S8: Parameters K_a, K_d, B and their standard error SE, measured for monomer **12** (n = 1).

n	KA(1/M)	KD(M)	Initial Conc B	Chi^2	KD	SE(KD)	B	SE(B)
1	3,04e7	3,29e-8	6,38e-8	3,23E-18	3,29E-08	3,20E-09	6,38E-08	4,22E-10

NMR DATA

Compound 4

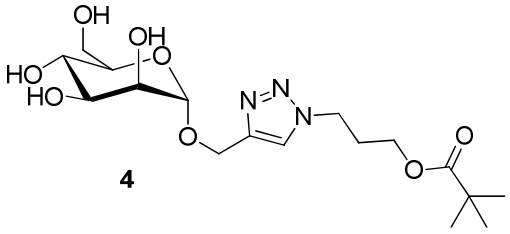

4

^{1}H NMR (400 MHz, D_2O)

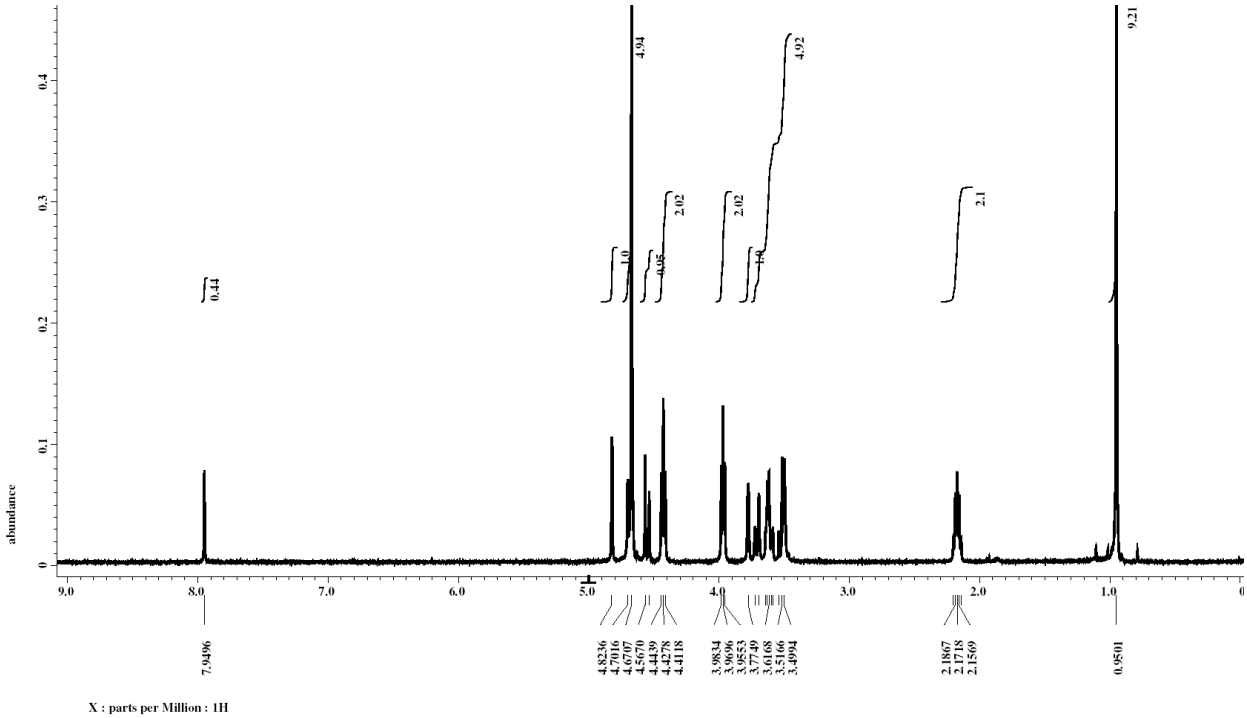

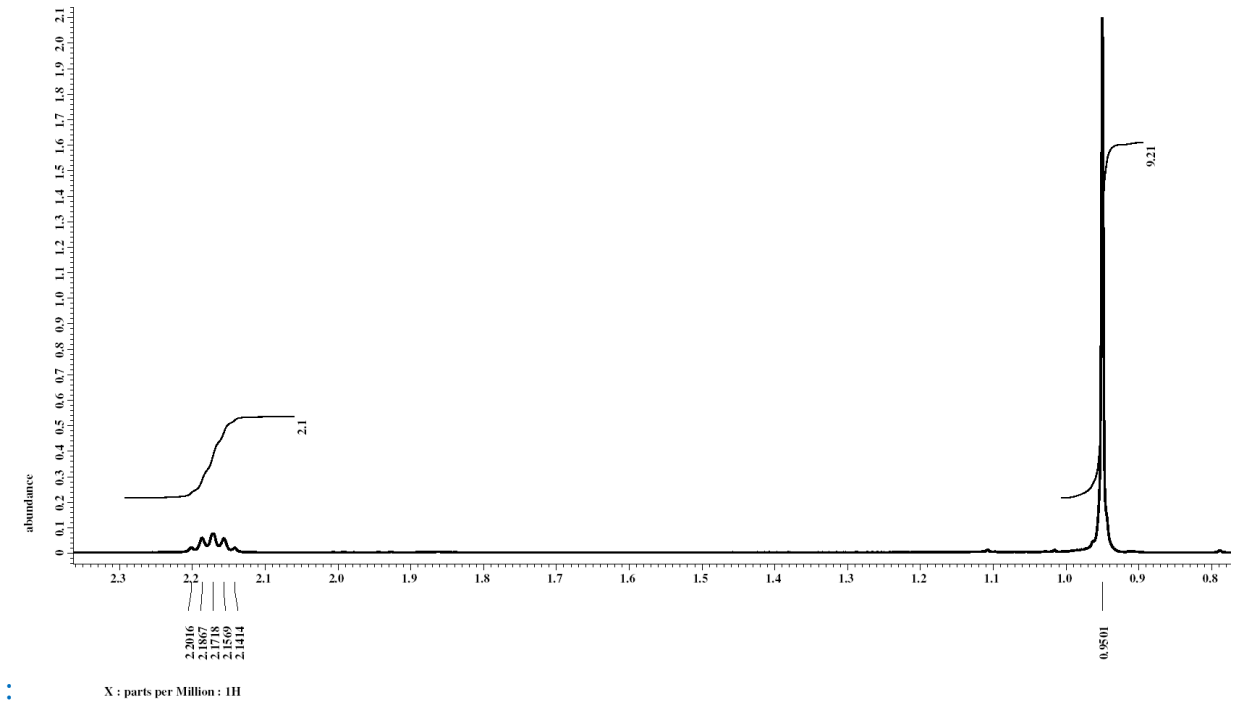
abundance
2.1
9.21
2.2016
2.1867
2.1718
2.1569
2.1414
0.9501
X : parts per Million : 1H

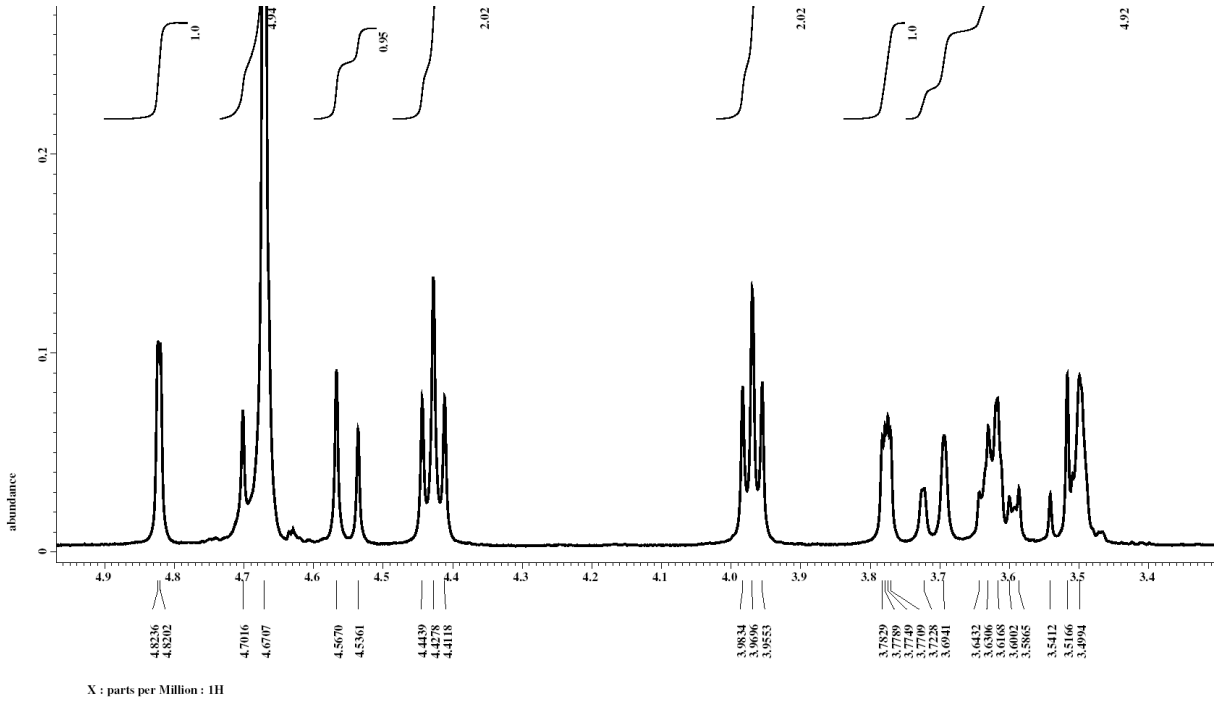
abundance
1.0
4.94
0.95
2.02
2.02
1.0
4.92
4.8236
4.8202
4.7016
4.6707
4.5670
4.5361
4.4439
4.4278
4.4118
3.9834
3.9696
3.9533
3.7829
3.7789
3.7749
3.7709
3.7228
3.6941
3.6432
3.6306
3.6168
3.6002
3.5865
3.5412
3.5166
3.4994
X : parts per Million : 1H

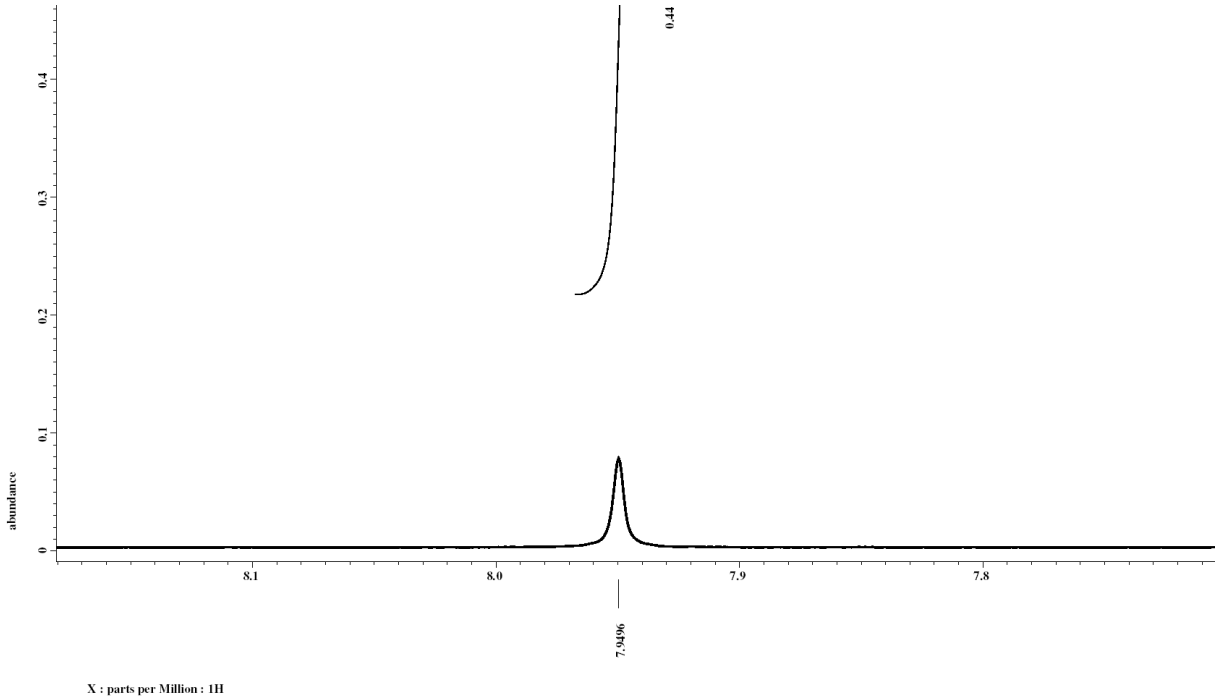

^{13}C NMR (101 MHz, D_2O)

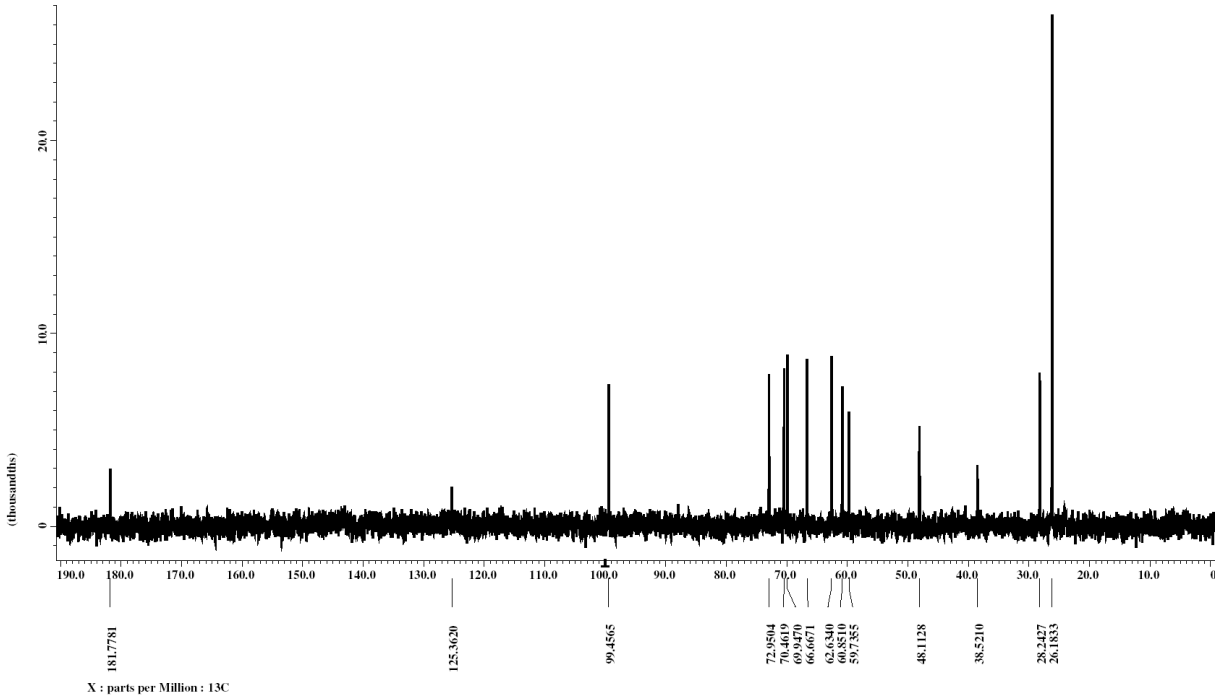

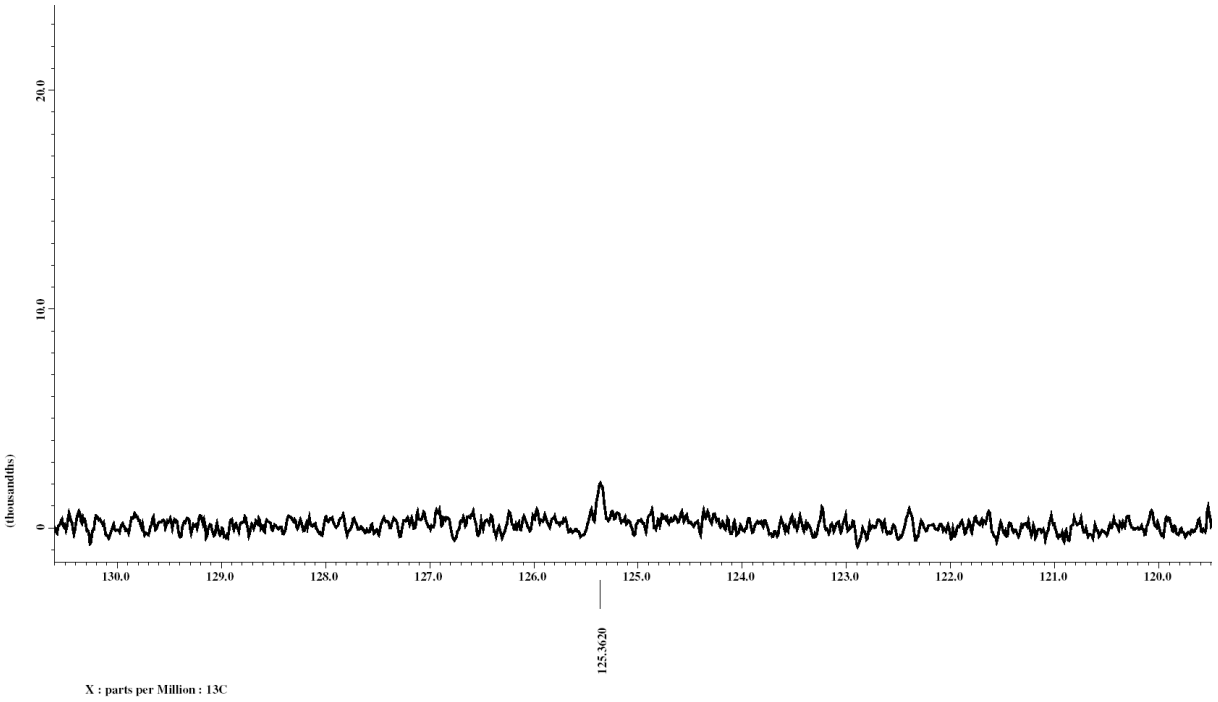

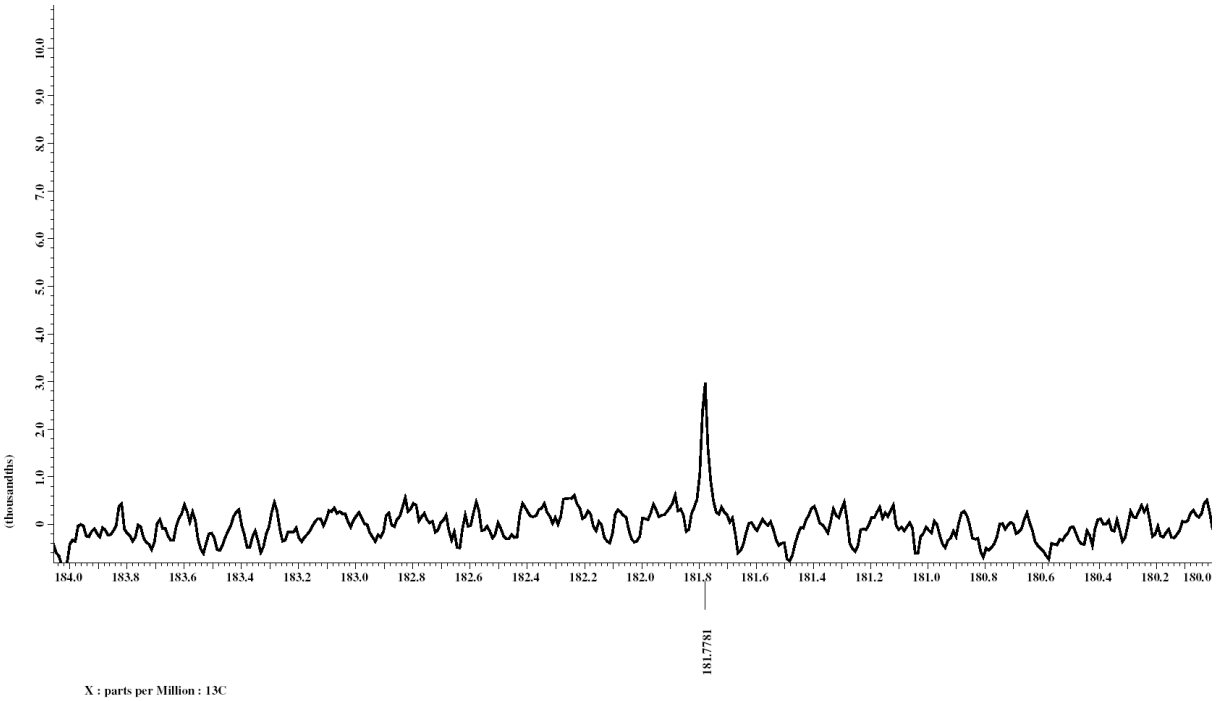

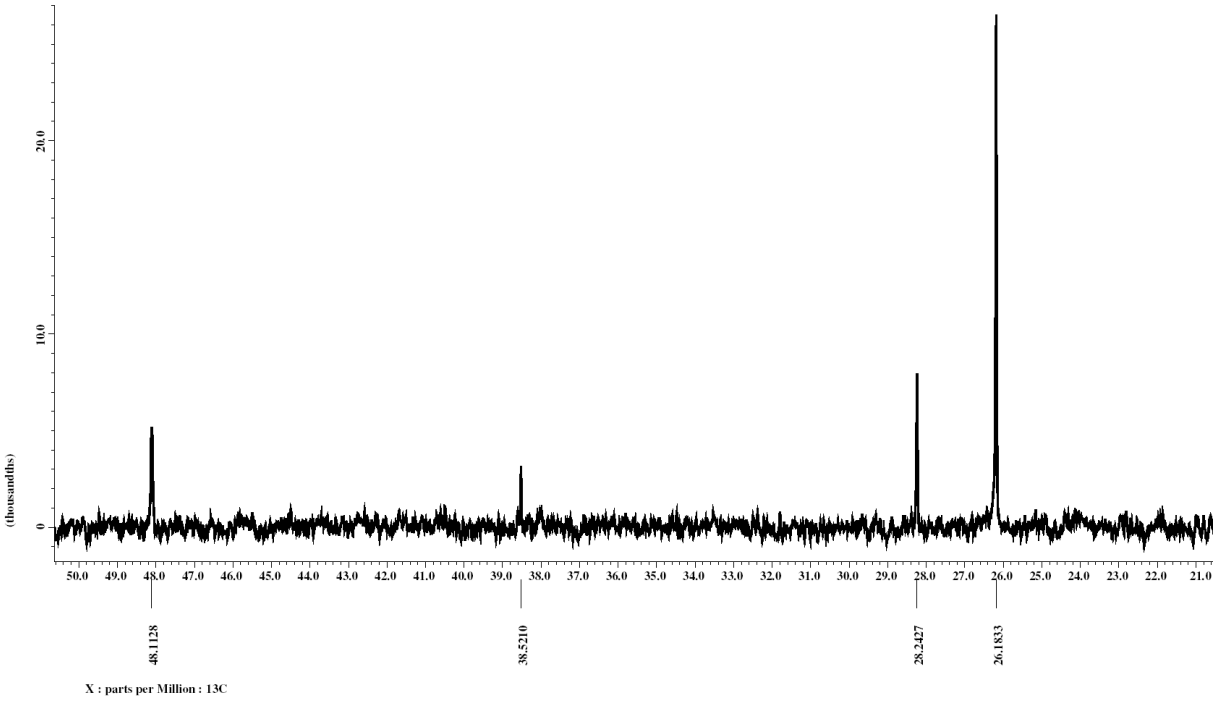
20.0
10.0
0
(thousandths)
50.0 49.0 48.0 47.0 46.0 45.0 44.0 43.0 42.0 41.0 40.0 39.0 38.0 37.0 36.0 35.0 34.0 33.0 32.0 31.0 30.0 29.0 28.0 27.0 26.0 25.0 24.0 23.0 22.0 21.0
48.1128
38.5210
28.2427
26.1833
X : parts per Million : 13C

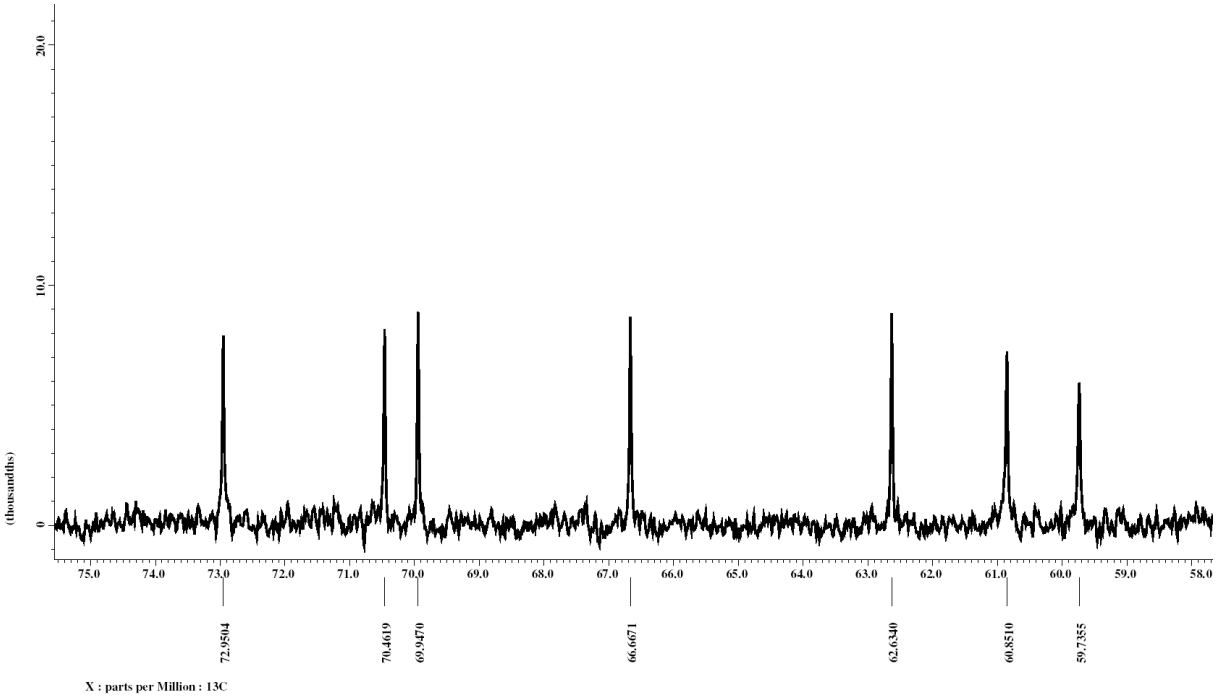
20.0
10.0
0
(thousandths)
75.0 74.0 73.0 72.0 71.0 70.0 69.0 68.0 67.0 66.0 65.0 64.0 63.0 62.0 61.0 60.0 59.0 58.0
72.9504
70.4619
69.9470
66.6671
62.6340
60.8510
59.7355
X : parts per Million : 13C

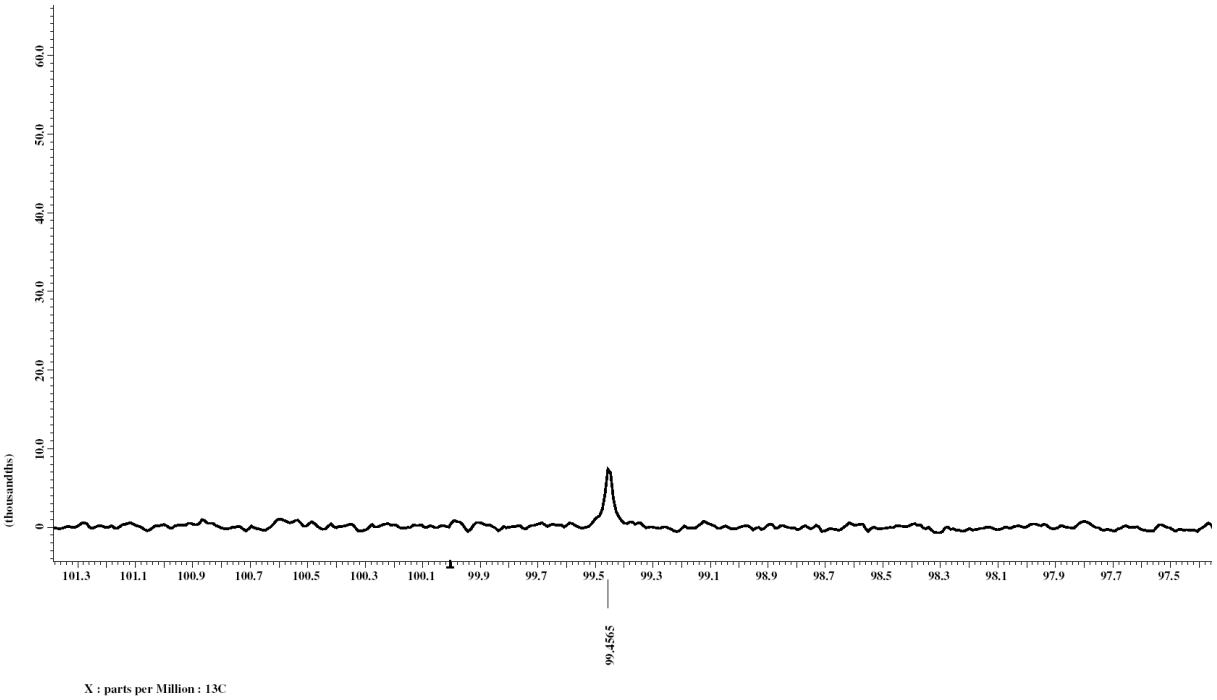
(thousandths)
60.0
50.0
40.0
30.0
20.0
10.0
0
101.3
101.1
100.9
100.7
100.5
100.3
100.1
99.9
99.7
99.5
99.3
99.1
98.9
98.7
98.5
98.3
98.1
97.9
97.7
97.5
99.4565
X : parts per Million : 13C

Compound 5

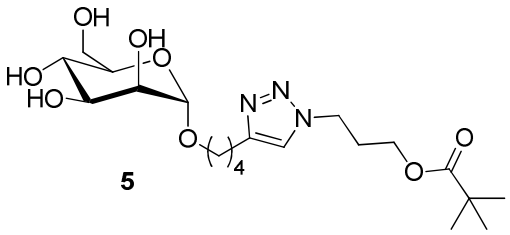

5

^{1}H NMR (400 MHz, D_2O)

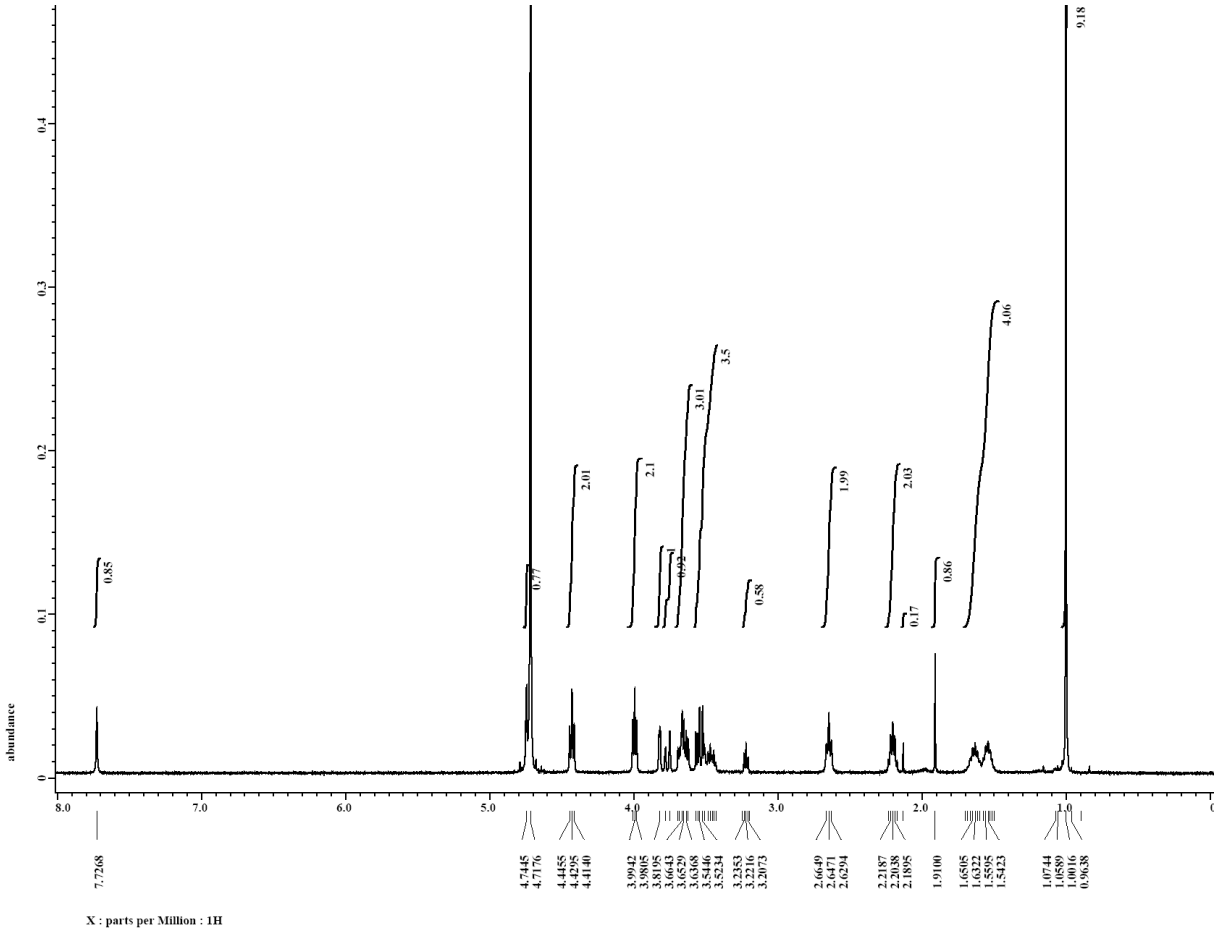

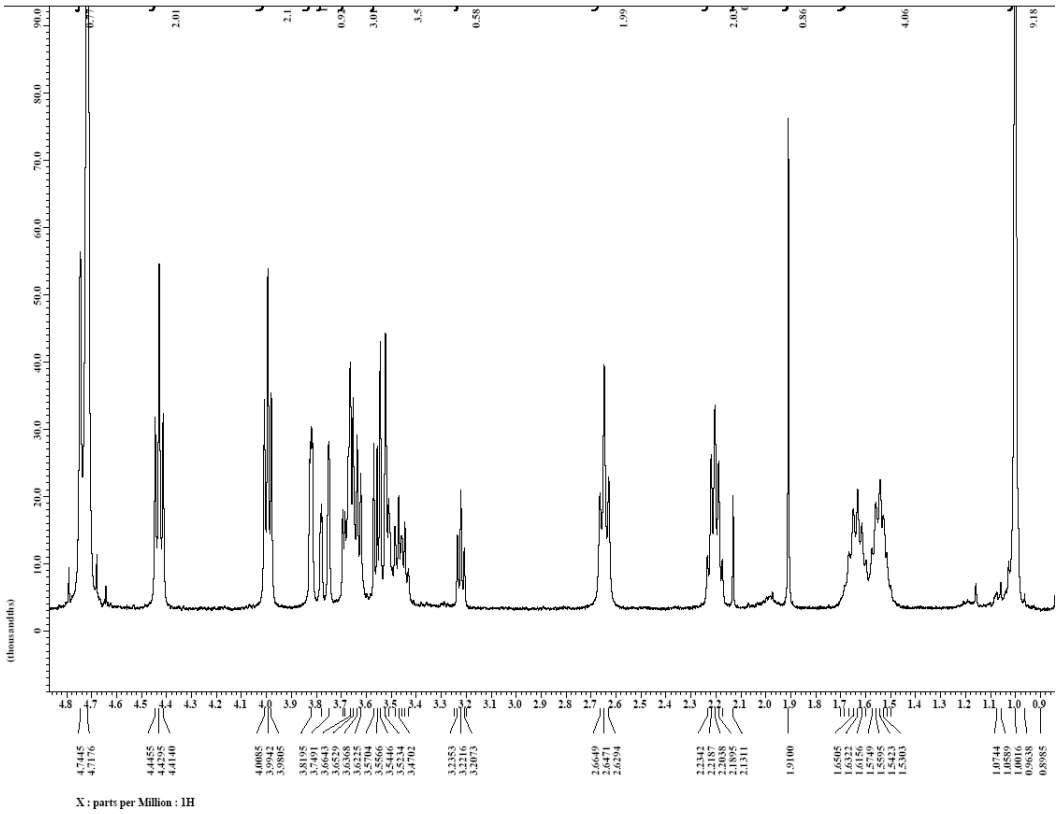

^{13}C NMR (101 MHz, D_2O)

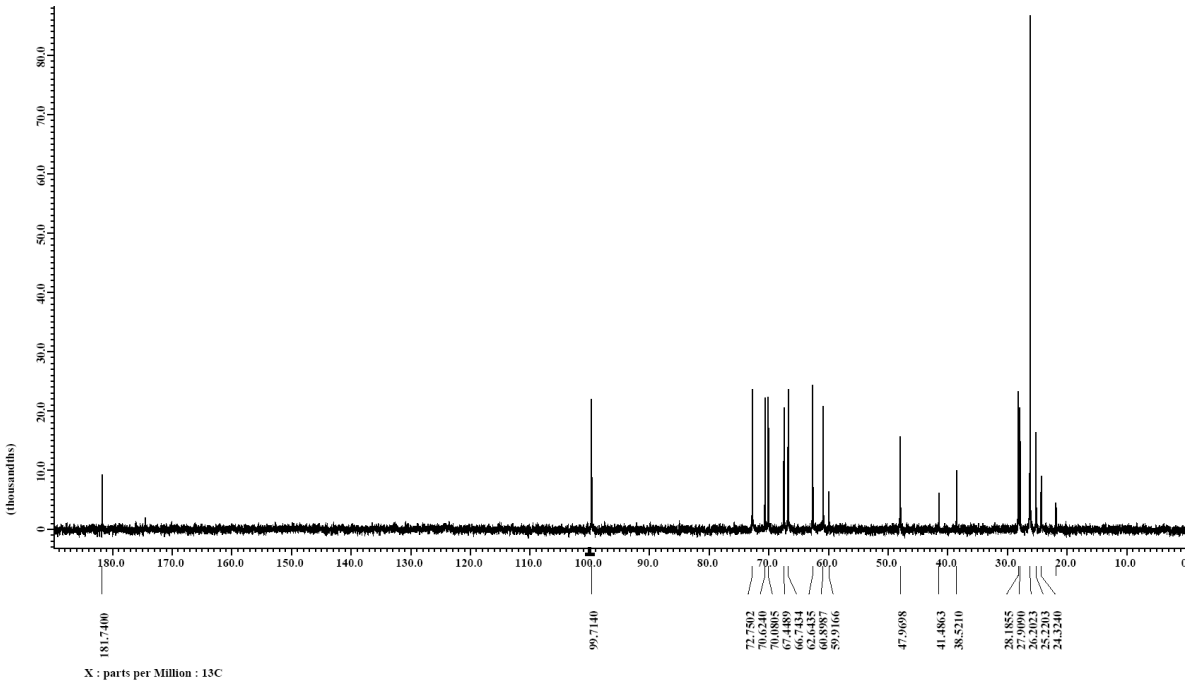

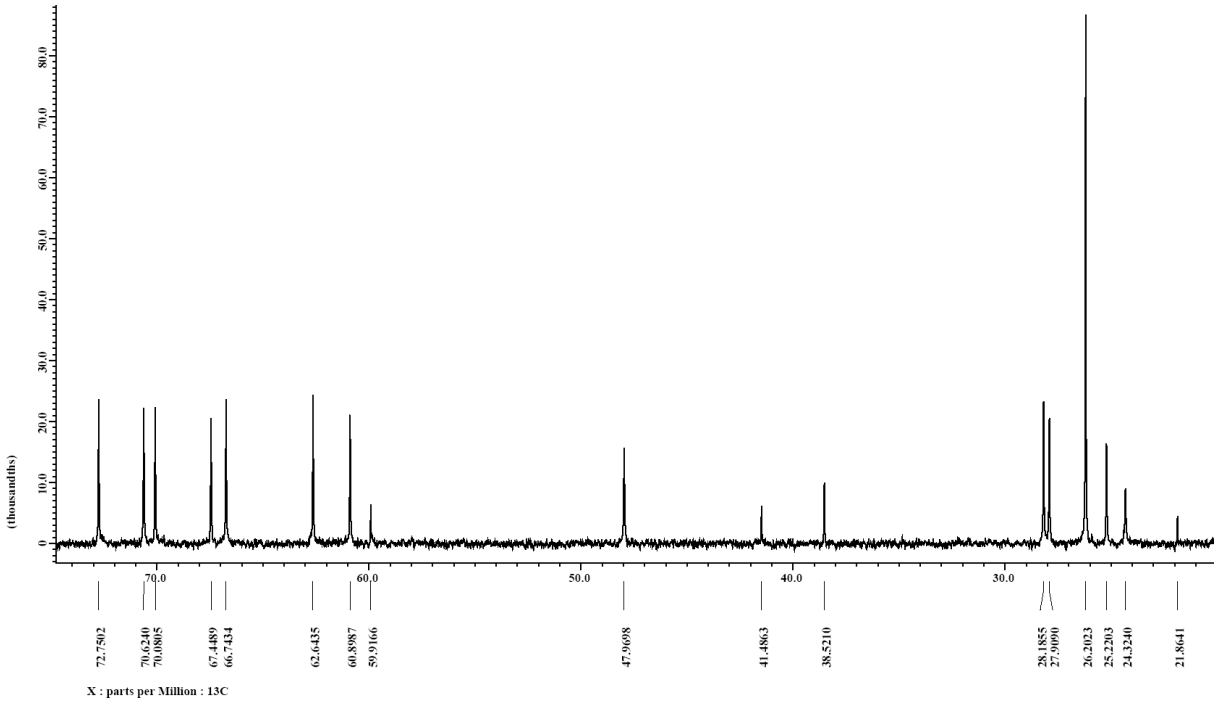
(thousandths)
0
10.0
20.0
30.0
40.0
50.0
60.0
70.0
80.0
70.0
60.0
50.0
40.0
30.0
72.7502
70.6240
70.0805
67.4489
66.7434
62.6435
60.8987
59.9166
47.9698
41.4863
38.5210
28.1855
27.9090
26.2023
25.2203
24.3240
21.8641
X : parts per Million : 13C

Compound 6

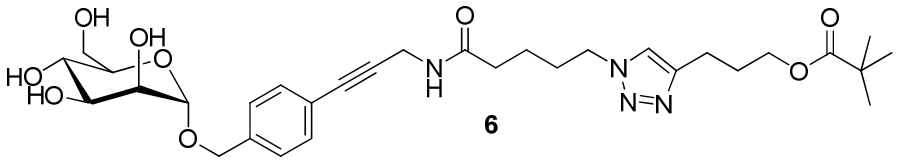

6

^{1}H NMR (400 MHz, CD_3OD)

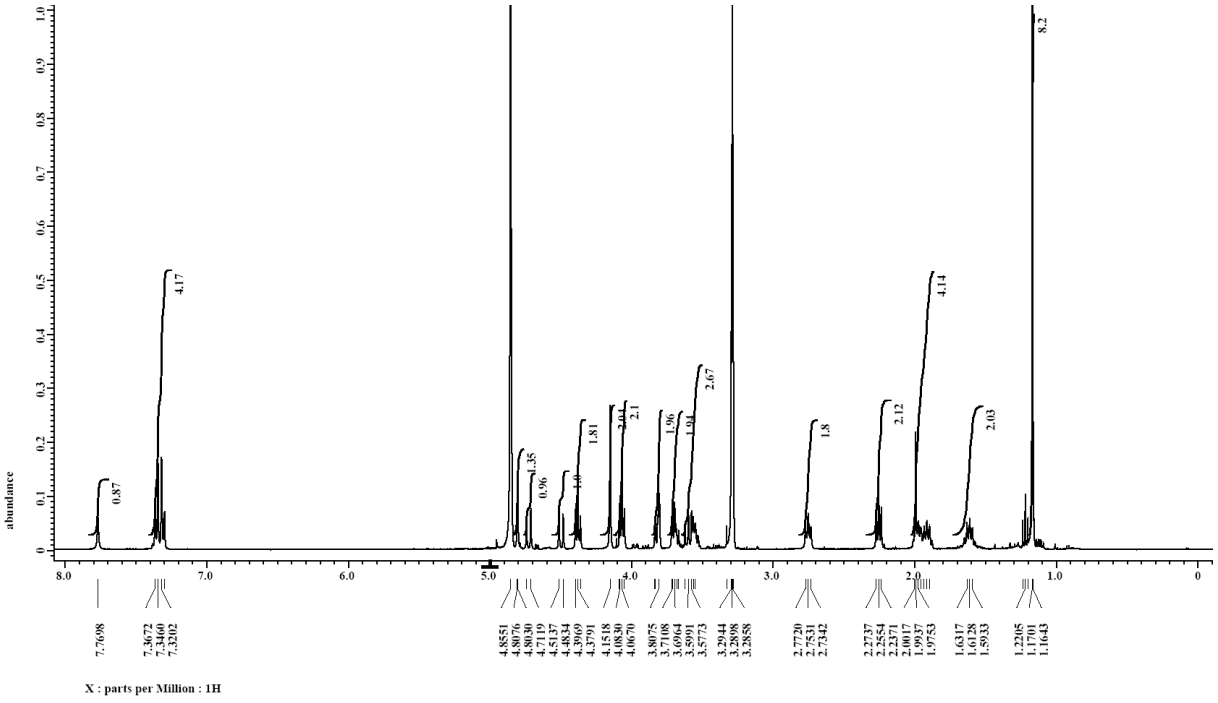

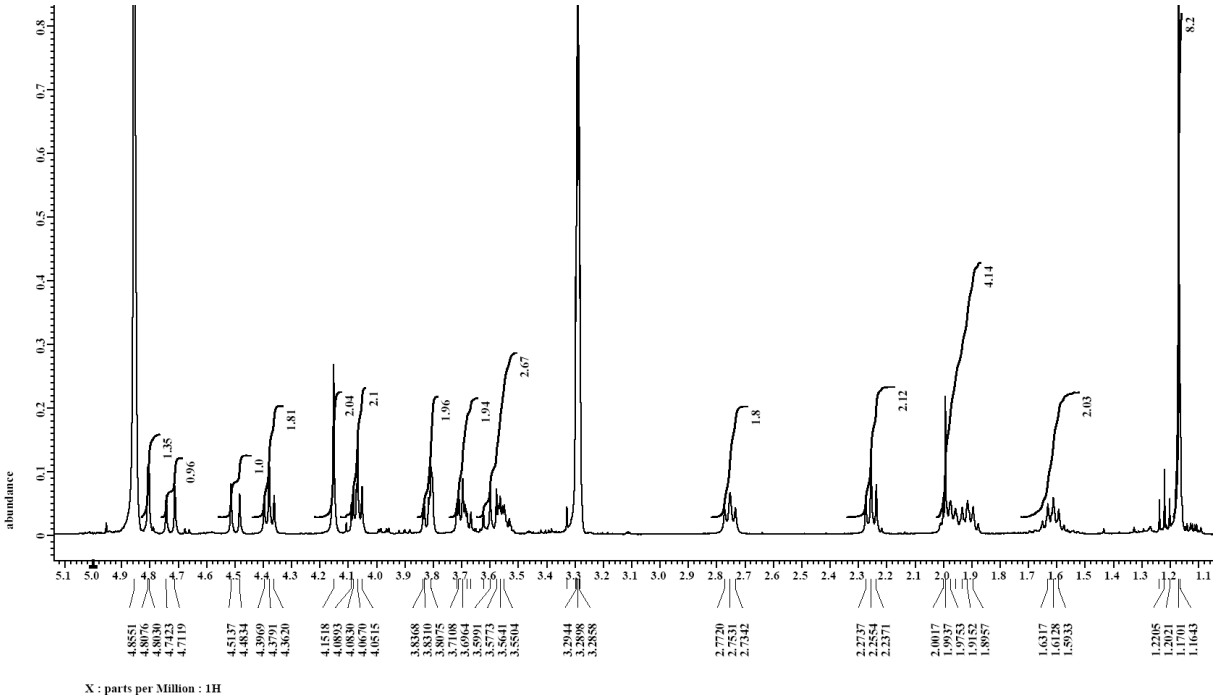

^{13}C NMR (101 MHz, CD_3OD)

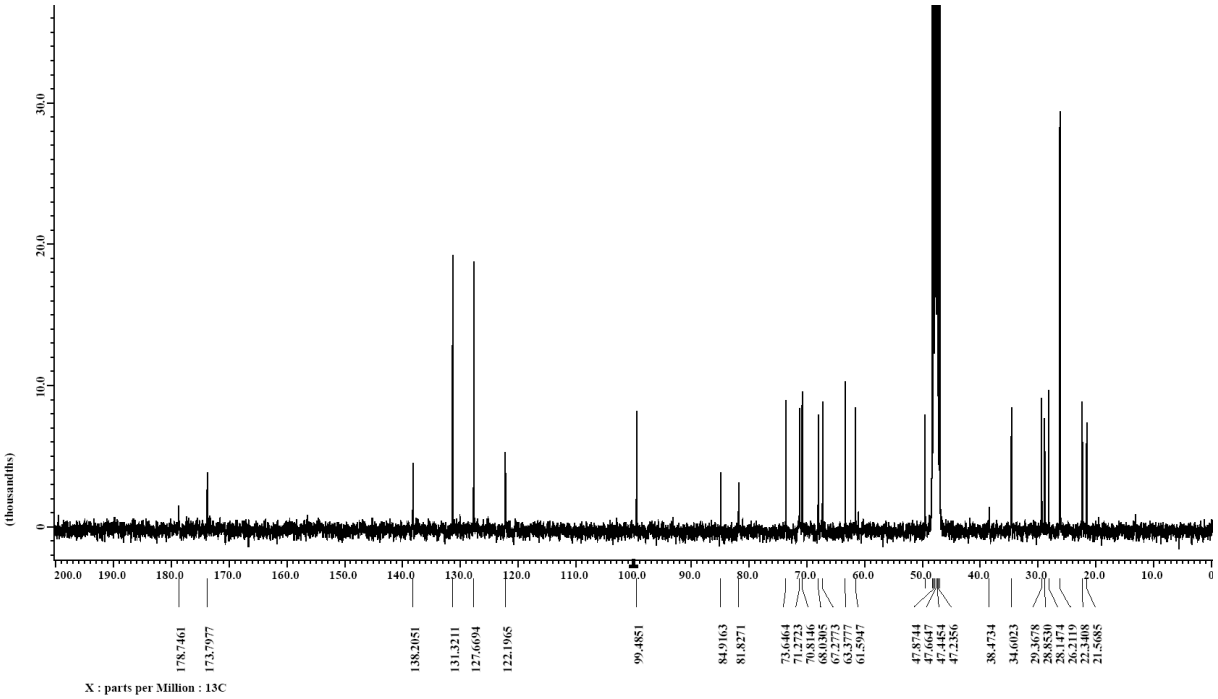

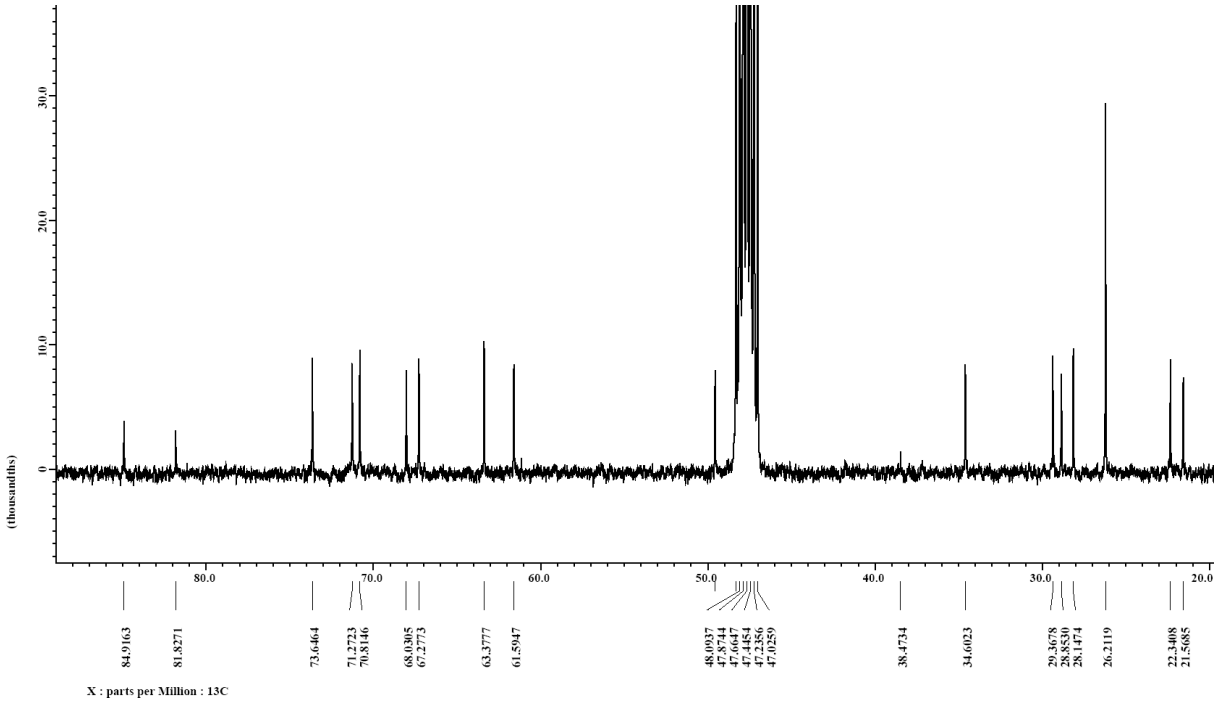
(thousandths)
30.0
20.0
10.0
0
80.0
70.0
60.0
50.0
40.0
30.0
20.0
84.9163
81.8271
73.6464
71.2723
70.8146
68.0305
67.2773
63.3777
61.5947
48.0937
47.8744
47.6647
47.4454
47.2356
47.0259
38.4734
34.6023
29.3678
28.8530
28.1474
26.2119
22.3408
21.5685
X : parts per Million : 13C

Compound 8

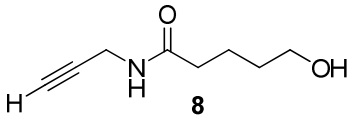

8

^{1}H NMR (400 MHz, $CDCl_3$)

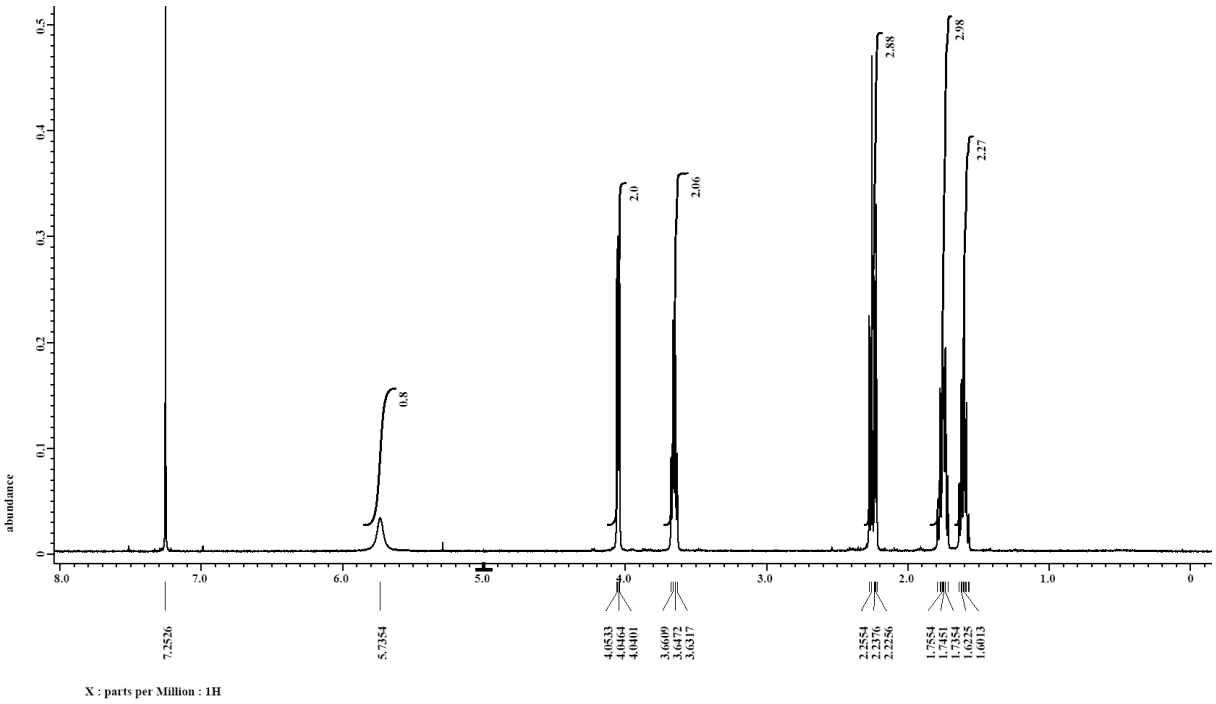

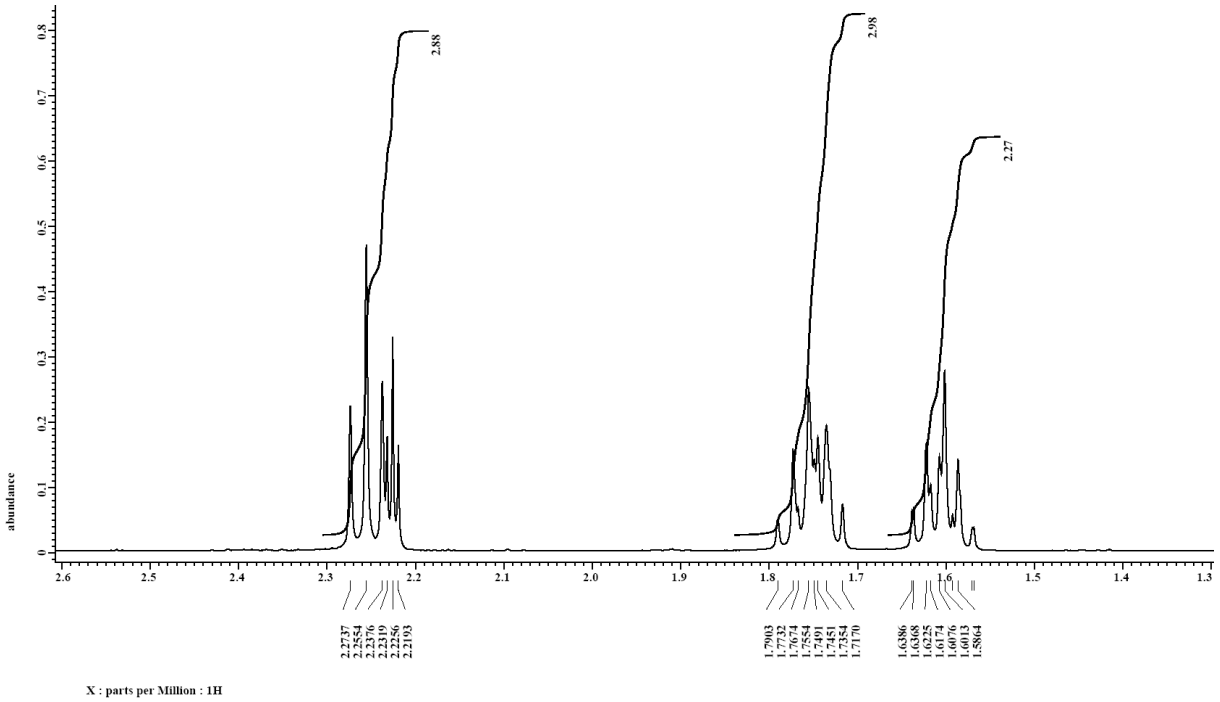
abundance
2.88
2.98
2.27
2.2737
2.2554
2.2376
2.2319
2.2256
2.2193
1.7903
1.7732
1.7674
1.7554
1.7491
1.7451
1.7354
1.7170
1.6386
1.6368
1.6225
1.6174
1.6076
1.6013
1.5864
X : parts per Million : 1H

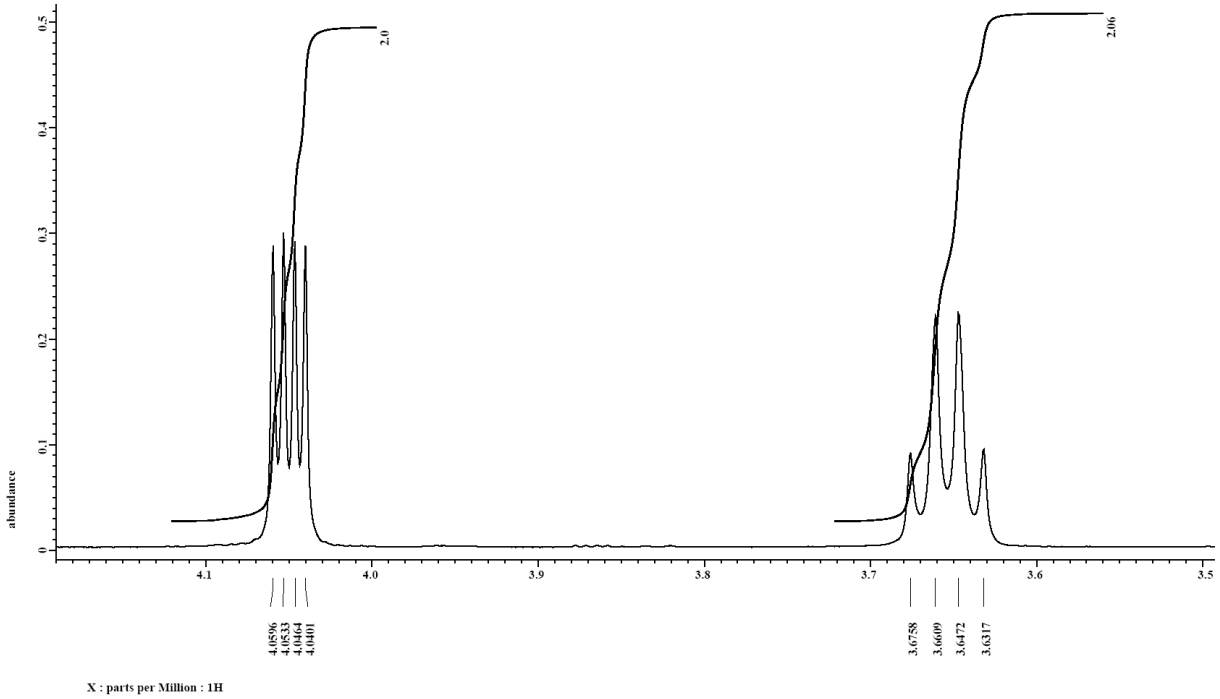
abundance
2.0
2.06
4.0596
4.0533
4.0464
4.0401
3.6758
3.6609
3.6472
3.6317
X : parts per Million : 1H

^{13}C NMR (101 MHz, $CDCl_3$)

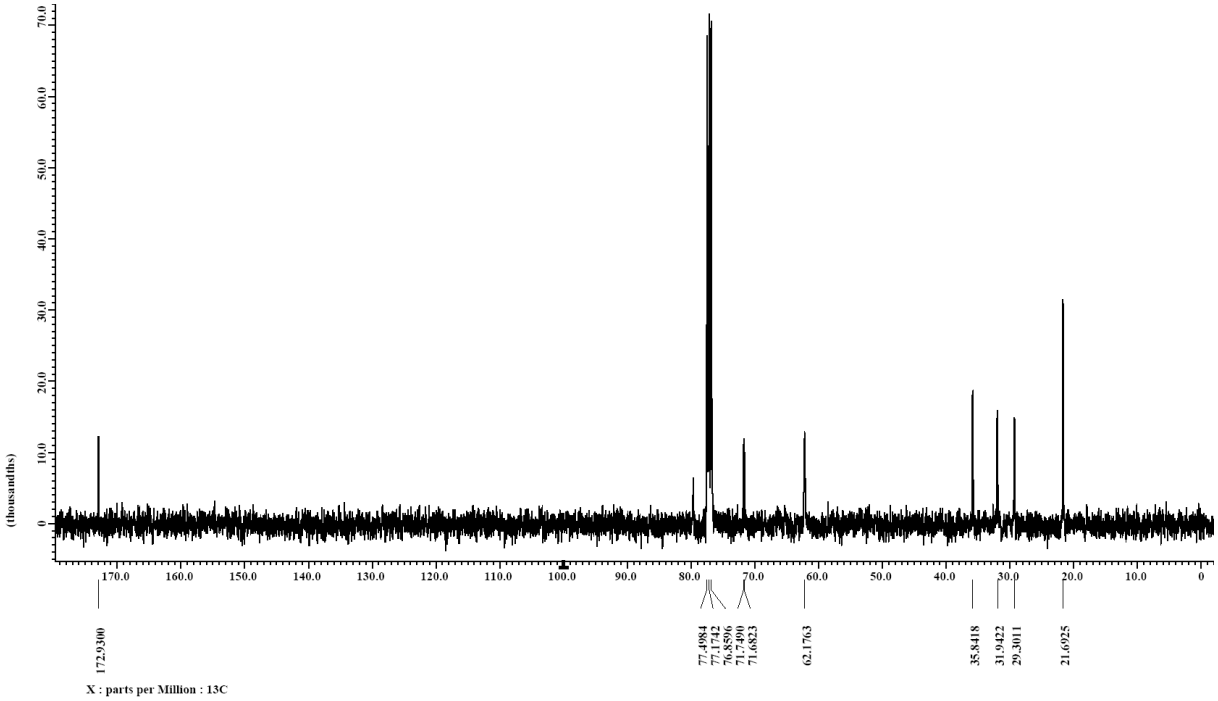

Compound 9

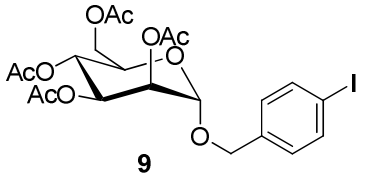

9

^{1}H NMR (400 MHz, $CDCl_3$)

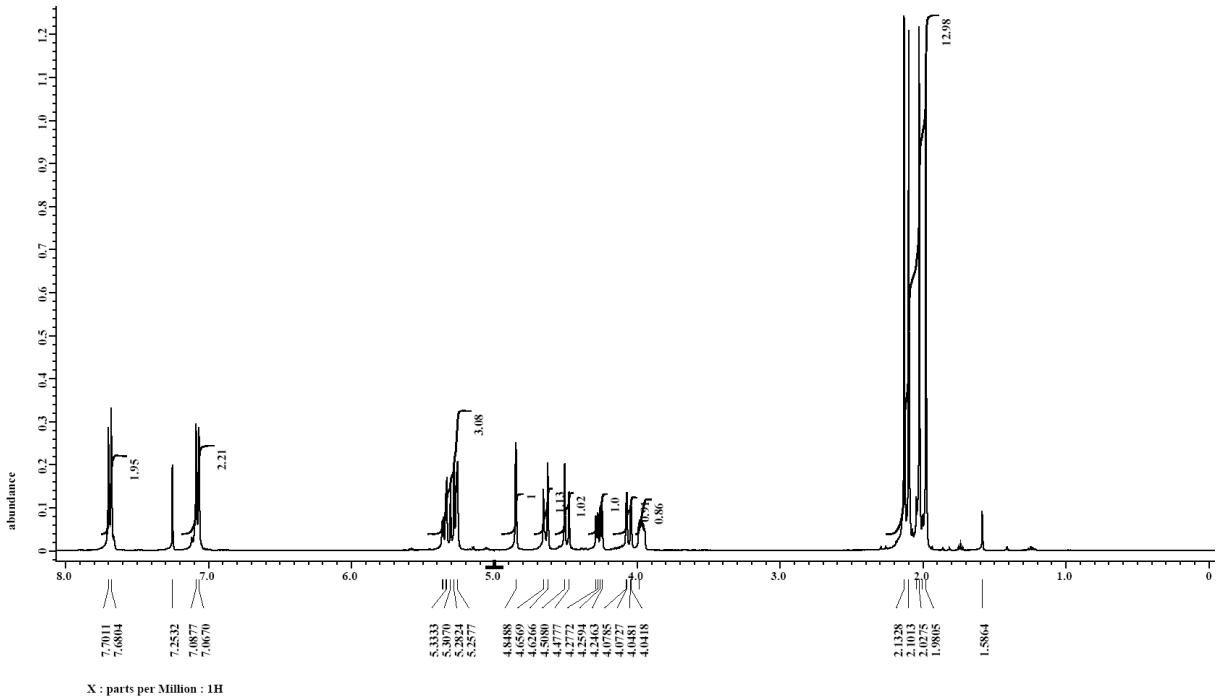

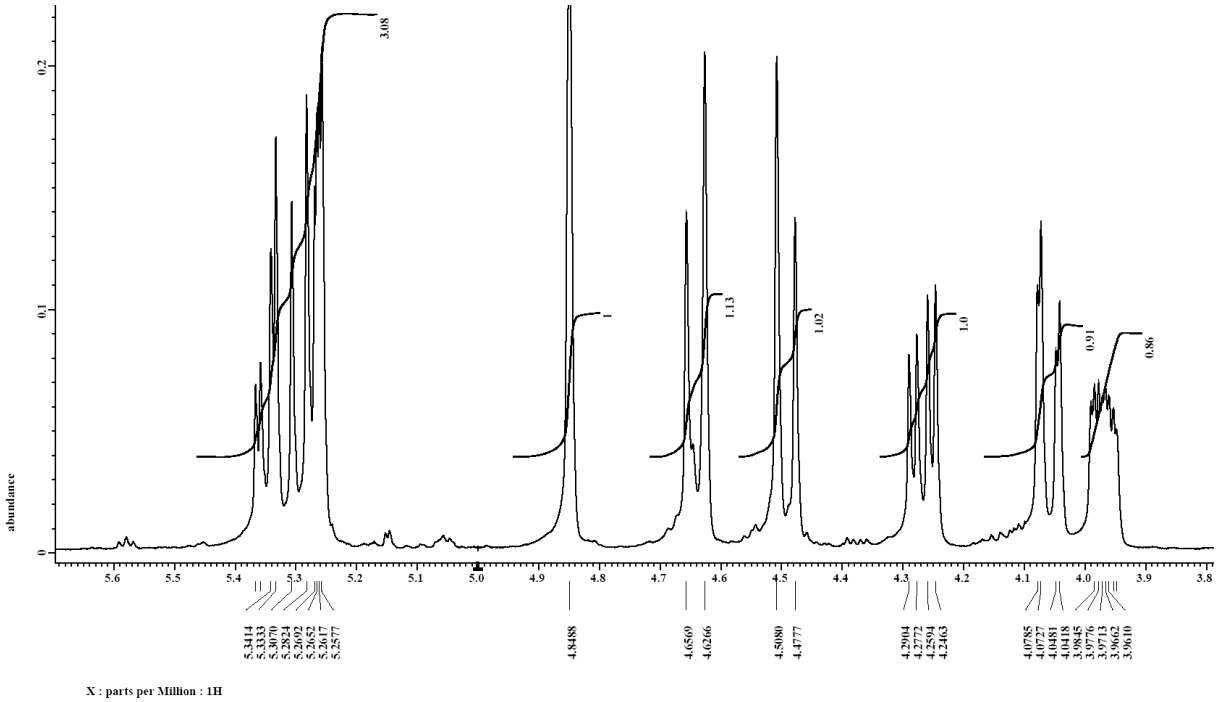

^{13}C NMR (101 MHz, $CDCl_3$)

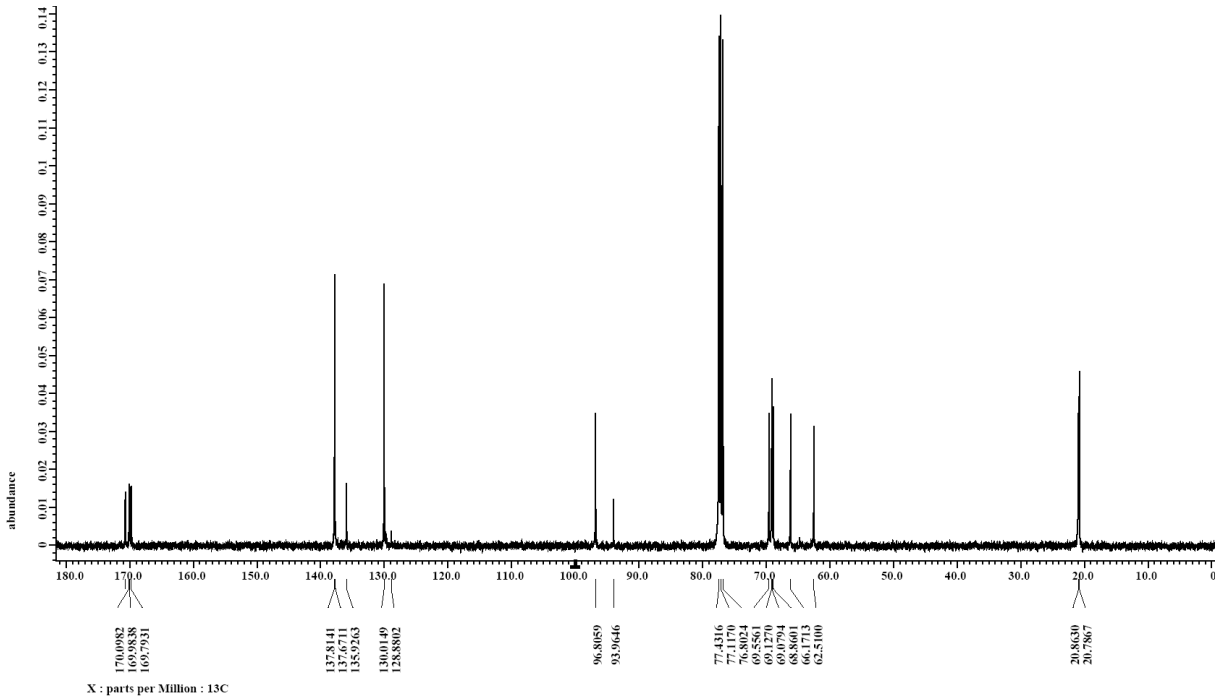

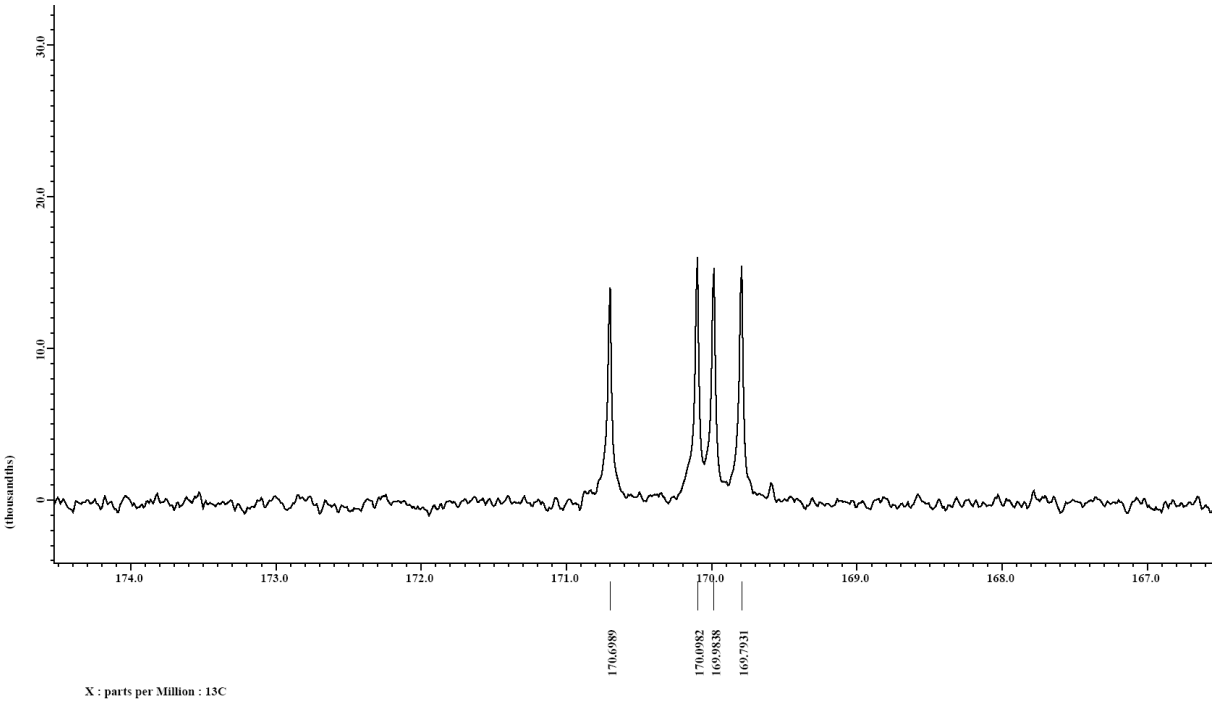
30.0
20.0
10.0
0
(thousandths)
174.0
173.0
172.0
171.0
170.0
169.0
168.0
167.0
170.6989
170.0982
169.9838
169.7931
X : parts per Million : 13C

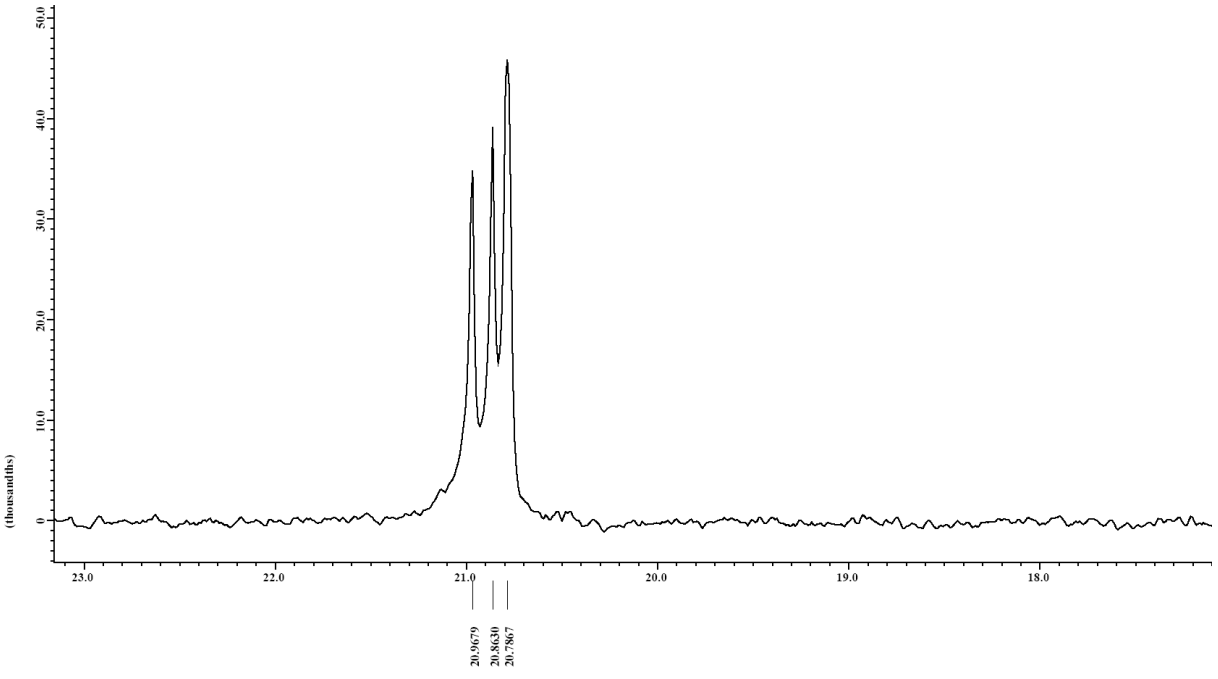
50.0
40.0
30.0
20.0
10.0
0
(thousandths)
23.0
22.0
21.0
20.0
19.0
18.0
20.9679
20.8630
20.7867
X : parts per Million : 13C

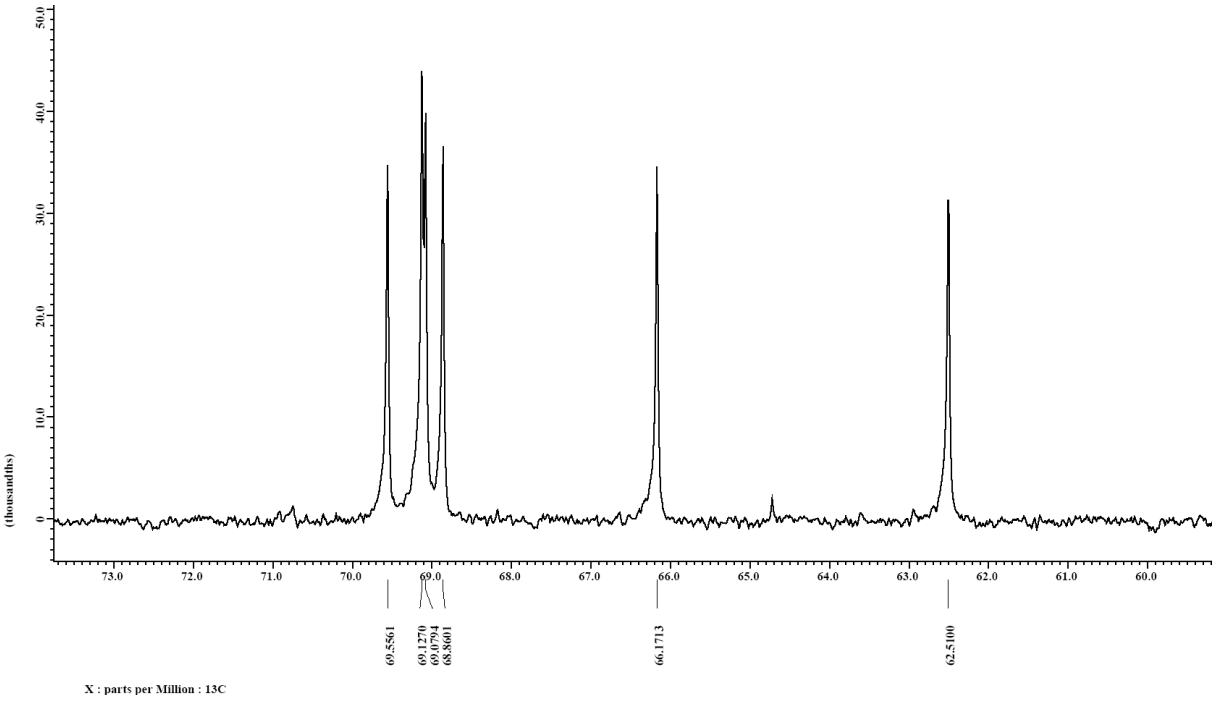
50.0
40.0
30.0
20.0
10.0
0
(thousandths)
73.0
72.0
71.0
70.0
69.0
68.0
67.0
66.0
65.0
64.0
63.0
62.0
61.0
60.0
69.5561
69.1270
69.0794
68.8601
66.1713
62.5100
X : parts per Million : 13C

Compound 10

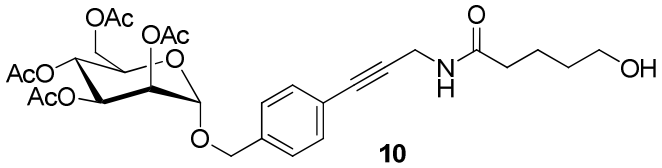

10

^{1}H NMR (400 MHz, $CDCl_3$)

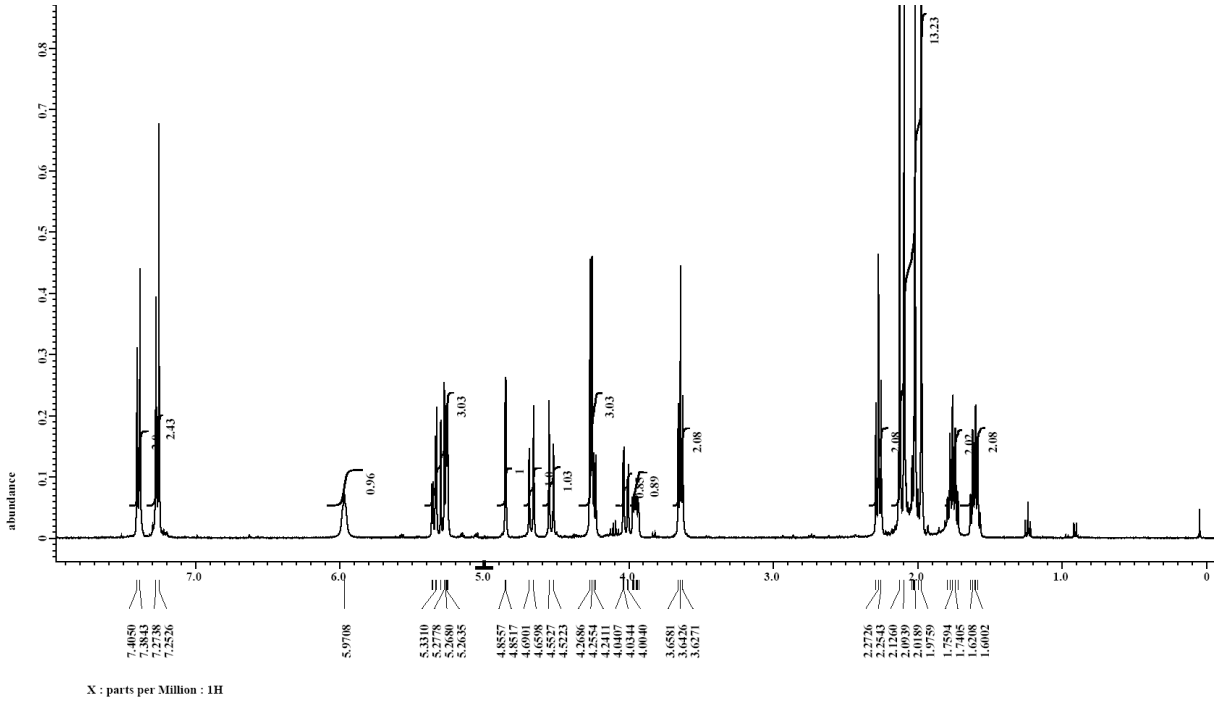

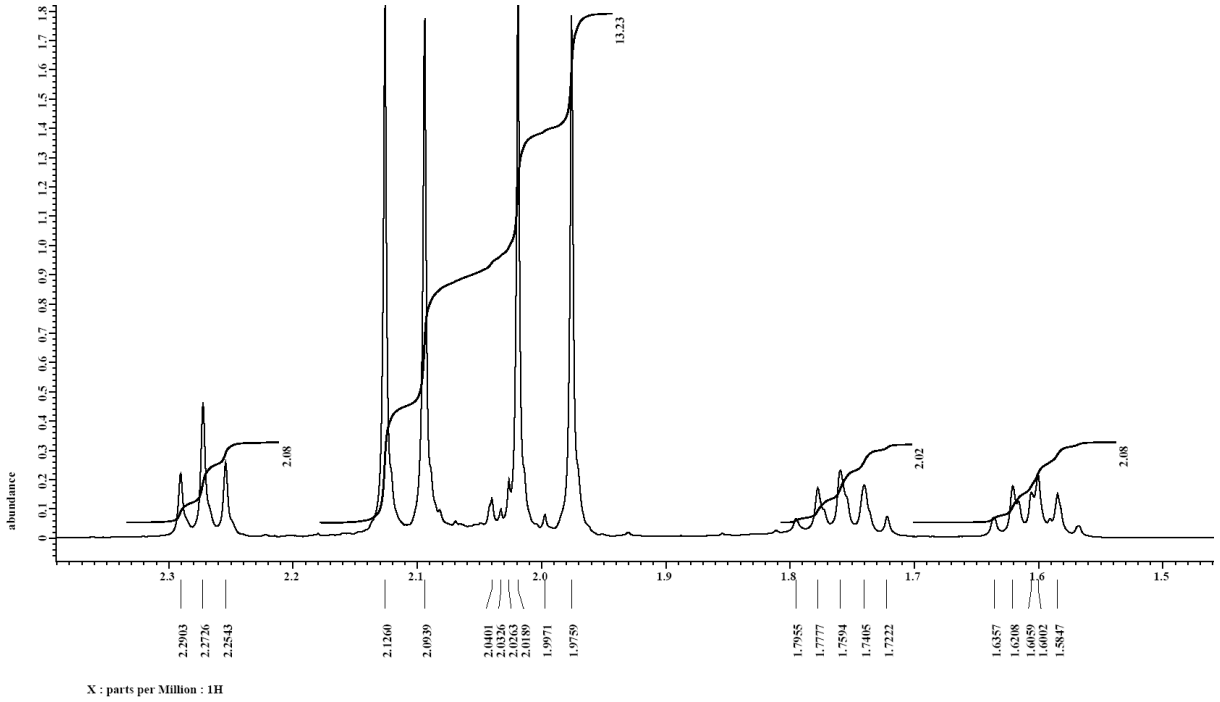
abundance
2.08
13.23
2.02
2.08
2.2903
2.2726
2.2543
2.1260
2.0939
2.0401
2.0326
2.0263
2.0189
1.9971
1.9759
1.7955
1.7777
1.7594
1.7405
1.7222
1.6357
1.6208
1.6059
1.6002
1.5847
X : parts per Million : 1H

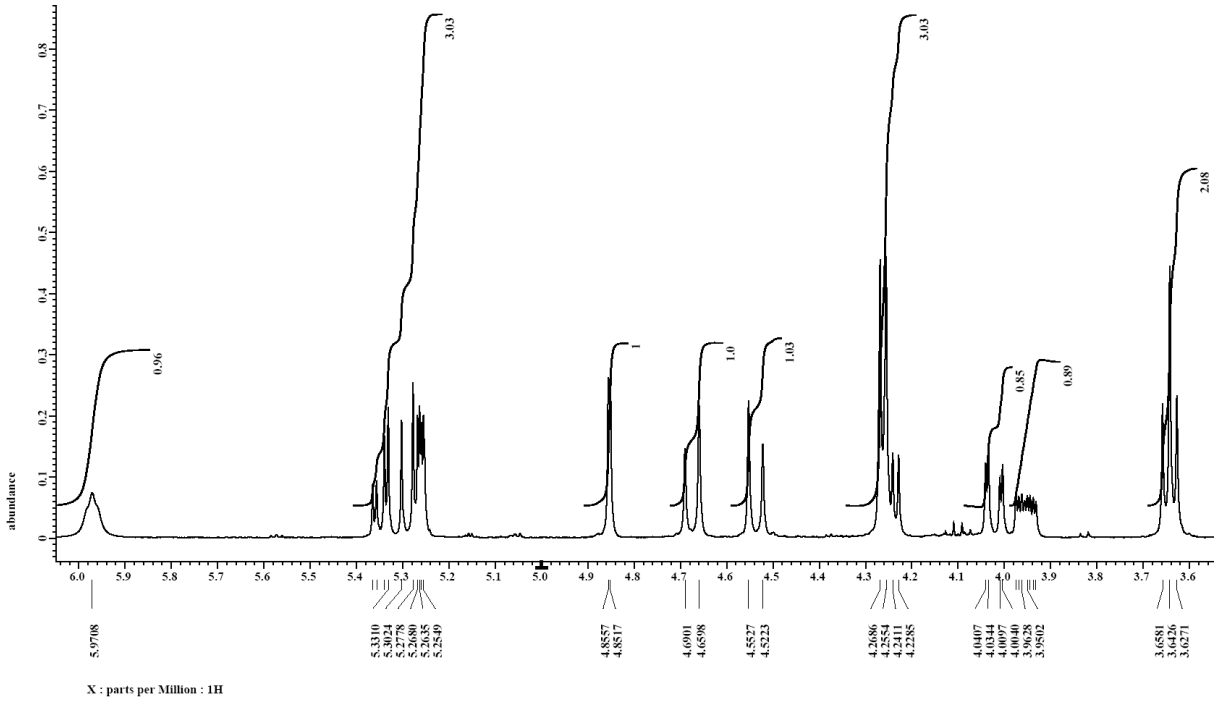
abundance
0.96
3.03
1
1.0
1.03
3.03
0.85
0.89
2.08
5.9708
5.3310
5.3024
5.2778
5.2680
5.2635
5.2549
4.8557
4.8517
4.6901
4.6598
4.5527
4.5223
4.2686
4.2554
4.2411
4.2285
4.0407
4.0344
4.0097
4.0040
3.9628
3.9502
3.6581
3.6426
3.6271
X : parts per Million : 1H

^{13}C NMR (101 MHz, $CDCl_3$)

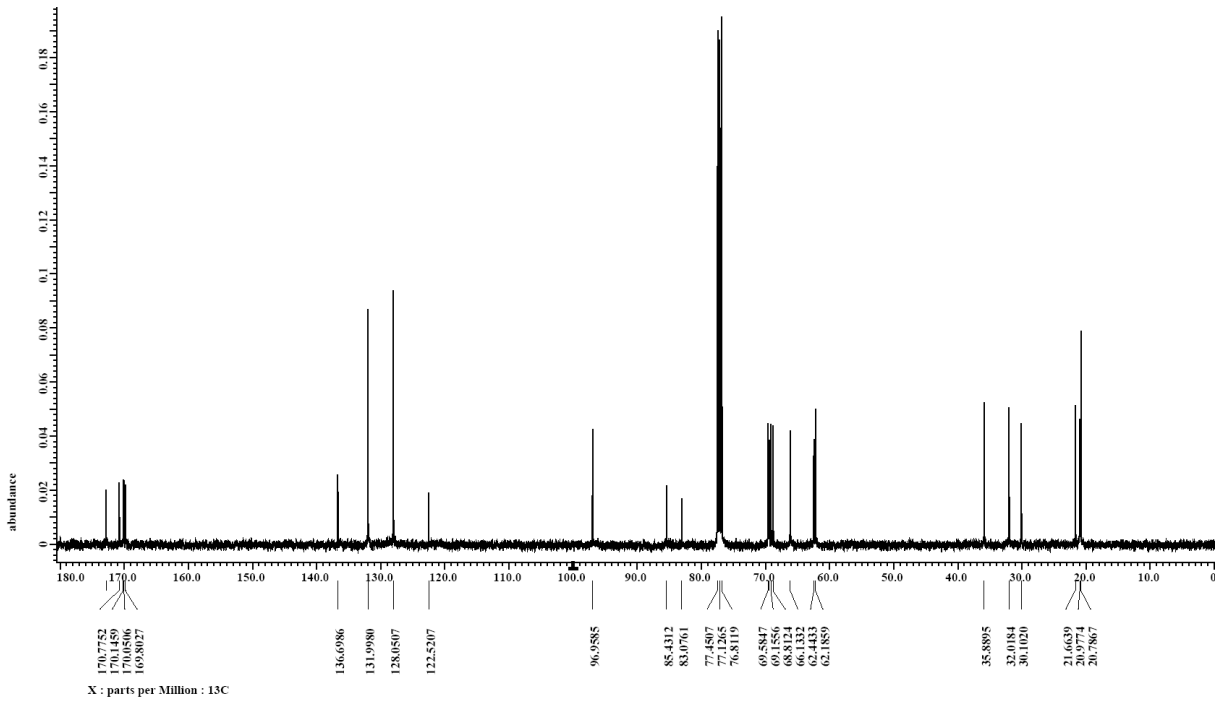

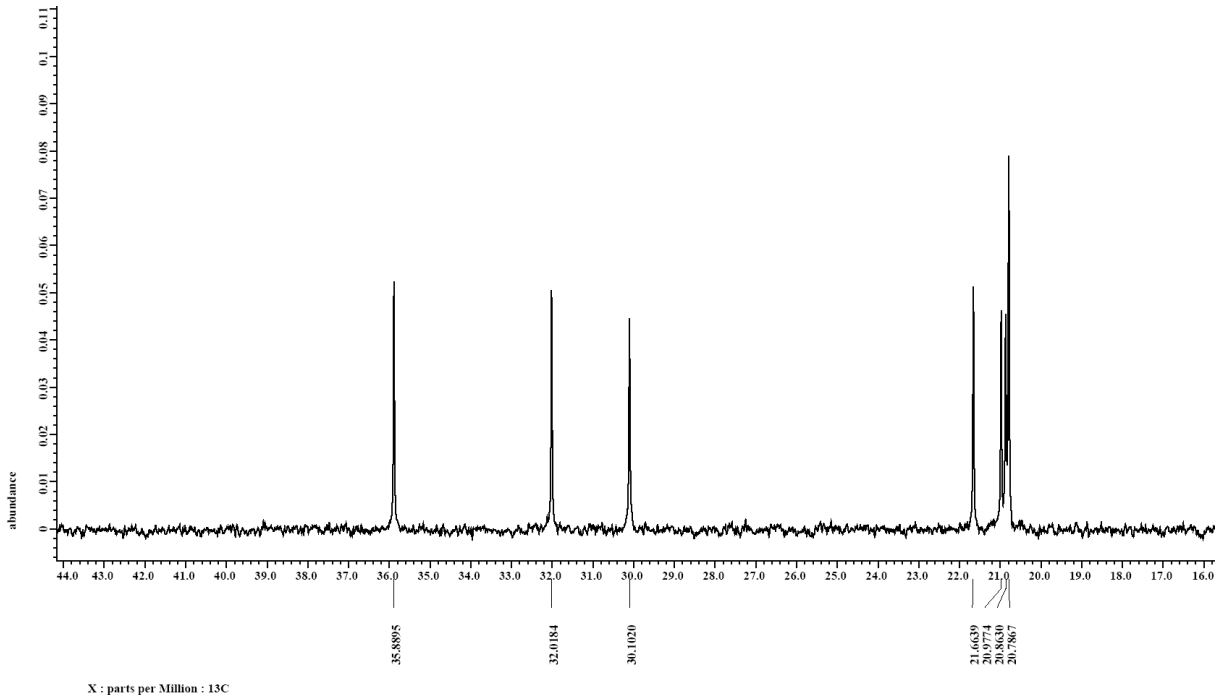

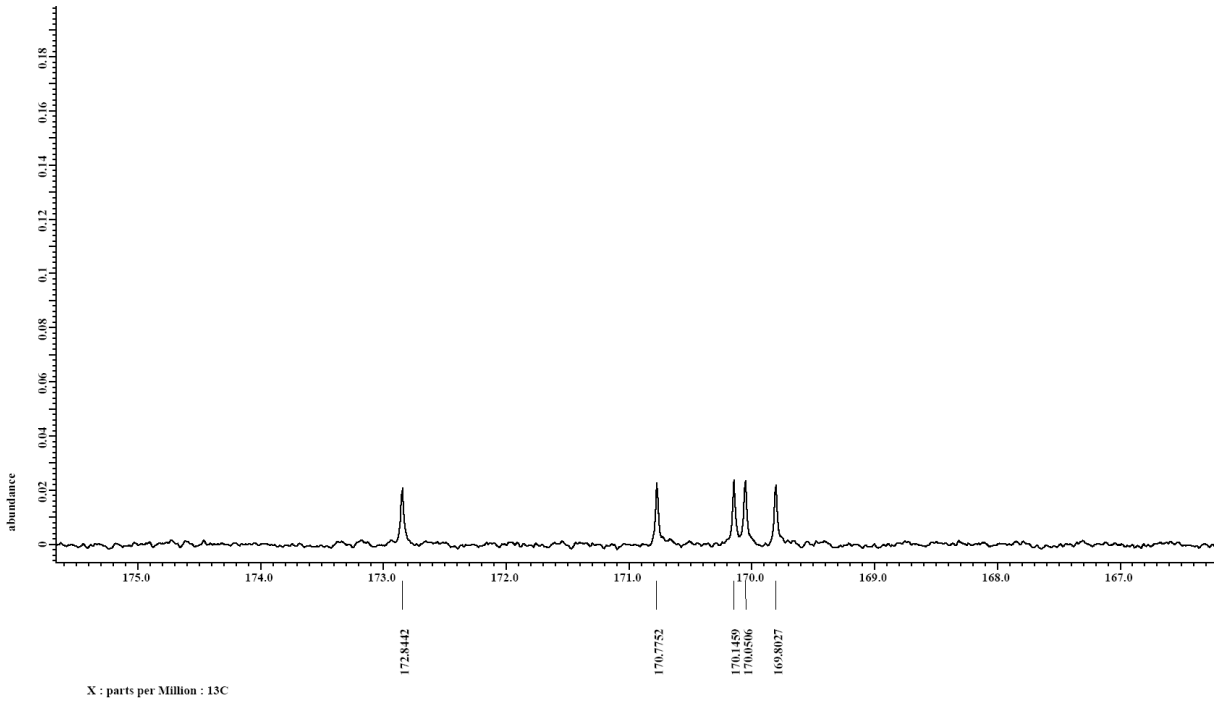
abundance
0
0.02
0.04
0.06
0.08
0.1
0.12
0.14
0.16
0.18
175.0
174.0
173.0
172.0
171.0
170.0
169.0
168.0
167.0
172.8442
170.7752
170.1459
170.0506
169.8027
X : parts per Million : 13C

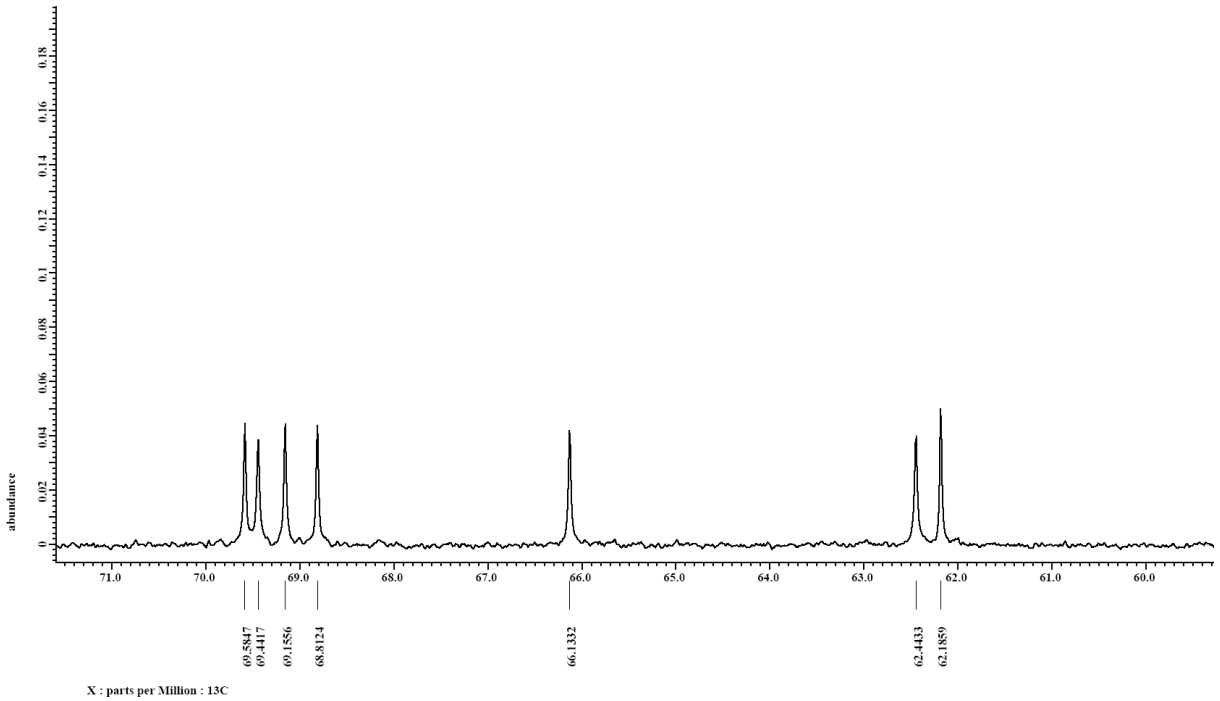
abundance
0
0.02
0.04
0.06
0.08
0.1
0.12
0.14
0.16
0.18
71.0
70.0
69.0
68.0
67.0
66.0
65.0
64.0
63.0
62.0
61.0
60.0
69.5847
69.4417
69.1556
68.8124
66.1332
62.4433
62.1859
X : parts per Million : 13C

Compound 11

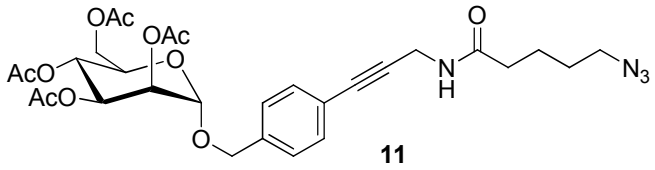

11

^{1}H NMR (400 MHz, $CDCl_3$)

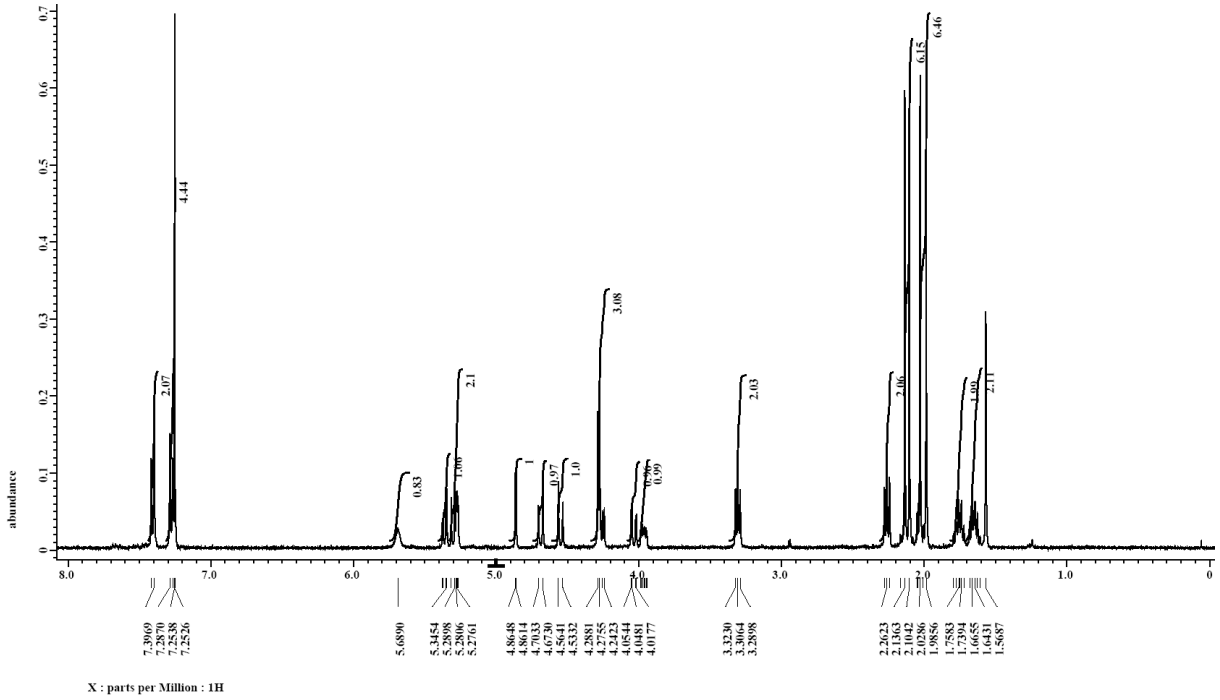

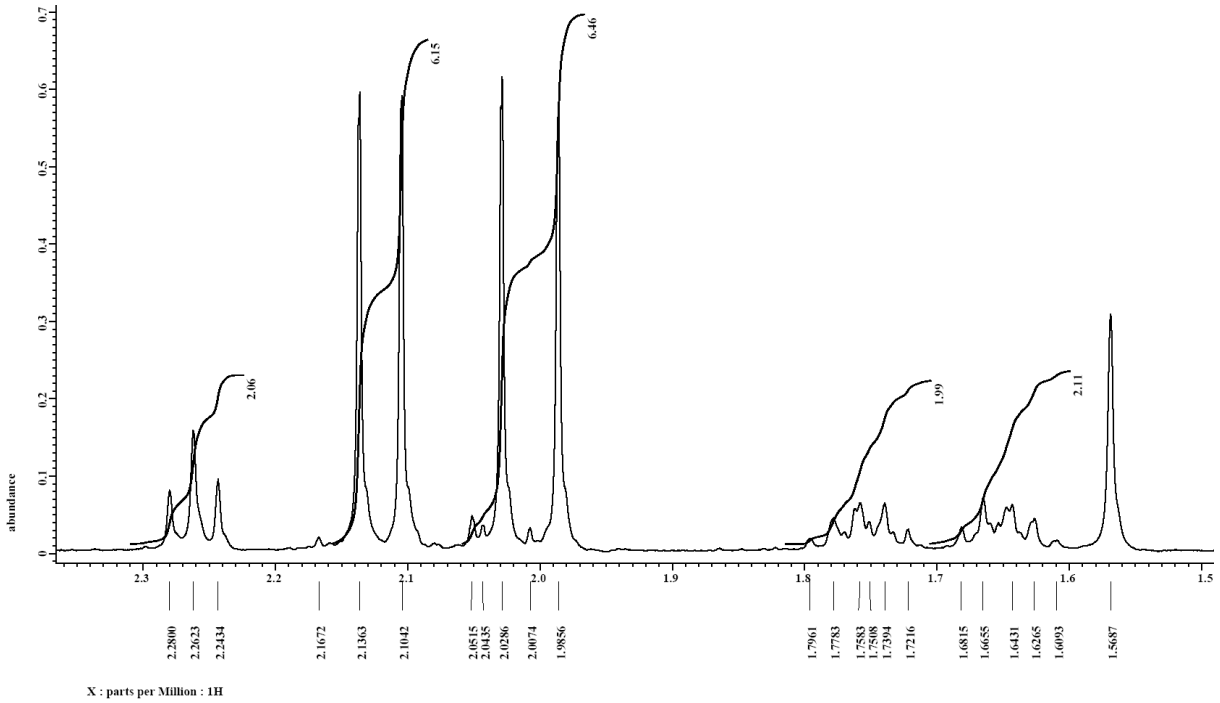
abundance
6.46
6.15
2.06
1.99
2.11
2.2800
2.2623
2.2434
2.1672
2.1363
2.1042
2.0515
2.0435
2.0286
2.0074
1.9856
1.7961
1.7783
1.7583
1.7508
1.7394
1.7216
1.6815
1.6655
1.6431
1.6265
1.6093
1.5687
X : parts per Million : 1H

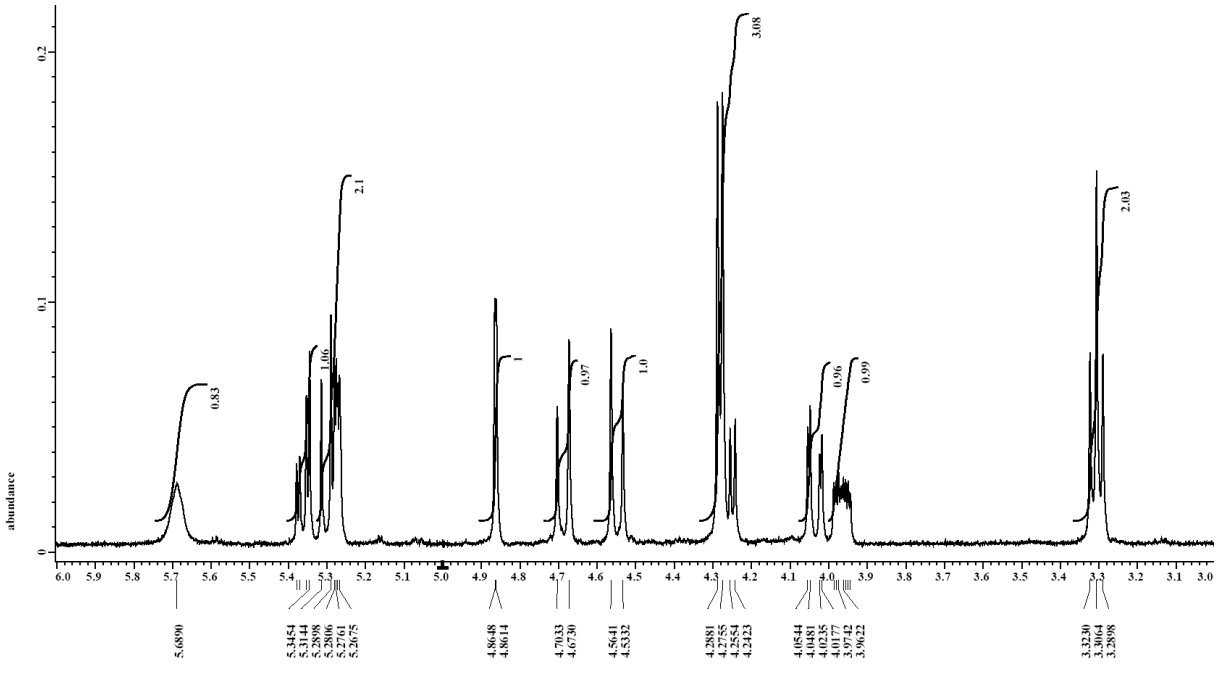
abundance
3.08
2.1
2.03
0.83
1.06
1
0.97
1.0
0.96
0.99
5.6890
5.3454
5.3144
5.2898
5.2806
5.2761
5.2675
4.8648
4.8614
4.7033
4.6730
4.5641
4.5332
4.2881
4.2755
4.2554
4.2423
4.0544
4.0481
4.0335
4.0177
3.9742
3.9622
3.3230
3.3064
3.2898
X : parts per Million : 1H

^{13}C NMR (101 MHz, $CDCl_3$)

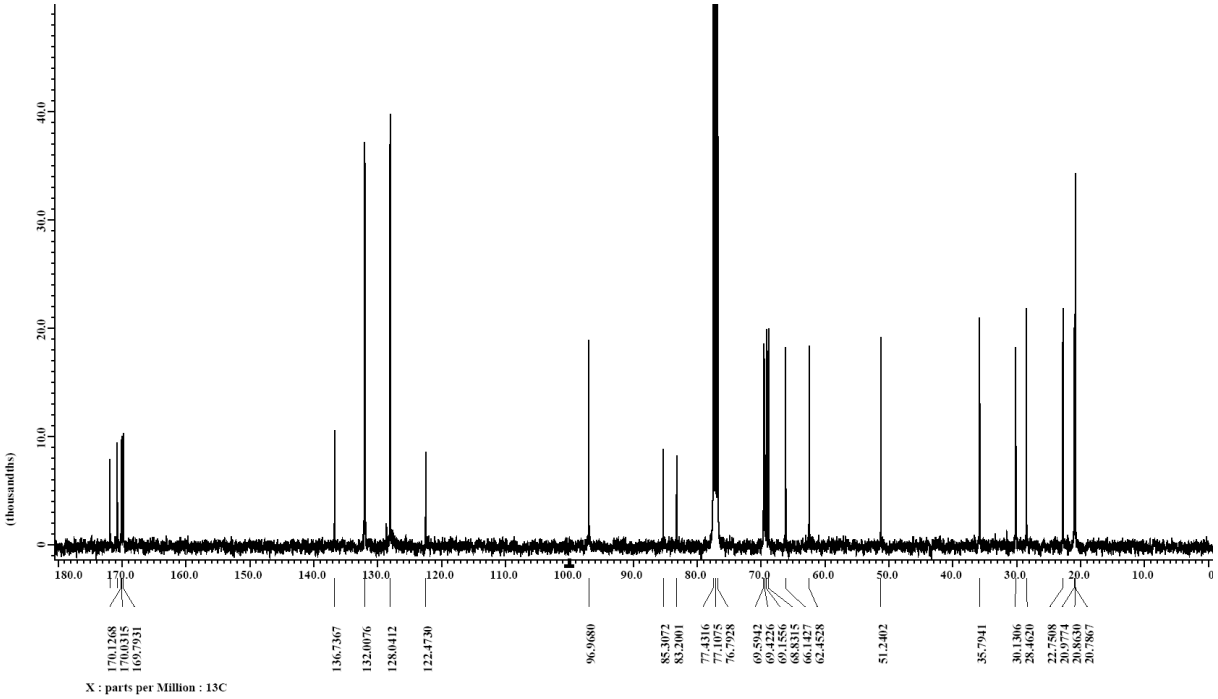

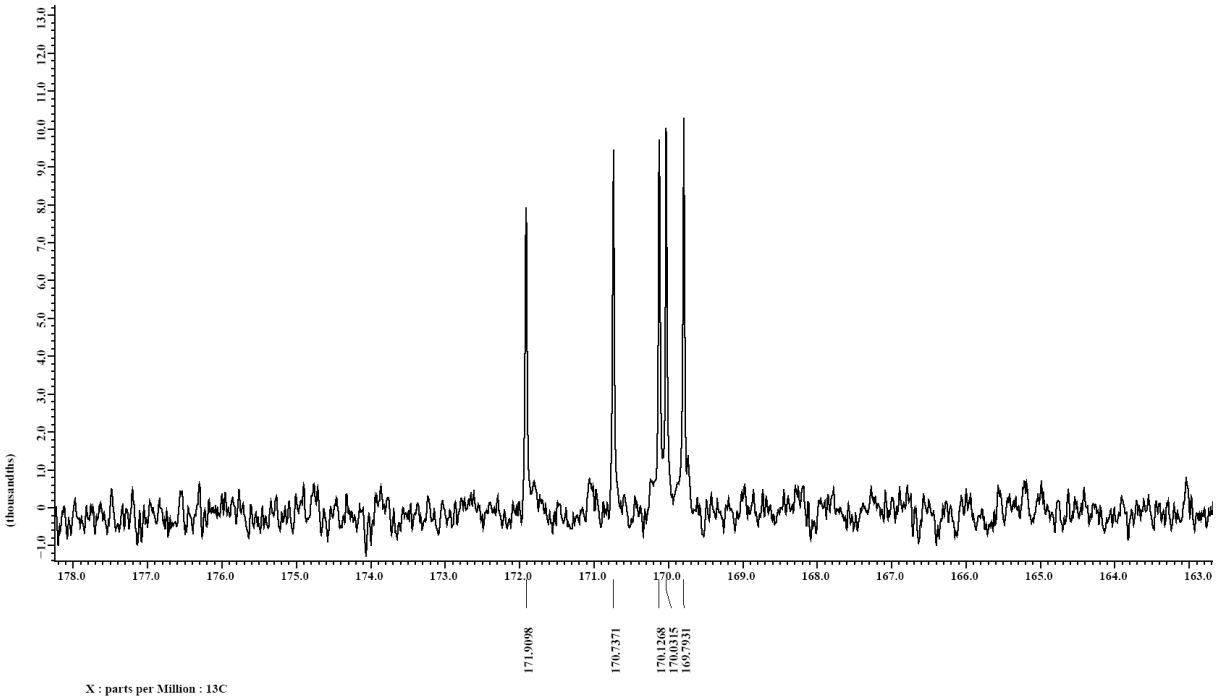

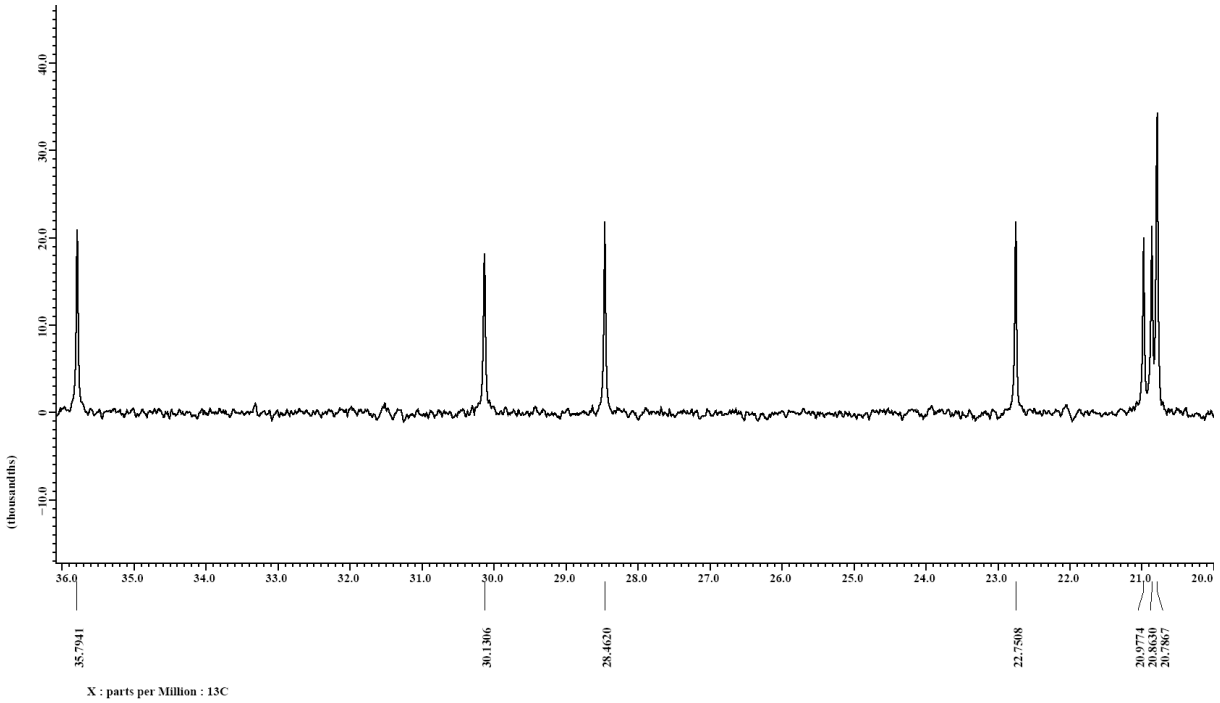
(thousandths)
40.0
30.0
20.0
10.0
0
-10.0
36.0
35.0
34.0
33.0
32.0
31.0
30.0
29.0
28.0
27.0
26.0
25.0
24.0
23.0
22.0
21.0
20.0
35.7941
30.1306
28.4620
22.7508
20.9774
20.8630
20.7867
X : parts per Million : 13C

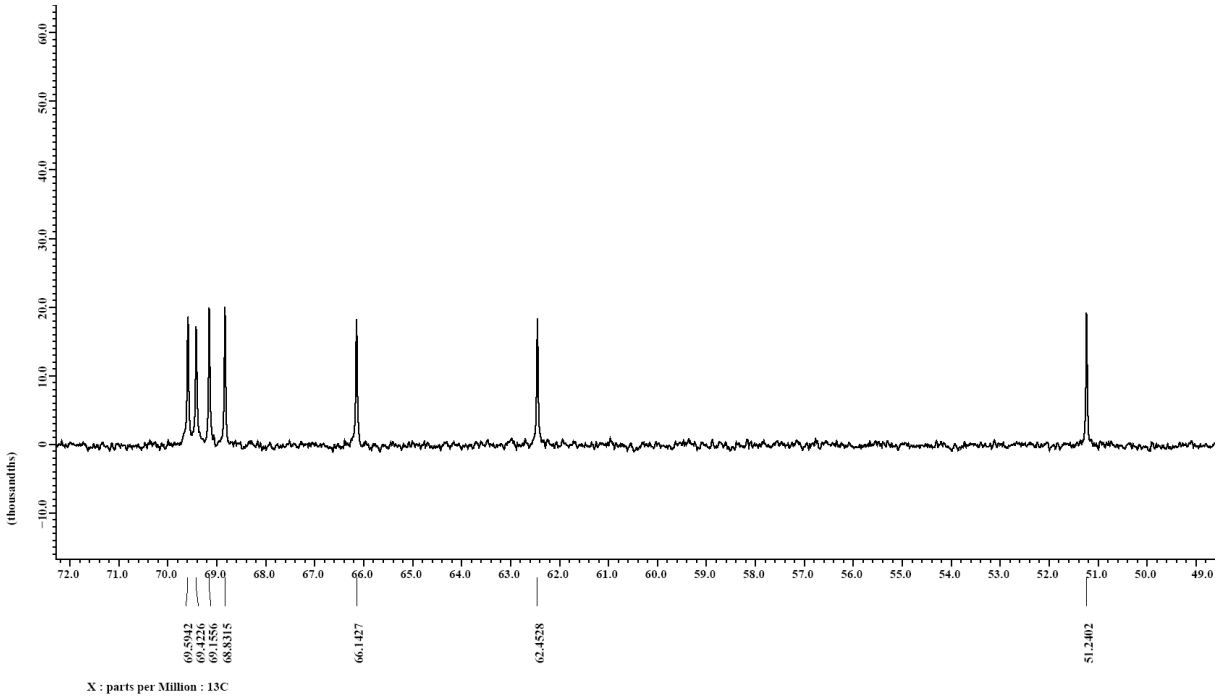
(thousandths)
60.0
50.0
40.0
30.0
20.0
10.0
0
-10.0
72.0
71.0
70.0
69.0
68.0
67.0
66.0
65.0
64.0
63.0
62.0
61.0
60.0
59.0
58.0
57.0
56.0
55.0
54.0
53.0
52.0
51.0
50.0
49.0
69.5942
69.4226
69.1556
68.8315
66.1427
62.4528
51.2402
X : parts per Million : 13C

Compound 12

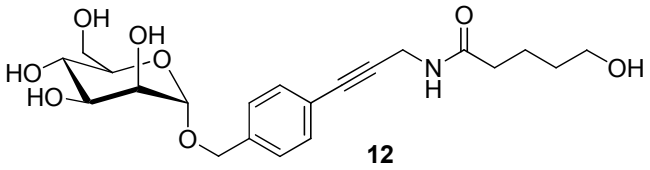

12

^{1}H NMR (400 MHz, D_2O)

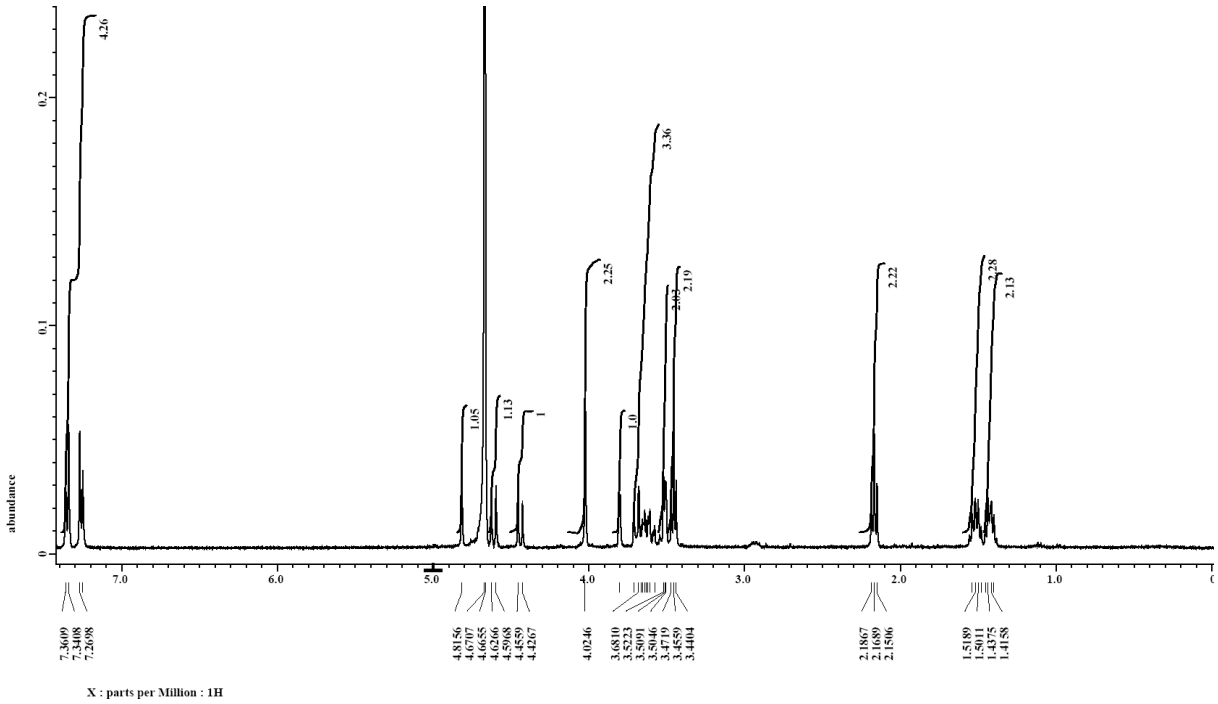

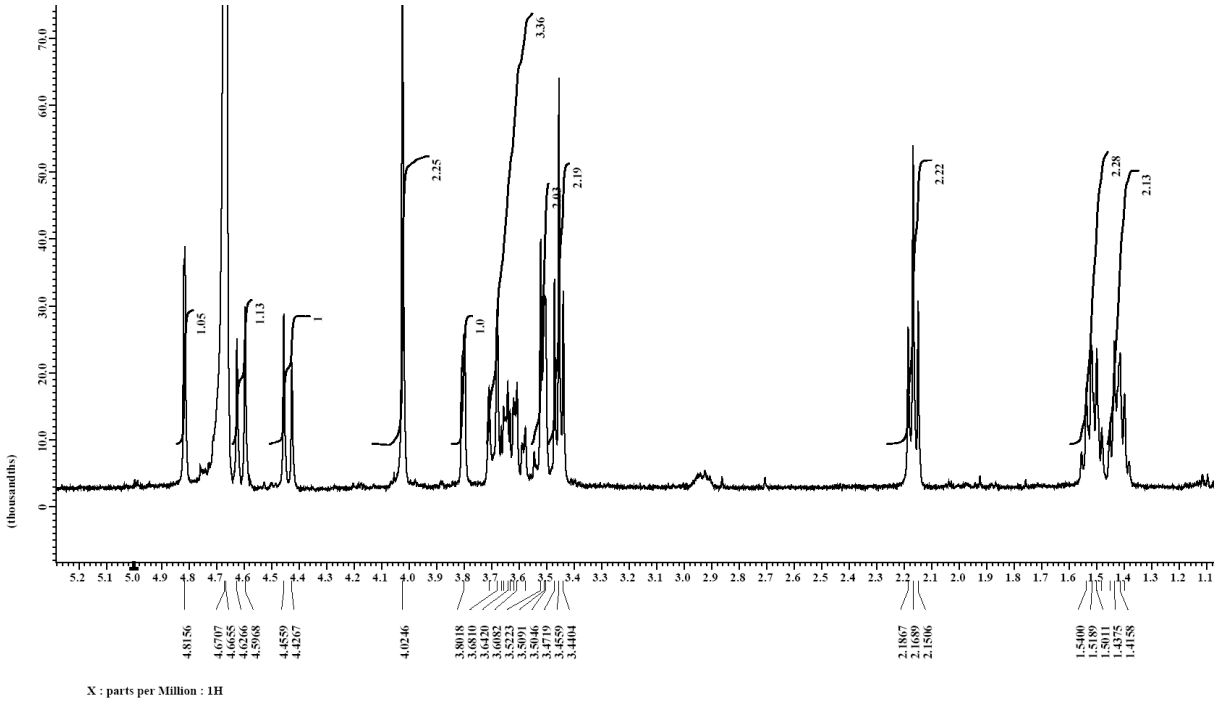

^{13}C NMR (101 MHz, D_2O)

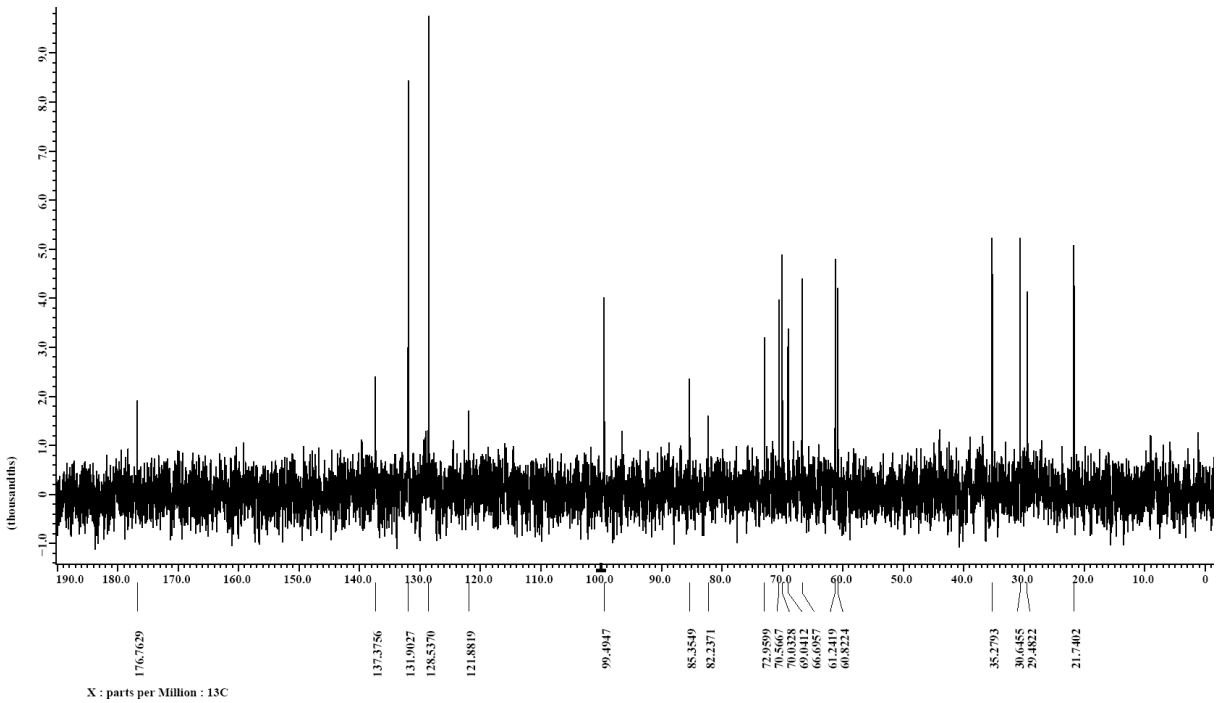

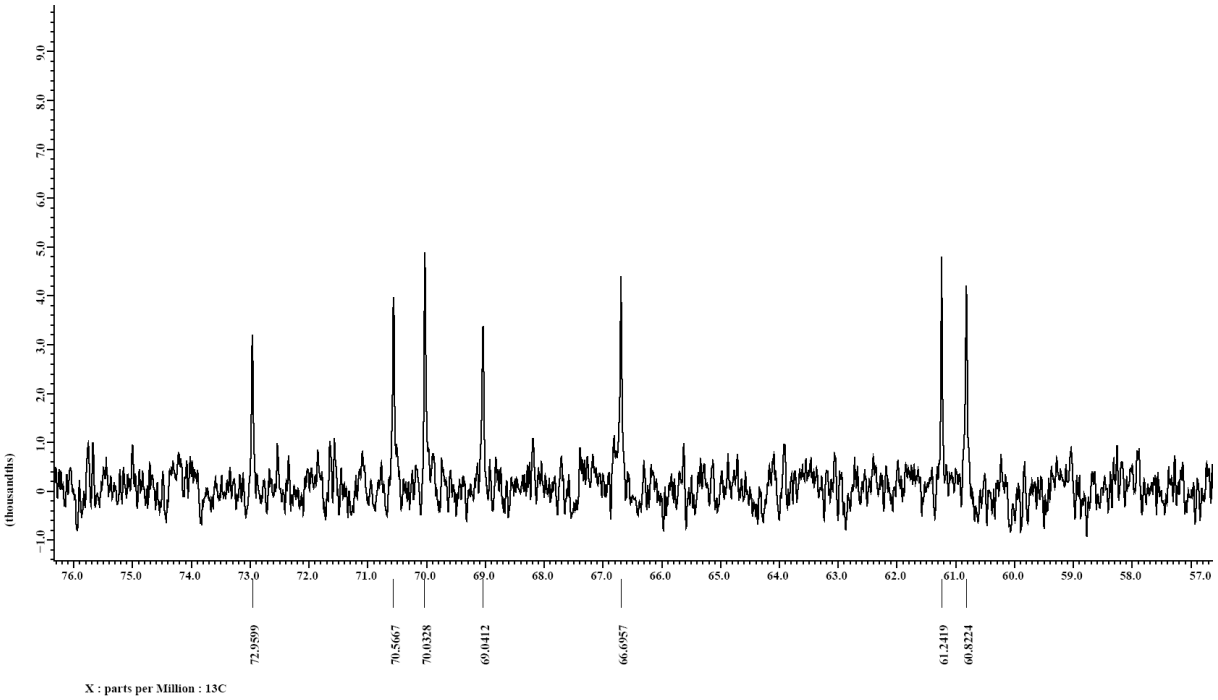
(thousandths)
9.0
8.0
7.0
6.0
5.0
4.0
3.0
2.0
1.0
0
-1.0
76.0
75.0
74.0
73.0
72.0
71.0
70.0
69.0
68.0
67.0
66.0
65.0
64.0
63.0
62.0
61.0
60.0
59.0
58.0
57.0
72.9599
70.5667
70.0328
69.0412
66.6957
61.2419
60.8224
X : parts per Million : 13C

Compound 13

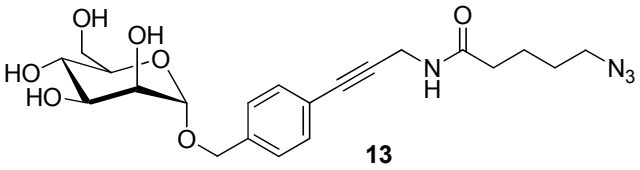

13

^{1}H NMR (400 MHz, CD_3OD)

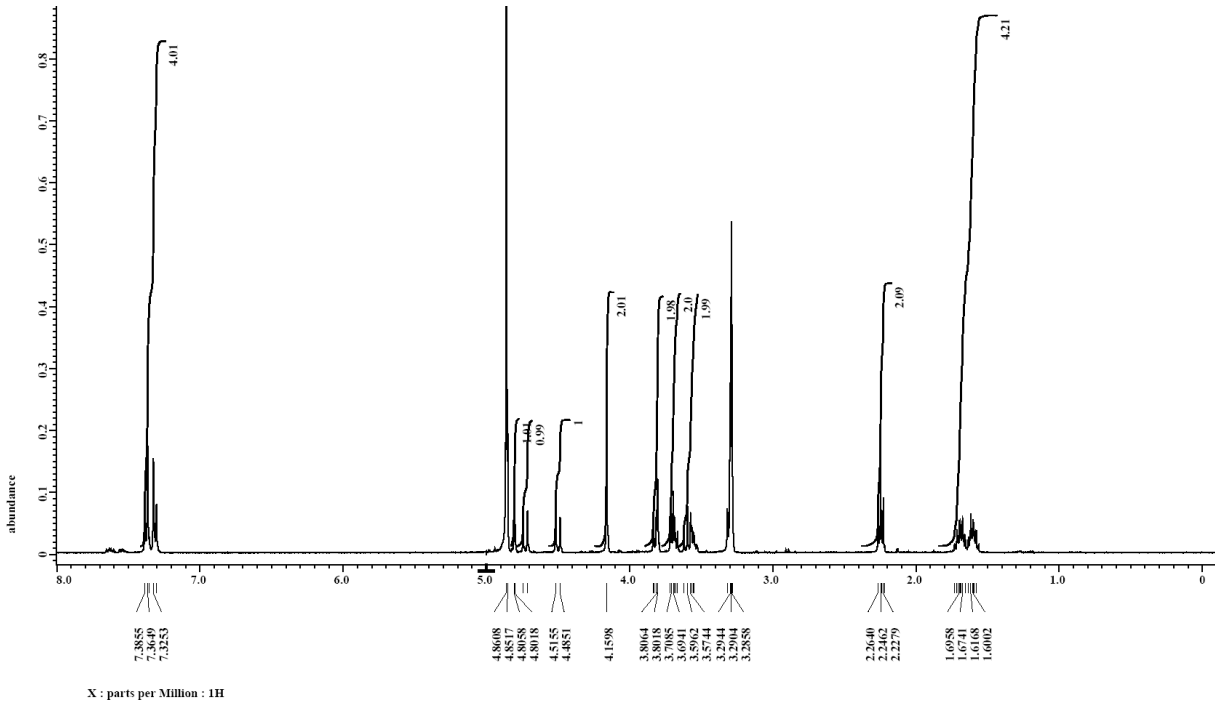

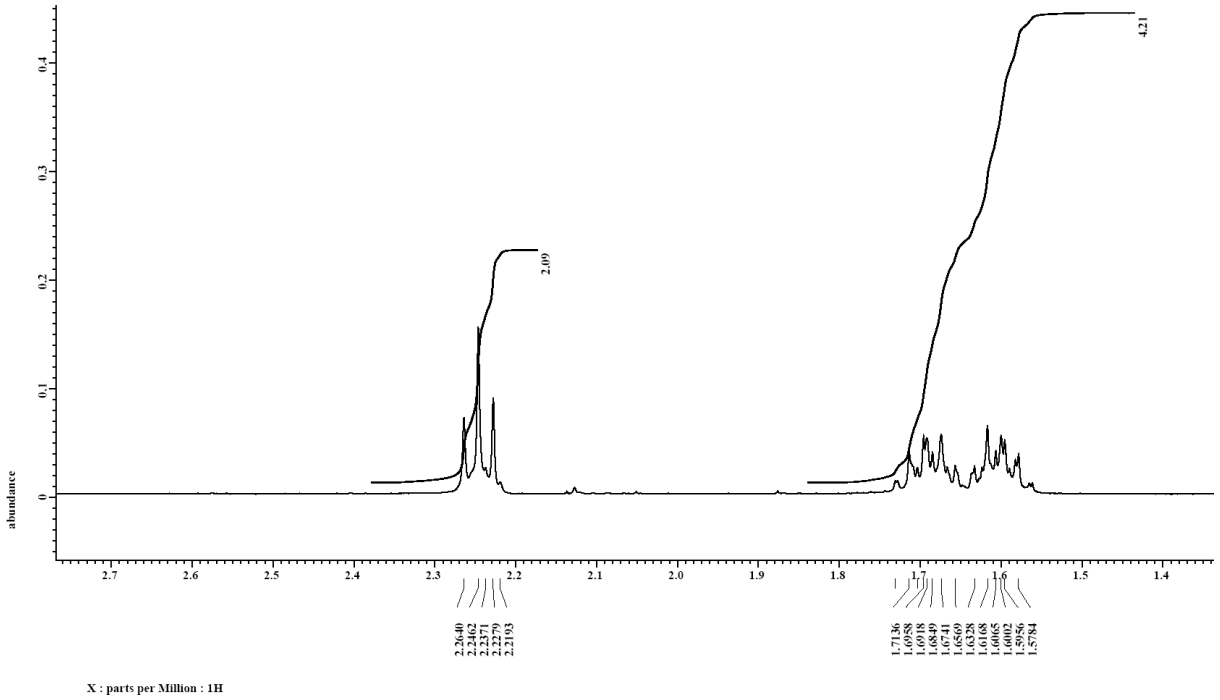
abundance
2.09
4.21
2.3640
2.2462
2.2371
2.2279
2.2193
1.7136
1.6988
1.6938
1.6849
1.6741
1.6569
1.6328
1.6168
1.6065
1.6002
1.5956
1.5784
X : parts per Million : 1H

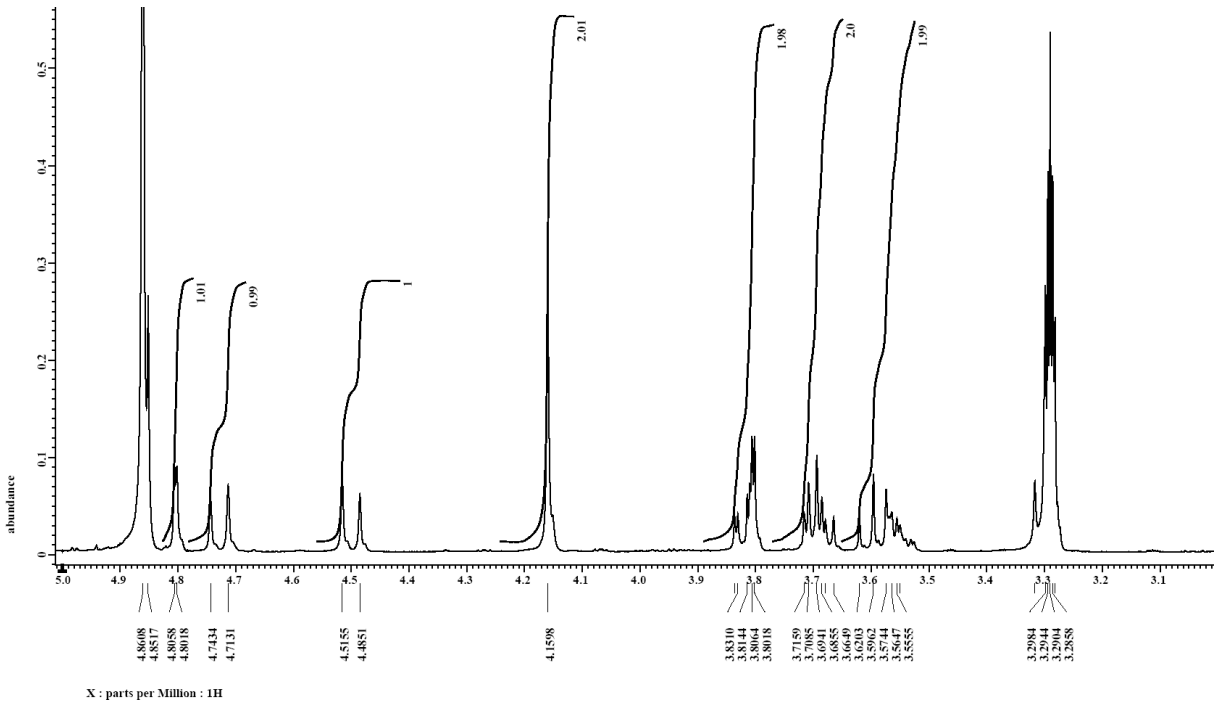
abundance
1.01
0.99
1
2.01
1.98
2.0
1.99
4.8608
4.8517
4.8058
4.8018
4.7434
4.7131
4.5155
4.4851
4.1598
3.8310
3.8144
3.8064
3.8018
3.7159
3.7085
3.6941
3.6855
3.6649
3.6203
3.5962
3.5744
3.5647
3.5555
3.2984
3.2944
3.2904
3.2858
X : parts per Million : 1H

^{13}C NMR (101 MHz, CD_3OD)

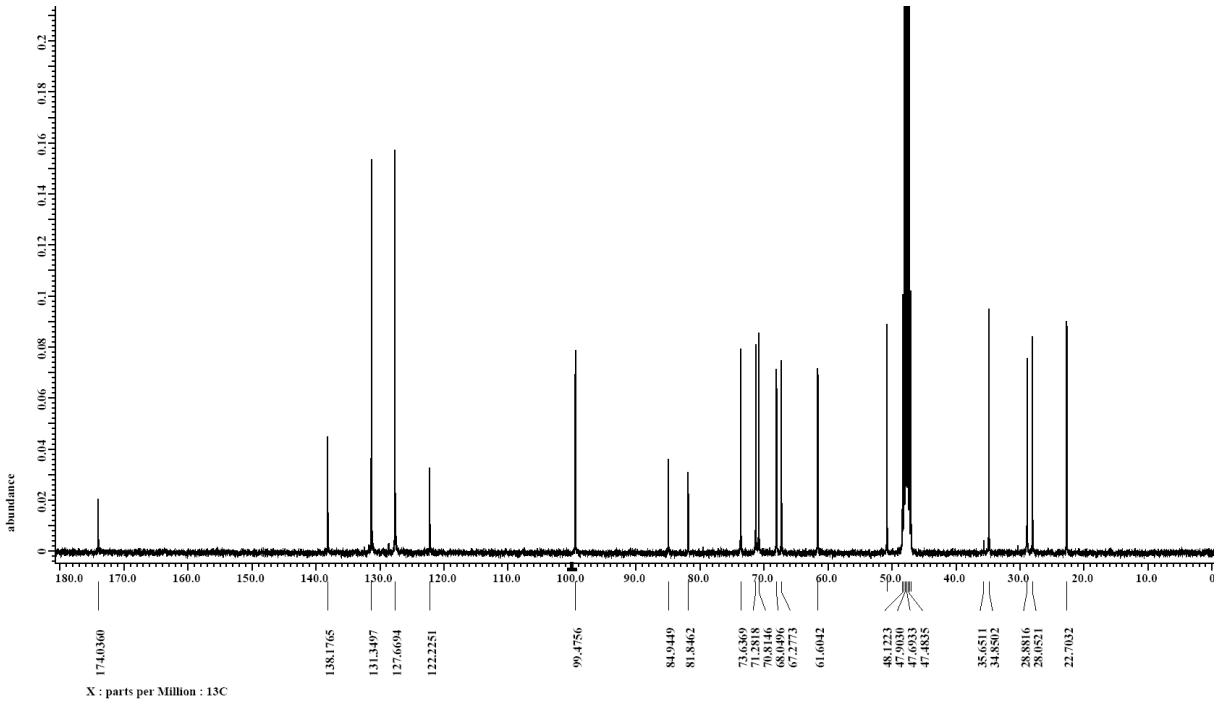

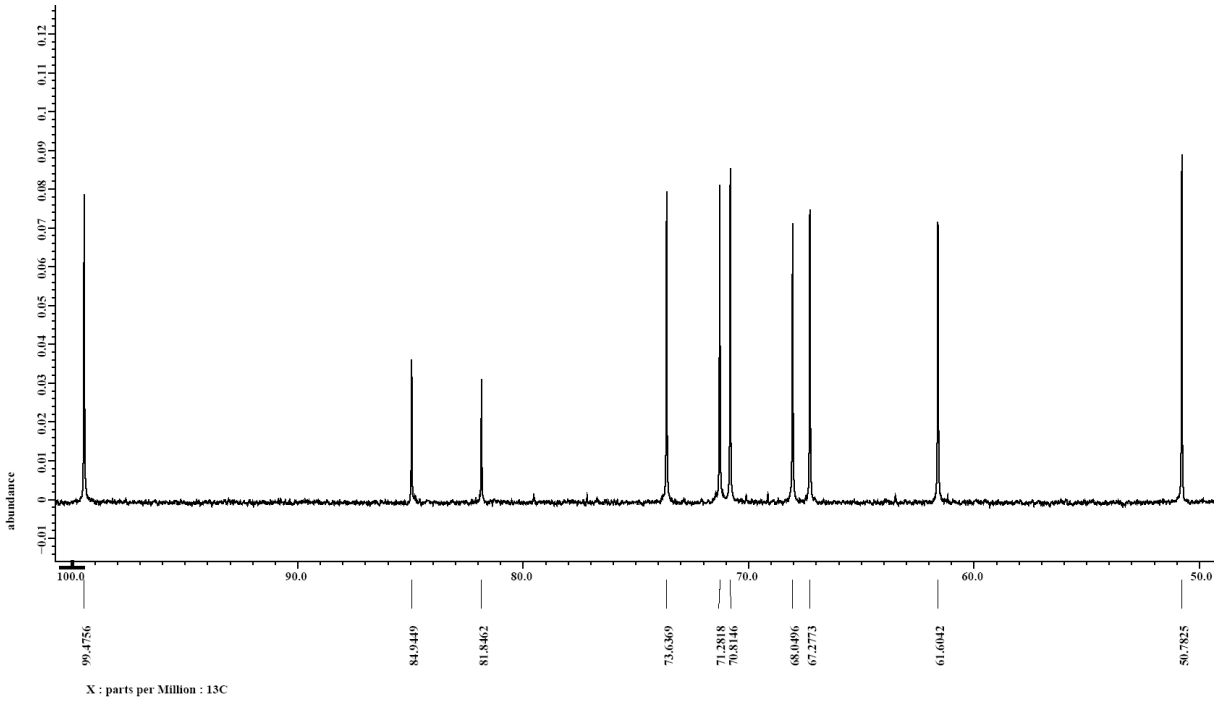

Compound 20

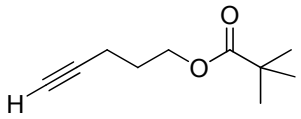

20

^{1}H NMR (400 MHz, $CDCl_3$)

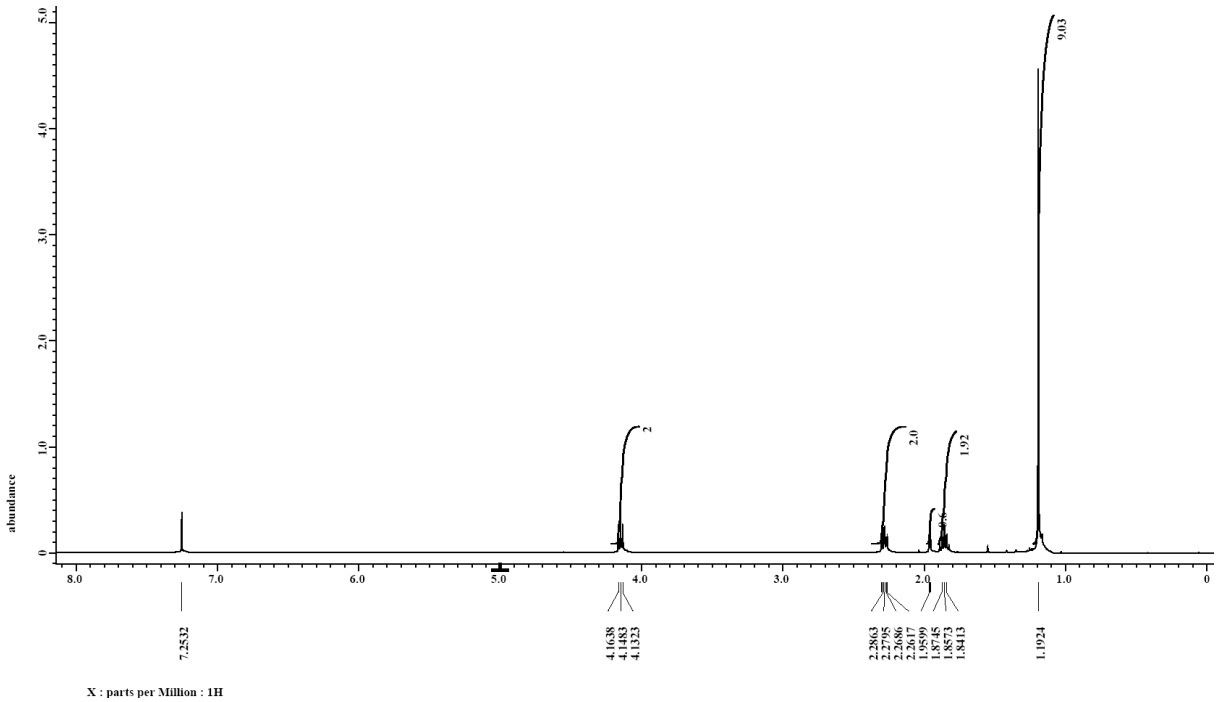

Compound 22

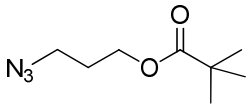

22

^{1}H NMR (400 MHz, $CDCl_3$)

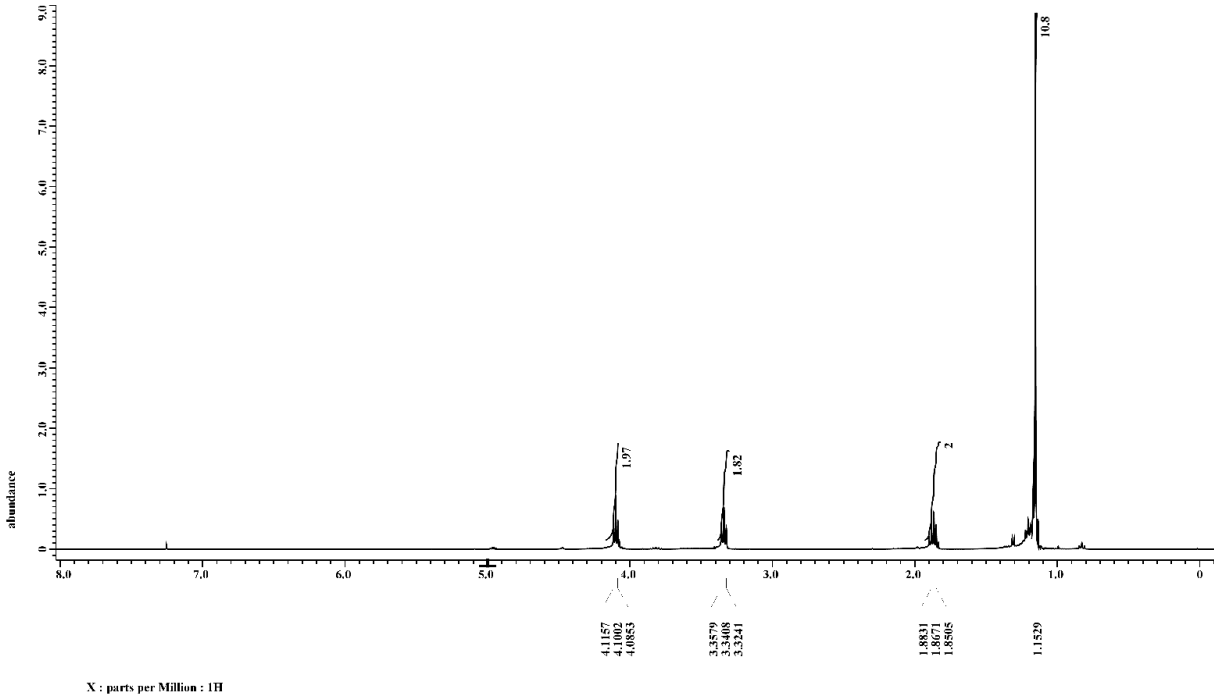

MODEL STRUCTURE OF MANNOSYLATED FULLERENE IN INTERACTION WITH 6 FIMH MOLECULES

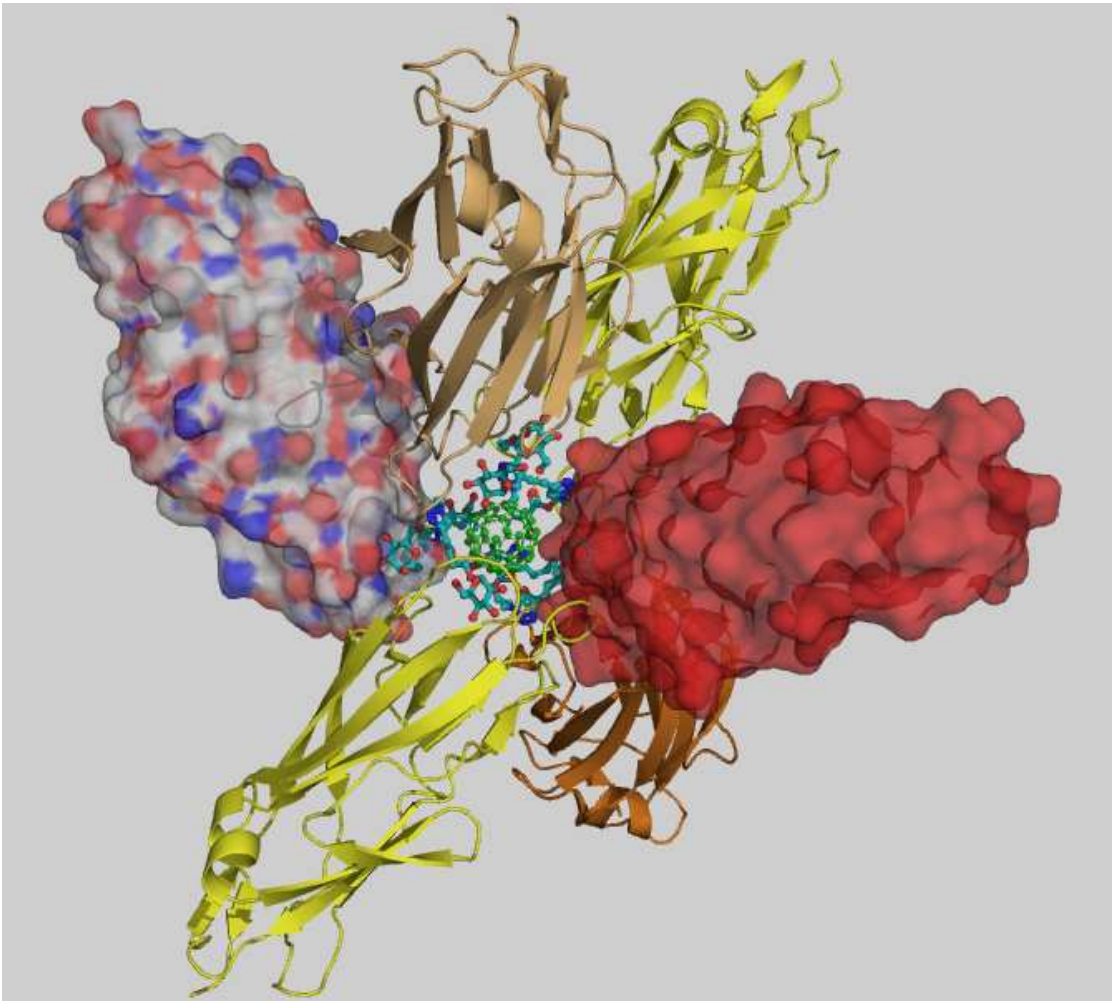

Presentation of a possible interaction model of the multivalent binding of FimH to a mannose-functionalized fullerene. The respective crystal structures of C60 fullerene[6] and the FimH receptor binding domain in complex with oligomannoside-3 have been employed to mimic the available interaction space for FimH binding to the fullerene on a molecular scale (using Pymol, version 0.99).

For the figure, fullerene **2** was created by coupling bivalent derivatives of monomer **5** (ball-and-stick model, blue for carbon, red for oxygen) onto the C60 architecture of the crystal structure (ball-and-stick presentation, green carbon, white bonds, the front face was left unmodified for clarity). The fullerene **2** adduct is displayed with six α-D-mannosides plugged into the mannose-binding pocket of FimH, through manual docking by superimposing the mannose onto the same mannose atomic positions in its crystal

[6] C60 crystal structure: I. Lamparth, C. Maichle-Mössmer, A. Hirsch, Angew. Chem.**1995**, *107*, 1755-1757; Angew. Chem. Int. Ed. Engl. **1995**, *34*,1607-1609. doi: 10.1002/anie.199516071

structure complex with FimH (reference 5 of the manuscript, Wellens et al.).[7] To better visualize mannose binding in the pocket of FimH, two out of six FimH molecules on opposite sides of the fullerene are shown as semi-transparant molecular surfaces. The electrostatic surface presentation (left) shows positively charged residues in blue and negatively charged residues in red. The tyrosine gate (tyrosines 48 and 137)[8] can be seen as two humps extending from the mannose binding pocket and pointing towards the fullerene structure. The four other FimH molecules are shown with their secondary structure.

[7] FimH crystal structure: Reference 5 of the manuscript (Wellens et al. *Plos One*, 2008, **3**, e2040).

[8] Reference 12 of the manuscript: Mol Microbiol. 2005 Jan;55(2):441-55. Receptor binding studies disclose a novel class of high-affinity inhibitors of the Escherichia coli FimH adhesin.
Bouckaert J, Berglund J, Schembri M, De Genst E, Cools L, Wuhrer M, Hung CS, Pinkner J, Slättegård R, Zavialov A, Choudhury D, Langermann S, Hultgren SJ, Wyns L, Klemm P, Oscarson S, Knight SD, De Greve H.